The ~~long–term sea–level~~ long-term sea-level commitment from Antarctica

Ann Kristin Klose[1,2], Violaine Coulon[3], Frank Pattyn[3], and Ricarda Winkelmann[1,2,4]

[1]Potsdam Institute for Climate Impact Research (PIK), Member of the Leibniz Association, P.O. Box 6012 03, 14412 Potsdam, Germany
[2]Institute of Physics and Astronomy, University of Potsdam, 14476 Potsdam, Germany
[3]Laboratoire de Glaciologie, Université libre de Bruxelles (ULB), Brussels, Belgium
[4]Department Evolutionary Earth Systems Science, Max Planck Institute of Geoanthropology, 07745 Jena, Germany

Correspondence: Ann Kristin Klose (annkristin.klose@pik-potsdam.de) and Ricarda Winkelmann (ricarda.winkelmann@pik-potsdam.de)

Abstract. The evolution of the Antarctic Ice Sheet is of vital importance given the coastal and societal implications of ice loss, with a potential to raise sea level by up to 58 m if melted entirely. However, future ~~ice–sheet~~ ice-sheet trajectories remain highly uncertain. One of the main sources of uncertainty is related to nonlinear processes and feedbacks of the ice sheet with the Earth ~~System~~ system on different timescales. Due to these feedbacks and ~~the ice–sheet~~ ice-sheet inertia, ice loss may already be triggered in the next decades or centuries and then unfolds delayed ~~on multi–centennial to millennial timescales~~over multiple centuries to millennia. This committed Antarctic ~~sea–level~~ sea-level contribution is not reflected in typical ~~sea–level~~ sea-level projections based on mass balance changes of ~~Antarctica~~the Antarctic Ice Sheet, which often cover ~~decadal–to–centennial~~ decadal-to-centennial timescales. Here, using two ~~ice–sheet~~ ice-sheet models, we systematically assess the ~~multi–millennial sea–level~~ long-term multi-millennial sea-level commitment from Antarctica in response to warming projected over the next centuries under ~~low– and high–emission~~ low- and high-emission pathways. This allows bringing together the time horizon of stakeholder planning with the much longer response times of the Antarctic Ice Sheet.

Our results show that warming levels representative of the ~~lower–emission~~ lower-emission pathway SSP1-2.6 may already result in an Antarctic mass loss of up to 6 m ~~sea–level equivalent on multi–millennial~~ sea-level equivalent on multi-millennial timescales. This committed mass loss is due to a strong ~~grounding–line~~ grounding-line retreat in the West Antarctic Amundsen Sea Embayment as well as a potential drainage from the Ross Ice Shelf catchment and onset of ice loss ~~in~~ from the Wilkes subglacial basin in East Antarctica. Beyond warming levels reached by the end of this century under the ~~higher–emission~~ higher-emission trajectory SSP5-8.5, a collapse of the West Antarctic Ice Sheet is triggered in the entire ensemble of simulations from both ~~ice–sheet~~ ice-sheet models. Under enhanced warming, next to ice loss from the marine parts, we also find a substantial decline in ice volume of regions grounded above sea level in East Antarctica. Over the next millennia, this gives rise to a ~~sea–level~~ sea-level increase of up to 40 m in our ~~experiments~~simulations, stressing the importance of including the committed Antarctic ~~sea–level~~ sea-level contribution in future projections.

1 Introduction

The future ~~sea–level~~ sea-level contribution from the Antarctic Ice Sheet, which stores enough ice to raise sea level by up to 58 m (Fretwell et al., 2013), is of vital importance for coastal communities ranging from small islands to the world's ~~mega–cities~~mega-cities, ecosystems and the global economy (Clark et al., 2016).

The Antarctic Ice Sheet has experienced changing environmental conditions on various timescales from decadal to ~~orbital–scale~~ orbital-scale climate variability since its presumed inception at the ~~Eocene–Oligocene~~ Eocene-Oligocene transition about 34 Mry ago (Zachos et al., 2001; DeConto and Pollard, 2003). This resulted in strong variations in its volume and extent linked to the slow ~~multi–millennial~~ multi-millennial changes in the Earth's astronomical configuration during the early to ~~mid–Miocene~~ mid-Miocene (Naish et al., 2001; Levy et al., 2016) and the Pliocene ~~(Naish et al., 2009; Pollard and DeConto, 2009). While large~~ (Naish et al., 2009). While terrestrial parts of the ~~terrestrial~~ East Antarctic Ice Sheet have persisted for millions of years (Sugden et al., 1995; Shakun et al., 2018), ~~ice–sheet~~ ice-sheet variability involved an occasional collapse of the West Antarctic Ice Sheet (Naish et al., 2009) and inward migration of ~~ice–sheet margins in marine–based~~ ice-sheet margins in marine-based sectors of East Antarctica (that is, where the ice sheet is grounded below sea level) during Pliocene warm periods (Cook et al., 2013; Patterson et al., 2014; Aitken et al., 2016). During Pleistocene Interglacials, Antarctic ice loss ~~contributed to sea–level high–stands (Wilson et al., 2018; Blackburn et al., 2020; Turney et al., 2020)~~from the East Antarctic Wilkes subglacial basin (Wilson et al., 2018; Blackburn et al., 2020) and across the Weddel Sea Embayment (Turney et al., 2020) may have contributed to sea-level high-stands of 6 m to 9 m higher than present (including a contribution from thermal expansion and mass loss from the Greenla
.

The future trajectory of the Antarctic Ice Sheet under progressing warming, however, is highly uncertain. This is due to uncertainties in the ~~(representation of) ice–sheet processes and ice–climate~~ understanding and representation of ice-sheet processes and ice-climate interactions (Fox-Kemper et al., 2021) as well as the potentially high magnitudes and rates of recent and projected warming. The present rate of warming is unprecedented in at least 2000 years, with an increase of 1.1 °C in the global mean surface temperature between 1850–1900 and 2011–2020 (Gulev et al., 2021). The amount of warming projected for the end of this century under the Shared Socioeconomic Pathways ~~(e.g., for the higher–emission scenario SSP5-8.5 with an increase in global a~~ (e.g. for the higher-emission scenario SSP5-8.5 with an increase in global annual mean surface air temperature of 3.6 °C to 6.5 °C relative is comparable to the transition from the Last Glacial Maximum to the beginning of the Holocene ~~,~~ approximately 11,700 years before present, but is expected to develop on much shorter timescales.

At present, accelerated mass loss of the Antarctic Ice Sheet is concentrated in West Antarctica and the East Antarctic Wilkes land (Otosaka et al., 2023; Rignot et al., 2019; Li et al., 2016; Miles et al., 2021), likely driven by ~~ocean–induced~~ ocean-induced melting due to the intrusion of warm water into the ~~ice–shelf~~ ice-shelf cavities (Paolo et al., 2015). In future projections so far, for instance provided by the recent Ice Sheet Model Intercomparison Project ~~ISMIP6 (Seroussi et al., 2020; Payne et al., 2021)~~ for CMIP6 (ISMIP6, Seroussi et al., 2020; Payne et al., 2021), the transient ~~sea–level~~ sea-level response to the projected warming ranges from a slight mass gain to a mass loss of ~~Antarctica~~ the Antarctic Ice Sheet by the end of this century under multiple emission scenarios (with the largest spread in ~~sea–level~~ sea-level change given by ~~higher–emission~~ higher-emission

pathways RCP8.5 and SSP5-8.5). The bulk of ~~sea-level~~ sea-level rise, however, is expected to unfold beyond the end of this century (Clark et al., 2016; Fox-Kemper et al., 2021) due to (1) the inertia of the ~~continental-scale~~ continental-scale ice sheet in combination with (2) the potential of crossing critical thresholds with ongoing ~~global warming . This long-term sea-level~~ warming (Lenton et al., 2023). This long-term *committed* sea-level response, that has already been triggered or may be triggered during the next decades or centuries (but unfolds ~~over the following centuries and~~ thereafter over multiple centuries to millennia), might be substantially higher than ~~and~~ the transient *realized* sea-level change, while it is not represented in typical ~~sea-level projections~~ sea-level projections (Seroussi et al., 2020; Edwards et al., 2021). Here, we assess this expected ~~long-term committed sea-level~~ long-term committed sea-level change, by stabilizing the climatic boundary conditions projected over the next centuries at specific points in time and letting the ice sheet evolve over several millennia. We furthermore ~~identify the gap~~ quantify the difference or offset between the transient ~~*realized*~~ ~~sea-level~~ realized sea-level contribution from Antarctica at a particular point in time and the respective ~~long-term *committed* sea-level contribution(Winkelmann et al., in review).~~ long-term committed sea-level contribution.

The slow ~~ice-sheet~~ ice-sheet response to perturbations in its climatic boundary conditions owing to high inertia results in a ~~time-lag~~ time-lag between forcing and the resulting mass change. As the ~~ice-sheet~~ ice-sheet response unfolds on centennial to ~~multi-millennial timescales, sea-level will~~ multi-millennial timescales, sea level may keep rising for millennia to come even if warming is ~~kept on a constant level~~ stabilized (Golledge et al., 2015; Winkelmann et al., 2015). This is especially due to the ~~softening-induced~~ softening-induced increase in the creep component of the ice flow and internal feedbacks ~~(Golledge et al., 2015; Clarke et al., 1977).~~ (Clarke et al., 1977; Golledge et al., 2015).

In addition, the Antarctic Ice Sheet is subject to several ~~positive (and negative~~ampliyfing (and dampening) feedback mechanisms determining its ~~long-term~~ long-term stability (Fyke et al., 2018; Garbe et al., 2020). For example, accelerated ice loss may be triggered once the ~~self-reinforcing surface melt-elevation feedback (Levermann and Winkelmann, 2016; Oerlemans, 1981)~~ amplifying surface melt-elevation feedback (Oerlemans, 1981; Levermann and Winkelmann, 2016) kicks in. With the lowering of the ~~ice-sheet~~ ice-sheet surface due to melting, it is exposed to higher air temperatures~~owing to the atmospheric lapse rate~~. Surface melting is, in turn, enhanced, promoting persistent ice loss upon crossing a critical temperature threshold. Furthermore, the marine parts of the ice sheet, e.g., in West Antarctica or the East Antarctic Aurora and Wilkes subglacial basins~~in East Antarctica~~, are found to be susceptible to ~~self-sustained~~self-sustained, potentially irreversible ~~grounding-line retreat (Garbe et al., 2020; Rosier et al., 2021; Mengel and Levermann, 2014; Feldmann et al., 2014)~~grounding-line retreat (Feldmann et al., 2014). The rapid ~~grounding-line~~ grounding-line retreat is often associated with ~~a self-amplifying~~ an amplifying feedback in which the increased ice flow across the grounding line caused by an initial retreat fosters further retreat. In a theoretical flowline setup, it was shown that, due to the ice flux being a nonlinear function of the ice thickness, ~~grounding lines of~~ ice sheets grounded below sea level on a retrograde, inland sloping bed are unstable (Marine Ice Sheet Instability; Weertman, 1974; Schoof, 2007). More complex stability conditions arise in three dimensions when accounting for additional processes such as, e.g., buttressing (Gudmundsson et al., 2012; Haseloff and Sergienko, 2018; Pegler, 2018), calving and submarine melting (Haseloff and Sergienko, 2022) or the presence of feedbacks between the ice sheet and its environment (Sergienko, 2022). Ice loss may be dampened, on the other hand, by negative feedbacks such as introduced by e.g., the isostatic rebound of

the solid Earth underlying the ice sheet~~to ice mass changes~~, which could potentially stabilize West Antarctic grounding lines ~~(Coulon et al., 2021; Barletta et al., 2018)~~(Barletta et al., 2018; Coulon et al., 2021).

Depending on the interplay of these feedbacks, persistent mass loss may be triggered once critical forcings or tipping points (Lenton et al., 2008; Armstrong McKay et al., 2022), for instance in temperature, are crossed. The Antarctic Ice Sheet was therefore classified as a tipping element of the climate system ~~(Lenton et al., 2008; Armstrong McKay et al., 2022)~~ (Lenton et al., 2008; Armstrong McKay et al., 2022; Lenton et al., 2023). Due to the inertia ~~in the system~~ of ice sheets and the related delay in ~~the ice-sheet response under realistic forcing~~their transient response following a realistic warming trajectory under e.g. a higher-emission pathway, the ice sheet's volume trajectory likely deviates from the ~~ice-sheet~~ ice-sheet equilibrium response to warming (Garbe et al., 2020; Rosier et al., 2021). While consequences of ~~self-sustained~~ self-sustained ice loss potentially triggered in the next decades or centuries may play out and become visible over millennial timescales (Reese et al., 2023) (characterized as a slow onset of tipping; Ritchie et al., 2021), tipping may also be sped up by forcing beyond the critical threshold. For the Greenland Ice Sheet, it was shown that the timescales of ~~ice-sheet~~ ice-sheet decline strongly depend on how far its critical temperature threshold is exceeded (Robinson et al., 2012).

Previous assessments of the ~~long-term contribution to sea-level~~ long-term contribution to sea-level rise from the Antarctic Ice Sheet have been primarily restricted to a single ~~ice-sheet~~ ice-sheet model and have ~~rarely explored intra- and inter-model uncertainties~~ thus rarely explored *model uncertainties*, including uncertainties in ice-sheet processes, their parameterisations in ice-sheet models and distinct initialisation approaches, as well as uncertainties in ~~climate forcing~~ the future climate (*climate forcing uncertainty*) (Golledge et al., 2015; Clark et al., 2016): They suggest that the grounding lines in the Amundsen Sea Embayment ~~may~~ might at present already be undergoing ~~or may be committed to a self-amplified retreat under sustained present-day climate conditions~~ a self-sustained retreat until a new stable geometric configuration is reached ~~(Reese et al., 2023; Joughin et a~~ or that this retreat might be imminent under sustained present-day climate (Joughin et al., 2014; Favier et al., 2014; Seroussi et al., 2017; Ar . The potential for pronounced ~~grounding-line recession in marine-based~~ grounding-line recession in marine-based portions of West Antarctica and the Wilkes subglacial basin in East Antarctica until the end of the millennium ~~(Golledge et al., 2015; Clark et al., 2016;~~ was illustrated for ~~higher-emission scenarios~~ higher-emission scenarios (Golledge et al., 2015; Winkelmann et al., 2015; Clark et al., 2016 , giving rise to an Antarctic mass loss of multiple meters ~~of sea-level~~ sea-level equivalent. On ~~multi-millennial~~ multi-millennial timescales, the loss of the portion of the ice sheet grounded above sea level in East Antarctica may be locked in for strong atmospheric warming, which would eventually commit the Antarctic Ice Sheet to contribute several tens of meter to ~~global mean sea-level rise (Clark et al., 2016; Winkelmann et al., 2015)~~sea-level rise (Winkelmann et al., 2015; Clark et al., 2016).

Here we systematically study the ~~long-term multi-millennial~~ long-term multi-millennial evolution of the Antarctic Ice Sheet in response to a wide range of possible future climate trajectories and thereby quantify its ~~sea-level~~ sea-level commitment for stabilized climate at different points in time over the course of the next centuries taking into account uncertainties in ~~climatic boundary conditions and ice-sheet~~ future Antarctic climate and ice-sheet processes, by means of two different ~~ice-sheet~~ ice-sheet models: PISM (Bueler and Brown, 2009; Winkelmann et al., 2011) and Kori-ULB (previously called f.ETISh; Pattyn, 2017). The remainder of this paper is structured as follows: In the following Sect. 2 we describe the methods for performing ~~sea-level projections on multi-millennial~~ sea-level projections on multi-millennial timescales. Results are presented in Sect. 3

and discussed in Sect. 4 with a focus on different sources of uncertainties, arising from the divergence of future climate trajectories (*climate forcing uncertainty*) as well as ~~structural uncertainties, distinct initialisations and certain processesand~~ from ice-sheet processes, their parameterisations in ~~ice–sheet models~~ ice-sheet models and related parameter choices next to distinct initialisation approaches (*model uncertainties*).

2 Methods

2.1 ~~Ice–sheet~~ Ice-sheet models

2.1.1 PISM

The Parallel Ice Sheet Model (PISM; Bueler and Brown, 2009; Winkelmann et al., 2011) is an ~~open–source, thermo–mechanically–coupled~~ open-source, thermo-mechanically-coupled ice sheet/stream/shelf model. In hybrid mode, the ~~shallow–ice~~ shallow-ice approximation (SIA) and ~~shallow–shelf~~ shallow-shelf approximation (SSA) are solved and superimposed, giving rise to different dynamic regimes from the ~~slow–flowing~~ slow-flowing ice in the ~~ice–sheet~~ ice-sheet interior to the ~~faster–flowing~~ faster-flowing streams and ice shelves. We here use a modified version of PISM release v1.0 (Garbe et al., 2020). In particular, centered differences of the ice thickness across the grounding line are calculated to derive the surface gradient, which have been shown to improve the representation of the driving stress at the grounding line (Reese et al., 2023). We use a rectangular grid of 16 km horizontal resolution and a vertical grid structure with the highest resolution at the base of the ice sheet and shelves.

Basal shear stress ~~τ_b and shallow–shelf~~ τ_b and shallow-shelf approximation basal sliding velocities ~~u_b~~ $\mathbf{u}_\mathrm{b}$ are related in a general power law of the form

$$\tau_\mathrm{b} = -\tau_c \frac{u_b}{u_{th}^q |u_b|^{1-q}} \frac{\mathbf{u}_\mathrm{b}}{\mathbf{u}_\mathrm{th}^q |\mathbf{u}_\mathrm{b}|^{1-q}} \tag{1}$$

with the threshold velocity ~~$u_{th} = 100$~~$u_\mathrm{th} = 100$ m yr^{-1} and the sliding exponent q. The yield stress ~~τ_c~~ τ_c is determined by the ~~Mohr–Coulomb~~ Mohr-Coulomb failure criterion (Cuffey and Paterson, 2010) as

$$\tau_\mathrm{c} = \tan(\phi N_\mathrm{till}) \tag{2}$$

including the till friction angle ϕ and the effective pressure N_till. The till friction angle is parameterized as piecewise linear with bed elevation (Martin et al., 2011), in our simulations with a lower value of 24° for topography below -700 m and an upper value of 30° for topography above 500 m (following Reese et al., 2023). The effective pressure N_till in PISM is a function of the overburden pressure P_0 and the fraction of the effective water thickness in the till layer $s = W_\mathrm{till}/W_\mathrm{max}$:

$$N_\mathrm{till} = \min\{P_0, N_0 \left(\frac{\delta P_0}{N_0}\right)^s 10^{(e_0/C_c)(1-s)}\} \tag{3}$$

where the values for the constants ~~N_0, e_0 and C_c~~ N_0, e_0 and C_c are chosen following Bueler and van Pelt (2015). The amount of water from basal melt in the till layer W_till with a maximum of ~~$W_\mathrm{max} = 2$~~$W_\mathrm{max} = 2$ m evolves according to the ~~non–conserving~~

non-conserving 'null' hydrology model (as described in Bueler and van Pelt, 2015) with a decay rate C of water in the till. The grounding-line position is simulated at a sub-grid scale evolving freely without imposing additional flux conditions. Basal resistance is linearly interpolated on a sub-grid scale around the grounding line (Feldmann et al., 2014), while sub-shelf melt in partially floating cells is not applied in the simulations presented here. We apply eigencalving, which linearly relates the calving rate to the spreading rate tensor with a proportionality factor of $K = 1\text{x}10^{17}$ m s (Levermann et al., 2012). Additionally, thin ice below 50 m is removed at the calving front (thickness calving) and a maximum extent for ice shelves is defined (Garbe et al., 2020; Albrecht et al., 2020). Our simulations include the effect of the viscous and elastic response of the bedrock to changes in ice load, following Lingle and Clark (1985) and Bueler et al. (2007), with an upper mantle viscosity $\eta = 1\text{x}10^{21}$ Pa s and density $\rho = 3300$ kg m^{-3} as well as a flexural rigidity of the lithosphere of $5\text{x}10^{24}$ N m.

2.1.2 Kori-ULB

The Kori-ULB ice flow model, which is the follow-up of the f.ETISh model (Pattyn, 2017), is a vertically-integrated, thermo-mechanically-coupled hybrid ice-sheet/ice-shelf model, and incorporates relevant features for studying the evolution of the Antarctic Ice Sheet such as the surface melt-elevation feedback, basal sliding, sub-shelf melting, calving, and bedrock deformation. The ice flow is governed by a combination of the shallow-ice (SIA) and shallow-shelf (SSA) approximations for grounded ice and by the shallow-shelf approximation for floating ice shelves (Bueler and Brown, 2009; Winkelmann et al., 2011). Simulations of the multi-millennial Antarctic sea-level contribution presented here were performed with Kori-ULB version 0.91 at a horizontal resolution of 16 km.

Basal sliding is parameterized using a Weertman sliding law, i.e.,

$$\tau_{\underline{b}\mathrm{b}} = {A_{\underline{b}\mathrm{b}}}^{-1/m} |\mathbf{v}_{\underline{b}\mathrm{b}}|^{1/m-1} \mathbf{v}_{\underline{b}\mathrm{b}} \tag{4}$$

where ~~τ_b and $\mathbf{v}_b$~~ τ_b and $\mathbf{v}_\mathrm{b}$ are the basal shear stress and the basal velocity, respectively, and with a basal sliding exponent ~~$m = 3.$~~ $m = 3$. The values of the basal sliding coefficient ~~A_b~~ A_b are inferred following the nudging method of Pollard and DeConto (2012b) and Bernales et al. (2017) ~~.~~ (compare Sect. 2.2.2).

At the grounding line, a flux condition (related to the ice thickness at the grounding line; Schoof, 2007) is imposed as in Pollard and DeConto (2012a) and Pollard and DeConto (2020) to account for grounding-line migration. This implementation can reproduce the steady-state behavior of the grounding line and its migration (Schoof, 2007) also at coarse resolution (Pattyn et al., 2013). Using this flux condition, the marine ice-sheet behavior in Antarctica was simulated by large-scale ice-sheet models (Pollard and DeConto, 2012a; DeConto and Pollard, 2016; Pattyn, 2017; Sun et al., 2020) ~~,~~ with similar results under buttressed conditions as in high-resolution models (Pollard and DeConto, 2020). Calving at the ice front depends on the parameterized combined penetration depths of surface and basal crevasses relative to the total ice thickness. Similar to Pollard et al. (2015) and DeConto and Pollard (2016), the parameterisation of the crevasse penetration depths involves the divergence of the ice velocity, the

accumulated strain, and the ice thickness. Bedrock adjustment in response to changes in ice and ocean load is taken into account by means of the commonly used Elastic ~~Lithosphere–Relaxed~~ Lithosphere-Relaxed Asthenosphere (ELRA) model, where the ~~solid–Earth~~ solid-Earth system is represented by a relaxing viscous asthenosphere below a thin elastic lithosphere plate (Le Meur and Huybrechts, 1996; Coulon et al., 2021). A spatially uniform relaxation time of ~~3000~~3000 years and a flexural rigidity of the lithosphere of 10^{25} N m is chosen in the simulations presented here.

2.2 Experimental design

2.2.1 Assessing Antarctic ~~sea–level~~ sea-level commitment

We aim to determine the ~~long–term multi–millennial sea–level~~ long-term multi-millennial sea-level contribution from the Antarctic Ice Sheet and thereby its sea-level commitment using the ~~ice–sheet~~ ice-sheet models PISM and Kori-ULB (compare Sect. ~~??~~2.1). After initializing the models to obtain initial Antarctic Ice Sheet ~~configurations~~ states and running historical simulations (described in more detail in the following Sect. 2.2.2 and Sect. 2.2.3, and illustrated in Figure 1), we assess the response of the Antarctic Ice Sheet to changes in the ~~oceanic and atmospheric~~ atmospheric and oceanic boundary conditions derived from ~~state–of–the–art~~ state-of-the-art climate model projections available from the sixth phase of the Coupled Model Intercomparison Project (CMIP6) under the Shared Socioeconomic Pathways SSP1-2.6 and SSP5-8.5 (thereby covering a wide range from ~~lower– to higher–emission~~ lower- to higher-emission scenarios). As we are interested in the ~~long–term~~ long-term ice-sheet response, we focus on a set of CMIP6 General Circulation Models (GCMs) that provide forcing until the year 2300. Thereby, we obtain the transient *realized* ~~sea–level~~ sea-level contribution of the Antarctic Ice Sheet at given points in time (for instance, in the year 2100, filled dots in Figure 1). We then quantify the ~~long–term~~ long-term *committed* ~~sea–level~~ sea-level contribution by stabilizing forcing conditions of the climate trajectories at regular intervals in time ('branching off' in the years 2050, 2100, 2150, 2200, 2250 and 2300; compare Table S1) and letting the ice sheet evolve over several millennia (until the year 7000) under ~~fixed~~ constant climatic boundary conditions characteristic for the respective branchoff year (Fig. 1, open dots). Climate conditions of the distinct branchoff years are determined as the mean over the previous ten years before the branchoff.

2.2.2 ~~initialisation~~Initialisation

Both ~~ice sheet~~ ice-sheet models are initialized using constant climatic boundary conditions representing the year 1950 (Fig. 1). ~~More specifically, 'historic'~~ The historical climatic boundary conditions for the year 1950 are constructed using the ~~historic changes in ocean and atmosphere~~ historical changes in atmosphere and ocean with respect to the reference period from 1995 to 2014 from the Norwegian Earth System Model (NorESM1-M; Bentsen et al., 2013) ~~. The oceanic and atmospheric anomalies in CMIP5.~~ The atmospheric and oceanic anomalies from NorESM1-M are averaged over the period ~~1945–1955~~ 1945-1955 and subsequently added to ~~present–day~~ present-day atmospheric temperatures and precipitation derived from Regional Climate Models (RCMs) as well as observed ~~present–day~~ present-day ocean temperatures and salinities. ~~Two distinct present–day~~ Present-day atmospheric climatologies are derived from the ~~Regional Climate Models (RCMs)~~ RCMs Modèle Atmosphérique

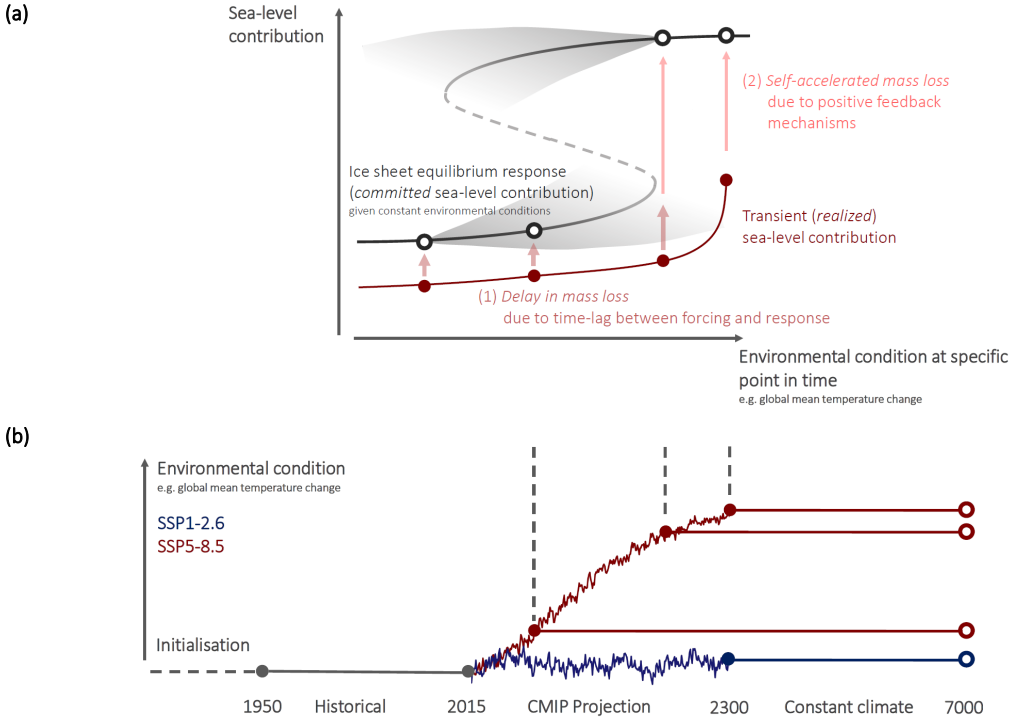

Figure 1. Schematic of the experimental design (a): Idealized and simplified stability diagram of the Antarctic Ice Sheet as possible tipping element, which illustrates some underlying factors potentially contributing to ~~a gap~~ the substantial difference or offset between the transient realized and ~~long-term~~ long-term committed ~~ice-sheet~~ ice-sheet response (in terms of ~~sea-level~~ sea-level contribution). For example, the crossing of critical thresholds with ongoing warming may result in accelerated mass loss. This is associated with the stepwise change (jump) towards a higher sea-level contribution indicated as (2). (b): Schematic summary of the experimental design used for assessing the ~~long-term~~ long-term committed contribution from the Antarctic Ice Sheet to ~~sea-level~~ sea-level rise with the ~~ice-sheet~~ ice-sheet models PISM and Kori-ULB. Starting with the initialisation of the ~~ice-sheet~~ ice-sheet models to build ~~ice-sheet representations~~ ice-sheet states in the year 1950, historical simulations are run until the year 2015 (~~present-day~~present-day). Using potential future climate trajectories based on CMIP6 under emission pathways SSP1-2.6 (blue) and SSP5-8.5 (red), the transient realized Antarctic ~~sea-level~~ sea-level change is projected until the year 2300. Additional simulations branching off at regular intervals in time determine the ~~sea-level~~ Antarctic sea-level commitment under stabilized climatic boundary conditions sustained over several millennia.

Régional (MARv3.11; Kittel et al., 2021) and the Regional Atmospheric Climate MOdel (RACMO2.3p2; van Wessem et al., 2018) to take into account uncertainties in the representation of ~~present-day~~ present-day Antarctic surface climate (compare Mottram et al., 2021). ~~Both present-day~~ While a recent intercomparison concluded that Antarctic climate is represented reasonably well compared to observations in state-of-the-art RCMs, disagreement between the RCMs with respect to surface mass balance components (such as precipitation and atmospheric temperatures as applied to the ice-sheet models here) exists for some areas (Mottram et al., 2021). Both present-day atmospheric climatologies are involved in the initialisation of each ~~ice-sheet~~ ice-sheet model, resulting in four (initial) ~~ice-sheet model configurations .~~ ice-sheet model configurations (Tab. S2). For ocean temperatures and salinities, ~~present-day~~ present-day observations based on Schmidtko et al. (2014) are used.

To build initial ~~ice-sheet representations~~ ice-sheet states with PISM, a ~~spin-up~~ spin-up approach is applied for each of the ~~atmospheric climatologies~~ historical atmospheric climatologies (around the year 1950, see above) individually. Uncertainties in ~~ice-sheet~~ ice-sheet model parameters are taken into account by running an ensemble of ~~spin-up~~ spin-up simulations and choosing the initial ice-sheet state which fits well to observations of ~~present-day~~ present-day ice thickness, ice velocities and ~~grounding-line~~ grounding-line position. More specifically, starting from Bedmap2 ice thickness and topography (Fretwell et al., 2013), PISM is run for 600 000 years with constant geometry to obtain a thermodynamic equilibrium. Applying the constant ~~historic~~ historical climatic boundary conditions associated with the year 1950, an ensemble of simulations with varying ~~model parameters (guided by recent PISM ensembles; Reese et al., 2023; Albrecht et al., 2020)~~ ice-sheet model parameters (guided by recent PISM ensembles; Albrecht et al., 2020; Reese et al., 2023) is run for several thousand years. Here, we include the SIA enhancement factor ($E_{SIA} \in 1.5, 2$; varied around the reference value of Albrecht et al., 2020) and parameters related to basal sliding, namely the ~~pseudo-plastic~~ pseudo-plastic sliding exponent ($q \in 0.25, 0.5, 0.75$, within the range investigated by Albrecht et al., 2020; Lowry et al., 2021), the till effective overburden fraction ($\delta \in 1.5, 2.0, 2.5$; Bueler and van Pelt, 2015) and the decay rate of till water content ($C \in 7, 10$ mm yr^{-1}, equivalent to the range explored by Albrecht et al., 2020). After 5000 years of simulation, the ensemble members are assessed with a scoring method following Albrecht et al. (2020) and Reese et al. (2020). The scoring method is based on the ~~mean-square-error~~ mean-square-error mismatch of grounded and floating ice area, ice thickness, ~~grounding-line~~ grounding-line location and surface velocity compared to ~~present-day observations (Fretwell et al., 2013; Rignot et al., 2011)~~present-day observations (Rignot et al., 2011; Fretwell et al., 2013). Each indicator is evaluated for the entire Antarctic domain as well as for the Amundsen, ~~Filchner-Ronne~~ Ronne-Filchner and Ross regions individually. The five ~~best-scoring~~ best-scoring ensemble members in terms of the continental as well as the ~~basin-scale~~ basin-scale indicators are continued until reaching 50 000 years of simulation, and ~~experiments~~ simulations are performed with the ~~ice-sheet~~ ice-sheet configuration performing well in the scoring after 50 000 years. Respective ice-sheet model parameters are given in Table S2.

For Kori-ULB, ~~ice-sheet initial conditions~~ initial ice-sheet states and basal sliding coefficients are obtained in an inverse simulation following Pollard and DeConto (2012b) for each of the ~~'historic'~~ historical atmospheric climatologies associated with the year 1950 (as described above). In this inverse ~~procedure~~simulation, the difference to the observed present-day ice thickness (Bedmachine; Morlighem et al., 2020) is minimized by iteratively adjusting the basal sliding coefficients under grounded ice and ~~sub-shelf~~ sub-shelf melt rates under floating ice (Bernales et al., 2017). The ~~resulting sub-shelf~~ optimized

field of basal sliding coefficients in Kori-ULB is characterized by high basal sliding coefficients at the ice-sheet margins, turning into regions of low slipperiness (low basal sliding coefficients) towards the interior of West Antarctica. It thus differs from the basal friction experienced by the Antarctic Ice Sheet in simulations with PISM, where overall slippery bed conditions in the interior of marine subglacial basins are found, given the parameterized, bed-elevation dependent material properties of the subglacial till (in particular, the till friction angle; Sect. 2.1). These inter-model differences in basal friction linked to the applied initialization approaches are expected to influence the ice-sheet response. The resulting sub-shelf melt rates may ~~therefore~~ be interpreted as ~~balance sub-shelf~~ balanced sub-shelf melt rates and are independent of the oceanic boundary conditions (forcing), while the ~~ice-sheet~~ ice-sheet states are in ~~steady-state with the initial~~ steady-state with the historical atmospheric climatologies. Applying constant ~~historic ocean and atmospheric~~ historical atmospheric and oceanic boundary conditions associated with the year 1950, a short relaxation is run for 10 years after the ice-sheet model initialisation and before the historical simulation. This limits an initial shock that may ~~results~~ result from the transition from the ~~balance sub-shelf~~ balanced sub-shelf melt rates derived during the transient ~~spin-up~~ inverse simulation to the imposed ~~sub-shelf~~ sub-shelf melt parameterisation scheme. The two initial ~~ice-sheet~~ ice-sheet states resulting from the ~~nudging spin-ups~~ inverse simulation are therefore in ~~quasi-equilibrium. They compare wellto~~ quasi-equilibrium.

Given that we include two common ways of initializing ice-sheet models (compare e.g. Seroussi et al., 2019, 2020), we sample uncertainties associated with the choice of the initialization approach. While an inverse simulation allows to reproduce the observed present-day ice-sheet geometry well, the resulting parameter fields (such as basal sliding coefficients in Kori-ULB) may compensate for errors or uncertainties in other ice-sheet processes (Aschwanden et al., 2013; Berends et al., 2023b). In addition, it is assumed that the field obtained in the inverse simulation to match present-day observations does not change in the future. In contrast, in the simulated ice-sheet state resulting from a spin-up the ~~observed ice dynamics, ice geometry, and grounding-line position (compare Fig.~~ ice-sheet variables may be modelled in a consistent way, but its geometry might differ from the observed ice sheet. It is the result of the covered ice-sheet physics in the ice-sheet model for a set of uncertain parameters, without any nudging.

The simulated grounding-line position and ice thickness of the initial ice-sheet states are compared to present-day observations in Figure S1~~), and are within the range of the ISMIP6 models (Seroussi et al., 2019)~~. As a result of the inverse simulation, the grounding-line position and ice thickness compare well to present-day observations in the initial ice-sheet states for Kori-ULB (Fig. S1a and c). With the spin-up approach applied in PISM, the initial ice-sheet states are characterized by larger ice thickness differences compared to present-day observations (Fig. S1b and d). Overall, ice in West Antarctica and in some coastal regions in East Antarctica (e.g. in Dronning Maud Land, upstream of Amery Ice Shelf and in Wilkes Land) is thicker than observed at present (comparable to Reese et al., 2023), while the ice thickness in the interior of East Antarctica is underestimated. In addition, the grounding line in the Siple Coast area (and in the catchment draining Ronne-Filchner Ice Shelf for the MAR atmospheric climatology) is located upstream of the observed grounding line in the present-day (Fig. S1 b and d), as previously seen in an ice-sheet model initialisation in a spin-up approach, e.g., Reese et al. (2023) and Sutter et al. (2023). These differences should be taken into account when interpreting the simulated long-term evolution of the Antarctic Ice Sheet.

2.2.3 Forcing and boundary conditions over the historical period and until 2300

Starting from the initial ~~ice-sheet configurations~~ ice-sheet states and climate conditions of the year 1950 described above, we run historical simulations for the time period from 1950 to 2015 (Fig. 1). Changes in ~~oceanic and atmospheric conditions~~ atmospheric and oceanic conditions over the historical period are derived from NorESM1-M, as recommended within ISMIP6 (Barthel et al., 2020; Nowicki et al., 2020). The ~~corresponding ice-sheet response (as determined by PISM and Kori-ULB) over the historical period is shown in Figure S2. The~~ atmospheric and oceanic forcing conditions until the year 2300, which are applied to the ~~ice-sheet~~ ice-sheet models for studying the future evolution of the Antarctic Ice Sheet, rely on a subset of ~~state-of-the-art~~ state-of-the-art GCM projections available within CMIP6 (MRI-ESM2-0, UKESM1-0-LL, CESM2-WACCM, and IPSL-CM6A-LR). We apply climate forcing under ~~both~~ the Shared Socioeconomic Pathways ~~SSP5-8.5 and~~ SSP1-2.6 and SSP5-8.5. The selection of CMIP6 GCMs was guided by the limited availability of extended climate projections until the year 2300 within ScenarioMIP (O'Neill et al., 2016), while the climate sensitivity of the available ~~GMCs~~ GCMs (Meehl et al., 2020) and their performance in comparison with observations ~~(e.g., Beadling et al., 2020; Purich and England, 2021; Bracegirdle et al., 2020)~~ (e.g. Beadling et al., 2020; Purich and England, 2021; Bracegirdle et al., 2020) were considered as secondary criteria.

Following Nowicki et al. (2020), ~~spatially-varying atmospheric (~~spatially-varying atmospheric (*~~near-surface~~ near-surface air temperature*) as well as oceanic (*salinity* and *temperature*) anomalies with respect to the ~~1995–2014~~ 1995-2014 mean climatology are ~~directly~~ derived from NorESM1-M over the historical period as well as from projections of the selected CMIP6 GCMs until the year 2300. Note that, for *precipitation*, ratios (instead of anomalies) with respect to the ~~1995–2014~~ 1995-2014 mean precipitation are determined to avoid 'negative' absolute precipitation ~~(e.g., Goosse et al., 2010, Equation 30)~~ (e.g. Goosse et al., 2010, Equation 30). The respective anomalies are added to the ~~present-day~~ present-day climatologies for the atmosphere (MAR, RACMO) and the ocean (Schmidtko et al., 2014). Thus, the resulting forcing matches ~~present-day~~ present-day climate conditions in the ~~1995–2014~~ 1995-2014 reference period (as in Reese et al., 2023). For the ~~oceanic~~ ocean properties, yearly averaged forcing is applied to the ~~ice-sheet~~ ice-sheet models. Missing values for the oceanic forcing on the continental shelf (arising due to the coarse resolution of CMIP6 GCMs) and in currently ~~ice-covered~~ ice-covered regions are filled following Kreuzer et al. (2021), i.e., by averaging over all existing values in neighbouring cells. In ~~contrast, monthly~~ addition, the ocean properties derived from CMIP6 GCMs are linearly interpolated to the basin-averaged continental shelf depth (Kreuzer et al., 2021) to determine sub-shelf melt (see below). Monthly forcing is used at the interface of the ice sheet to the atmosphere (as in Golledge et al., 2019).

Surface melt and runoff are determined from monthly atmospheric temperature and precipitation (i.e., accounting for the seasonal cycle) using a ~~positive-degree-day~~ positive-degree-day (PDD) scheme (Reeh, 1991). The amount of PDD follows the approach presented in Calov and Greve (2005), with a default value for the standard deviation of $\sigma = 5$ °C and $\sigma = 4$ °C for PISM and Kori-ULB, respectively. Snow accumulation rates are derived from precipitation via an atmospheric temperature threshold with a linear transition between snow and rain. In Kori-ULB, natural variability is considered when determining snow accumulation rates (similar to the calculation of the amount of ~~positive-degree-days~~positive-degree-days) using a standard deviation of $\sigma = 3.5$ °C. Melt coefficients of 3 mm w.e. per PDD for snow and 8 mm w.e. per PDD for ice are used in both

~~ice–sheet~~ ice-sheet models after a comparison to MAR estimates until the year 2100 (Kittel et al., 2021; Coulon et al., 2024). A constant fraction of surface melt refreezes in PISM (Reeh, 1991), while Kori-ULB applies a simple thermodynamic parameterisation of the refreezing process (Huybrechts and De Wolde, 1999; Coulon et al., 2024). Computing surface melt and runoff in a PDD approach follows ~~Garbe et al. (2020) and DeConto et al. (2021)~~ DeConto et al. (2021) and Garbe et al. (2020), likewise studying the future Antarctic ~~response to changing environmental conditions and the ice–sheet stability on multi–millennial~~ Ice Sheet response to a changing climate and the ice-sheet stability on multi-millennial timescales. Applying the surface mass balance determined by RCMs, which are in turn forced by ~~climate projections of GCMs~~GCM climate projections, would be an alternative approach for projecting Antarctic ~~sea–level~~ sea-level change. However, surface mass balance estimates from RCMs are not yet available beyond the end of this century and may be biased by the use of a static ~~ice–sheet~~ ice-sheet geometry neglecting, for example, the surface ~~melt–elevation~~ melt-elevation feedback (Kittel et al., 2021).

To account for the **surface ~~melt–elevation~~ melt-elevation feedback**, the ~~near–surface~~ near-surface air temperature is corrected for changes in ~~ice–sheet~~ the ice-sheet surface elevation. More specifically, air temperatures T_{forcing} provided to the ~~ice–sheet~~ ice-sheet models are shifted linearly with a change in surface elevation Δh as

$$T = T_{\text{forcing}} + \Gamma \Delta h \tag{5}$$

following the atmospheric lapse rate Γ of 8°C / km.

~~Sub–shelf~~ Sub-shelf melt rates are computed by using the Potsdam ~~Ice–shelf~~ Ice-shelf Cavity mOdel (PICO; Reese et al., 2018). PICO calculates ~~sub–shelf~~ sub-shelf melt rates from ~~far–field~~ far-field salinities and temperatures and parameterizes the overturning circulation in ~~ice–shelf cavities. Ocean properties derived from CMIP6 GCMs are linearly interpolated to the continental shelf depth (Kreuzer et al., 2021) to be applicable to PICO . The~~ ice-shelf cavities. The values of the PICO overturning strength parameter C and the turbulent heat exchange coefficient γ_T^* are an individual choice for each ice-sheet model to match sub-shelf melt sensitivities and / or observed melt rates. $C = 3\text{x}10^6$ m^6 s^{-1} kg^{-1} and ~~the turbulent heat exchange coefficient~~ $\gamma_T^* = 7\text{x}10^{-5}$ m s^{-1} (with correction of ocean properties of Schmidtko et al. (2014) to match observed ~~present–day~~ present-day melt rates from Adusumilli et al. (2020)) are used for PISM ~~experiments~~simulations, as they have been found to fit melt sensitivities well (Reese et al., 2023). For Kori-ULB ~~experiments~~simulations, the overturning strength and the turbulent heat exchange coefficient are chosen as $C = 1\text{x}10^6$ m^6 s^{-1} kg^{-1} and ~~$\gamma_T = 4\text{x}10^{-5}$~~ $\gamma_T^* = 4\text{x}10^{-5}$ m s^{-1}, respectively.

3 Results

We here present the transient response of the Antarctic Ice Sheet over the historical period (Sect. 3.1) and to a range of possible future climate trajectories until ~~the year~~ 2300 (Sect. 3.2) along with the associated committed ~~ice–sheet evolution on multi–millennial~~ ice-sheet evolution on multi-millennial timescales (Sect. 3.3). The dependency of the committed ~~sea–level~~ Antarctic sea-level contribution on the ~~environmental~~ climate conditions in Antarctica sustained over several thousands of years after their stabilization at different points in time during the next centuries is assessed in Sect. 3.4.

3.1 ~~Transient ice–sheet response until 2300~~Historical ice-sheet evolution

~~Following the lower–emission pathway SSP1-2.6 results in a sea–level change ranging~~ The pattern of observed present-day rates of ice-thickness change (e.g. Smith et al., 2020) is overall captured by both ice-sheet models in response to the historical NorESM1-M climate trajectory from 1950 to 2015 (Fig. 2a - c), with a thinning in the Amundsen and Bellingshausen Sea region and the Antarctic Peninsula and a thickening in the ice-sheet interior. The magnitude of ice-sheet thinning in the Amundsen Sea Embayment is, however, underestimated compared to present-day observations in the historical simulations with PISM presented here (Fig. 2a and c). In addition, we find ice loss for Ross, Ronne-Filchner and Amery ice shelves in PISM in contrast to present-day observations (Fig. 2a and c).

The evolution of the continent-wide integrated surface mass balance is relatively similar for both ice-sheet models, but occurs on a higher, though still within RCM uncertainties, level in PISM than in Kori-ULB (Fig. 2d). While sub-shelf melt increases in PISM from about 300 Gt yr^{-1} in 1950 towards 1100 Gt yr^{-1} in 2015 at the lower end of present-day observations (Fig. 2e, solid lines), the basal mass balance is on the order of the observational record in Kori-ULB over the entire historical period, slightly exceeding its upper end in 2015 with about 1800 Gt yr^{-1} (Fig. 2e, dashed lines). The continent-wide aggregated sub-shelf melt rates observed in present-day are thus reproduced with both sets of PICO parameters (compare Sect. 2.2.3), but they result in different sensitivities of sub-shelf melt rates to ocean temperature changes over the historical period (Fig. 2e; Reese et al., 2023) .

Mass loss in the Amundsen Sea Embayment dominates the overall observed ice sheet mass changes in Antarctica to date (Otosaka et al., 2023). Given the lower magnitude of ice-sheet thinning of Pine Island and Thwaites glaciers in PISM, and stronger sub-shelf melt in Kori-ULB, we find diverging ice-sheet trajectories with both ice-sheet models in terms of the Antarctic sea-level contribution over the **historical period** from 1950 to 2015: Kori-ULB shows an integrated mass loss with a sea-level contribution of about +4 mm in 2015 (Fig. 2f, dashed lines), while the ice sheet overall gains mass equivalent to a sea-level change ranging between -4 mm and -6 mm in PISM (Fig. 2f, solid lines; within spread of recent ensemble of historical ice-sheet tr .

In the future evolution of the Antarctic Ice Sheet determined by PISM (Sect. 3.2 - 3.4), changes in the regions of Ross and Ronne-Filchner ice shelves could thus be overestimated, while the lower thinning rates over the historical period in the Amundsen Sea Embayment could suggest a reduced sensitivity of Thwaites and Pine Island glaciers to changes in Antarctic climate in these simulations.

3.2 Future transient ice-sheet response until 2300

By the end of this century, the projected Antarctic sea-level contribution varies between -5.0 cm to +8.0 cm ~~by the~~ and -6.0 cm and +6.0 cm compared to present-day in response to SSP1-2.6 and SSP5-8.5 climate trajectories, respectively (Fig. 3a and c, Tab. 1). Projected ice-sheet changes by 2100 are comparable across emission pathways (Fig. 3; in line with Lowry et al., 2021; Edwards et a , given a very similar evolution of Antarctic climate at least during the first half of the 21st century (Fig. 4). The sea-level contribution due to mass balance changes of the Antarctic Ice Sheet projected by Kori-ULB and PISM by the end of this century

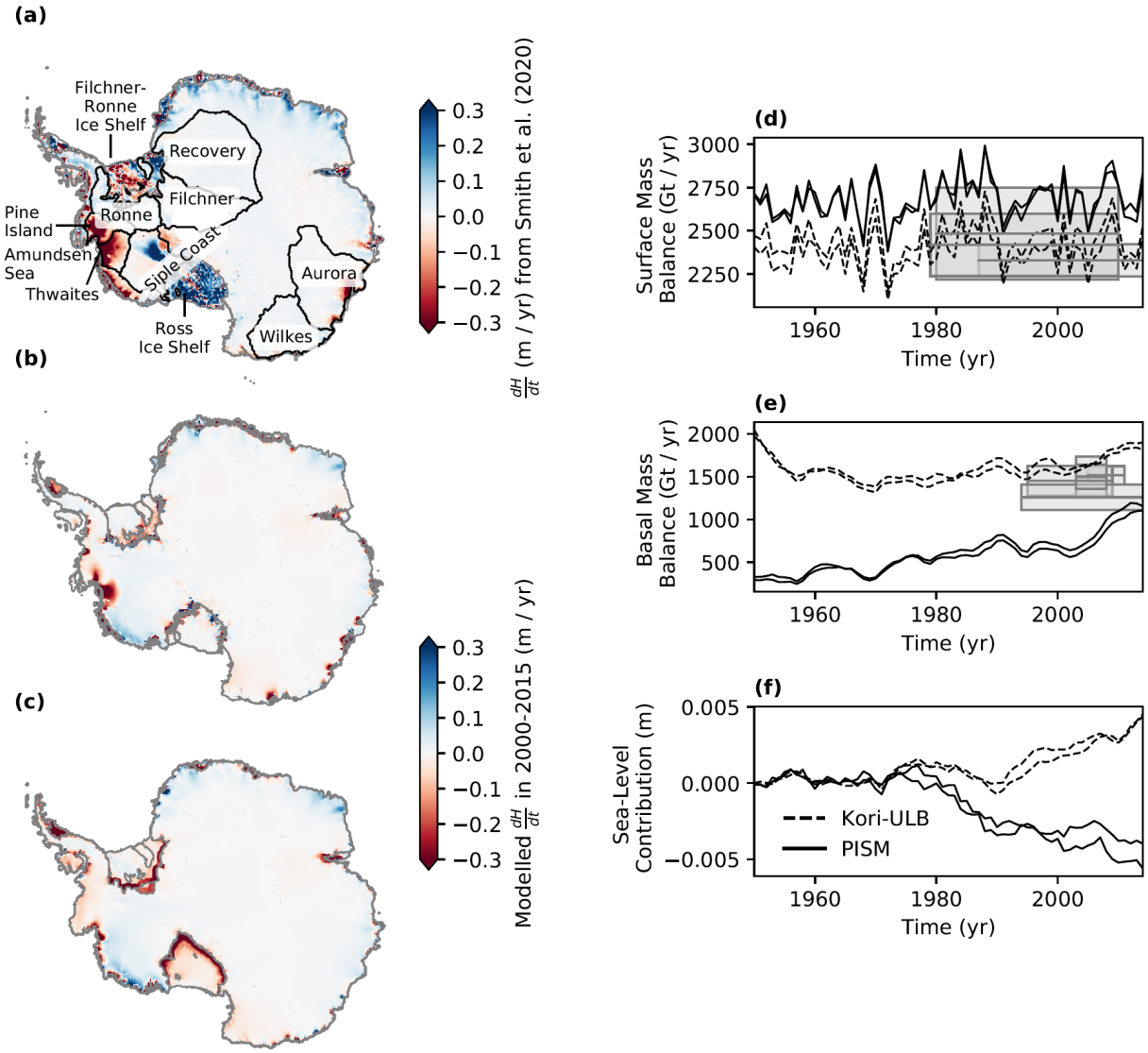

Figure 2. **Trajectories of the Antarctic Ice Sheet over the historical period** from 1950 to 2015. (a) - (c): Rates of ice-thickness change as observed based on Smith et al. (2020) (a) and as determined by the ice-sheet models Kori-ULB (b) and PISM (c) in response to historical changes in Antarctic climate derived from NorESM1-M. The modelled ice-thickness change is averaged across the ice-sheet model configurations associated with atmospheric climatologies based on MAR and RACMO (Tab. S2). (d) - (e): Evolution of the Antarctic Ice Sheet as determined by the ice-sheet models Kori-ULB (dashed lines) and PISM (solid lines) using atmospheric climatologies based on MAR and RACMO in terms of the surface mass balance (d), sub-shelf melt (e), and sea-level contribution (f), based on volume above floatation. Observations of the ice-sheet mass balance components (as in Coulon et al., 2024) are given by grey boxes (indicating the time period and uncertainties of the respective observations), where the solid line shows the mean.

and from is also within the range of recent estimates by ISMIP6, ranging from -9 cm to +30 cm under higher-emission pathways and from -1.4 cm to +15.5 cm under lower-emission pathways (Seroussi et al., 2020; Payne et al., 2021). The simulated trends of ice-sheet changes over the historical period are continued in these projections over this century with both ice-sheet models. That is, Kori-ULB projects a positive sea-level contribution (Fig. 3a and c, dashed lines). PISM projects a sea-level drop by 2100 compared to present-day (Fig. 3a and c, solid lines).

Following the **lower-emission pathway SSP1-2.6** to 2300 results in a sea-level change ranging from -0.2 m to +0.5 m in 2300 compared to present-day (Fig. 2a; 3a, Tab. 1). Therein, Kori-ULB projects a positive sea-level contribution for this lower-emission scenario (steadily increasing Antarctic contribution to sea-level rise (Fig. 3a, dashed lines), while PISM projects a sea-level drop (. While some PISM ice-sheet trajectories show the onset of mass loss after an initial mass gain (e.g. for CESM2-WACCM climate, indicated in blue), the Antarctic sea-level contribution projected by PISM in 2300 compared to present-day remains negative (Fig. 3a, solid lines).

The overall sign of ice-sheet ice-sheet mass changes contributing to a change in sea-level sea level depends on the balance between the dynamic response to sub-shelf melting and ice-shelf sub-shelf melting and ice-shelf thinning and the surface mass balance-, driven by changes in Antarctic climate (Fig. 4): We find that, with a projected Antarctic-averaged atmospheric warming of up to 3.6°C in 2300 (Fig. 4a, Tab. S1), the integrated surface mass balance remains positive for both ice-sheet models until 2300 under SSP1-2.6 and on its present-day level until 2300 for both ice-sheet models under this lower-emission pathway, with strong GCM-dependent variability (Fig. S3a). However, the response in dynamic discharge contributing to a sea-level increase on centennial timescales is higher in 4b). The evolution of sub-shelf melt to 2300 is overall consistent across Kori-ULB and PISM and follows the characteristics of the projected changes in circumantarctic ocean temperatures by each GCM (Fig. 4d and e): Abrupt circumantarctic ocean warming to 2050 in UKESM-1-0-LL and IPSL-CM6A-LR (of about 0.5°C and 0.3°C, respectively) results in a strong initial increase in sub-shelf melt (Fig. 4d and e, grey and pink). In contrast, a steady rise in CESM2-WACCM circumantarctic ocean temperatures to 0.7°C in 2300 is accompanied by a continuous increase in sub-shelf melt (Fig. 4d and e, blue). Overall, the magnitude of sub-shelf melt is higher for projections by Kori-ULB (with ice-sheet thinning in the Amundsen Sea Embayment extending inlanddashed lines) compared to PISM (solid lines), following the respective levels reached at the end of the historical period (Fig. 4e, Fig. S4–S5)2e). The response in dynamic discharge contributing to a sea-level increase is thus stronger in Kori-ULB than in PISM (see in the Amundsen Sea Embayment and the East Antarctic Totten Glacier (Fig. S6–S7 for comparison3b), explaining the diverging sea-level sea-level contribution under SSP1-2.6 until 2300.

Under climate trajectories following the With significant changes in Antarctic climate from 2100 onwards under the **higher-emission pathway SSP5-8.5emission pathway** , the Antarctic ice loss varies between -6.0 cm and +6.0 cm sea-level equivalent by the end of this century, increasing (Fig. 4a and d), Antarctica's sea-level contribution increases to +0.7 —- +3.1 m by 2300 (Fig. 2b; 3c, Tab. 1). The initial sea-level drop by 2100 is again found in simulations from PISM and can be attributed to increasing snowfall with warming, which dominates the ice-sheet mass balance until the end of this century.Simulations by Kori-ULB show an earlier grounding-line retreat in the Amundsen Sea Embayment, outweighing the initial increase in the integrated surface mass balance and resulting in a positive sea-level contribution already during the 21st century. Beyond

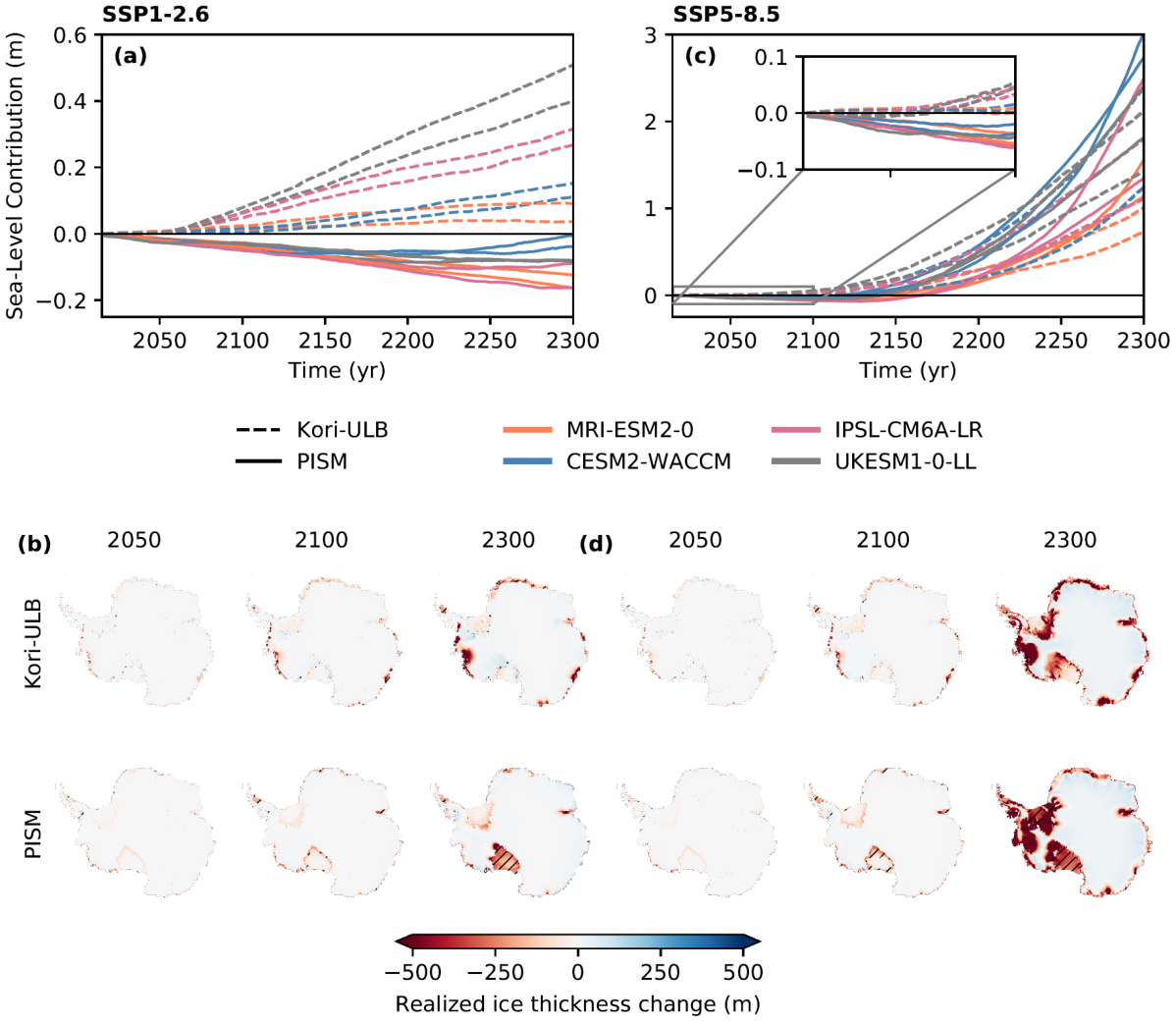

Figure 3. **Projected Antarctic ice loss on multi-centennial timescales** in response to changing climate conditions under emission pathways SSP1-2.6 (left column) and SSP5-8.5 (right column). (a) and (c): Transient sea-level contribution (in meters sea-level equivalent) from Antarctica until 2300 in response to changing climate conditions as projected by four CMIP6 GCMs (given by the colour), as determined by the ice-sheet models Kori-ULB (dashed lines) and PISM (solid lines). (b) and (d): Mean ice-thickness change in the years 2050, 2100 and 2300, as determined by the ice-sheet models Kori-ULB (uppper row) and PISM (lower row). The ice-thickness change is averaged across the applied GCMs and the respective ice-sheet model configurations (Tab. S2). A potential loss of ice shelves is indicated by hatches.

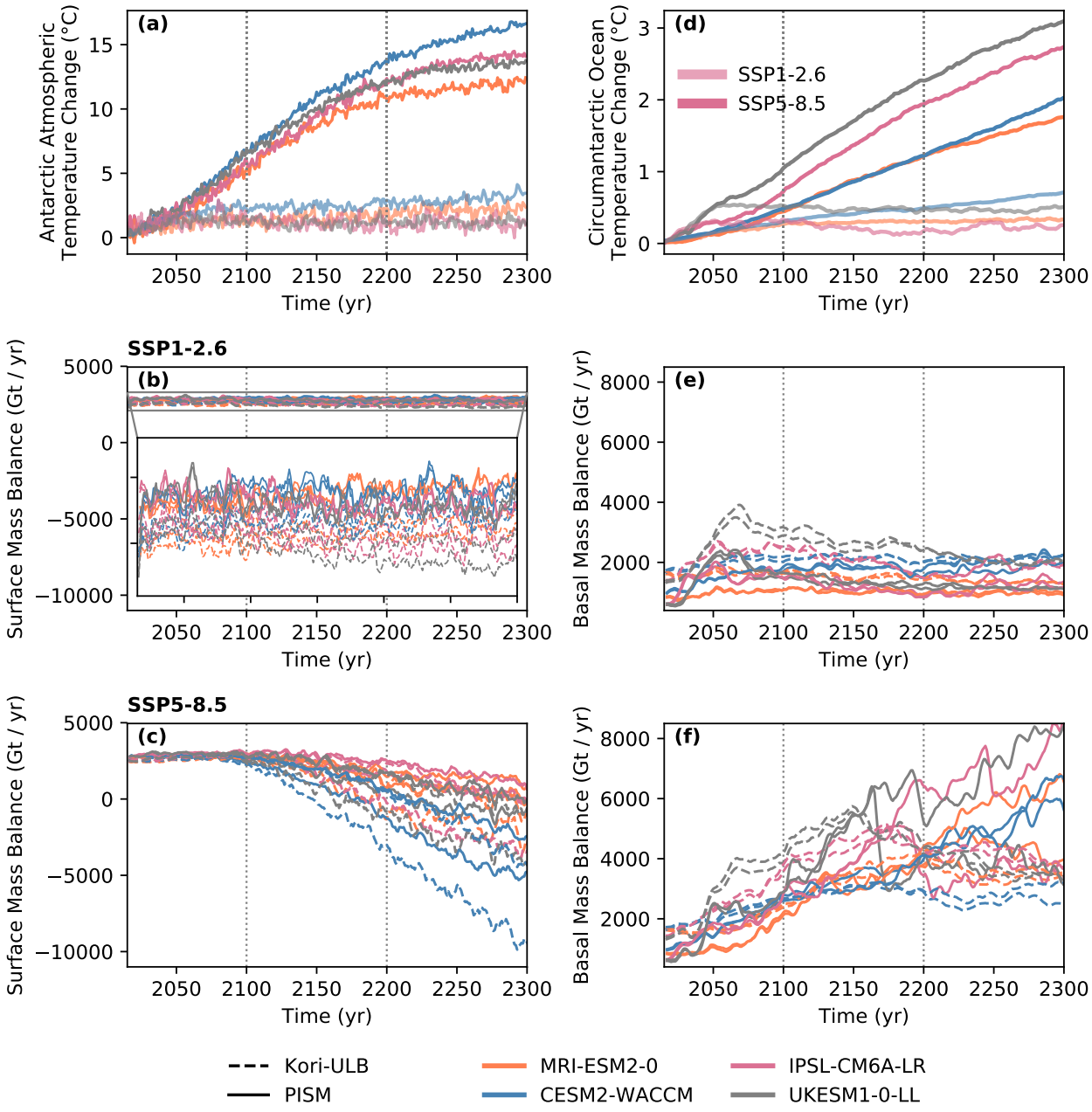

Figure 4. **Future Antarctic climate and projected ice-sheet mass balance components on multi-centennial timescales**, under emission pathways SSP1-2.6 (transparent colors / upper row) and SSP5-8.5 (opaque colors / lower row) for four CMIP6 GCMs (given by the colour) in terms of (a): Antarctic-averaged atmospheric temperature change, (b) and (c): Surface mass balance, (d): Circumantarctic oean temperature change, and (e) and (f): Sub-shelf melt, as determined by the ice-sheet models Kori-ULB (dashed lines) and PISM (solid lines).

2100 and over the course of the following two centuries, the grounding line in the Amundsen Sea Embayment may retreat substantially transient contribution of the Antarctic Ice Sheet to sea-level change until 2300 is in line with the results of e.g. Golledge et al. (2015) (showing an ice loss of +1.6 m - +2.96 m sea-level equivalent under RCP8.5) and is consistent with the Antarctic contribution to sea-level rise reported in the latest IPCC assessment of -0.3 m - +3.2 m sea-level equivalent (Fox-Kemper et al., 2021). It is caused by pronounced mass loss of the West Antarctica Thwaites and Pine Island glaciers as well as upstream of Ronne-Filchner and Ross ice shelves projected with both ice-sheet models (Fig. 3b, realized)depending on the sensitivity of the initial state to the imposed ocean warming (being strongest under IPSL-CM6A-LR and UKESM1-0-LL; d). The grounded ice-sheet response is accompanied by thinning of the major Antarctic ice shelves including the Ross and Ronne-Filchner ice shelves, that are (in PISM only) eventually lost sequentially by 2150 and 2300, respectively (Fig. S8–S11 show the individual ice–sheet response determined by both ice–sheet models to the different centennial climate trajectories). 3d).

At the same time, the integrated surface mass balance starts to decrease and may even turn negative for turn negative during the next centuries with strong atmospheric warming (Fig. S3b). The major ice shelves including the Ross Ice Shelf as well as the Filchner–Ronne Ice Shelf thin, in particular near the grounding line, and are (in PISM only)even lost sequentially by 2150 and2300, respectively 4c). This pattern is evident in projections by both Kori-ULB and PISM. The decline in the ice sheet's surface mass balance is most pronounced for CESM2-WACCM (Fig. 4a and c, blue), projecting an Antarctic temperature increase of more than 15°C beyond 2200 and, thereby, covering atmospheric warming ranges that are not found in any of the other GCMs (Fig. 3b, realized; Fig. S10–S11). As a consequence of reduced buttressing, the grounding line in the Siple Coast region starts to show retreat.

Overall, the global mean sea–level contribution due to mass balance changes of the Antarctic Ice Sheet projected by PISM and Kori-ULB on centennial timescales 4a, blue, Tab. S1). Following the progressing ocean warming under SSP5-8.5 (reaching an ocean temperature change of up to 3°C for UKESM1-0-LL in 2300; Fig. 4d), sub-shelf melt continues to increase beyond 2100 (Fig. 4f). It eventually levels off after 2150 with the loss of West Antarctic ice shelves (Fig. 4f, also compare Coulon et al., 2024) . An additional increase of sub-shelf melt beyond 2150 occurs in some PISM simulations (Fig. 2a and b; Tab. 1)is within the range of recent estimates: by the end of this century, estimates by the Ice Sheet Model Intercomparison Project ISMIP6 range from -9 cm to +30 cm under higher–emission pathways and from -1.4 cm to +15.5 cm under lower–emission pathways (Seroussi et al., 2020; Payne et al., 2021). The forced response of the Antarctic Ice Sheet until 2300 is 4f, solid lines) with a substantial contribution from smaller ice shelves in the Ross and Amundsen Sea Embayment formed during the grounding-line retreat in combination with the chosen PICO parameters (characterized by a relatively higher melt sensitivity; Reese et al., 2023) , overtaking magnitudes of aggregated sub-shelf melt determined in Kori-ULB (Fig. 4f, dashed lines).

In summary, while the ice-sheet trajectories under the SSP1-2.6 scenario are still influenced by the simulated historical trends and differences in ice-sheet modelling choices (Seroussi et al., 2023), we find that climate drivers dominate the projected multi-centennial ice-sheet changes under the higher-emission pathway SSP5-8.5. In particular, in line with the results of both Golledge et al. (2015) and Chambers et al. (2022) and is consistent with the range of -0.3 m – +3.2 m sea–level equivalent given as estimate for the Antarctic sea–level contribution in the latest IPCC assessment (Fox-Kemper et al., 2021)Coulon et al. (2024)

, our projections indicate that the atmosphere becomes an amplifying driver of Antarctic mass loss beyond the end of this century, irrespective of the ice-sheet model.

3.3 ~~Long–term~~ Long-term committed ~~ice–sheet~~ ice-sheet evolution over the next millennia

~~Oceanic and atmospheric~~ Atmospheric and oceanic warming projected for the upcoming centuries may trigger changes in the dynamics and geometry of the Antarctic Ice Sheet that are not realized on the same timescales (as the forcing), but unfold thereafter over the course of the following millennia, due to ~~ice–sheet~~ ice-sheet inertia and nonlinear feedbacks. After determining the transient realized ~~sea–level response~~ sea-level contribution over the next centuries (Sect. 3.2), we investigate this ~~long–term~~ long-term committed evolution of the Antarctic Ice Sheet by ~~keeping environmental conditions constant~~ stabilizing climatic boundary conditions at different points in time and letting the ice sheet evolve over several millennia (~~see~~ compare Sect. 2.2.1; Fig. 1).

~~Our simulations confirm~~ The bulk of our simulations shows that sea level may keep rising for centuries to millennia to come even if warming is ~~kept at a constant level (Fig. 2c and d, consistent with, e.g., Winkelmann et al., 2015; Van Breedam et al., 2020)~~ stabilized (Fig. 5a - d; consistent with, e.g. Winkelmann et al., 2015; Van Breedam et al., 2020). The delayed response of the Antarctic Ice Sheet on millennial timescales gives rise to a substantial ~~gap~~ difference between the transient *realized* (described in the previous Sect. 3.2) and the ~~long–term~~ long-term *committed* Antarctic ~~sea–level~~ sea-level contribution, being more than the 100 (10)~~–fold of the sea–level~~ -fold of the sea-level change projected by ~~the year~~ 2100 (2300) (~~compare Figure 2a – d;~~ Fig. 3, Fig. 5, Tab. 1). ~~This commitment gap (Winkelmann et al., in review) depends on the specific climate trajectory and the warming levels that are reached at the respective (branchoff) point in time.~~

We find a sharp increase in the Antarctic ~~sea–level~~ sea-level contribution over the next millennium, irrespective of the emission ~~scenario.~~pathway (Fig. 5a - d).

3.3.1 Antarctic sea-level commitment under lower-emission pathway SSP1-2.6

When following the ~~**lower–emission**~~ **lower-emission pathway SSP1-2.6**, the ~~ice–sheet~~ ice-sheet response levels off after a peak in the rate of Antarctic ice loss within this millennium or at the latest by the beginning of the following millennium ~~. It then stabilizes at qualitatively different stages of ice–sheet decline~~ (Fig. 5a and c). Some of the ice-sheet trajectories eventually show a decline in the Antarctic sea-level contribution on multi-millennial timescales (Fig. ~~2c and e).In some cases, abrupt~~ 5a and c; e.g. for sustained MRI-ESM2-0 climate indicated in orange), with a thickening trend upstream of Ross Ice Shelf (in Kori-ULB only, see below) and in the ice-sheet interior towards the year 7000, outweighting the initial mass loss. Abrupt changes in the Antarctic ~~sea–level contribution occur delayed (compared to other trajectories under the lower–emission pathway)in PISM~~sea-level contribution may also occur delayed for MRI-ESM2-0 climate (Fig. 5a and c, orange), with a lag of up to multiple millennia to the onset of the perturbation in ~~ice–sheet boundary conditions . These ice–sheet trajectories , however, eventually converge to the same magnitude of sea–level contribution on multi–millennial timescales.In~~ climatic boundary conditions in PISM simulations. This delay is related to a later onset of substantial grounding-line retreat in the Amundsen

Sea Embayment in these simulations with comparably smaller projected oceanic changes in MRI-ESM2-0 (compared to other climate trajectories under the lower-emission pathway; Fig. 4a and d).

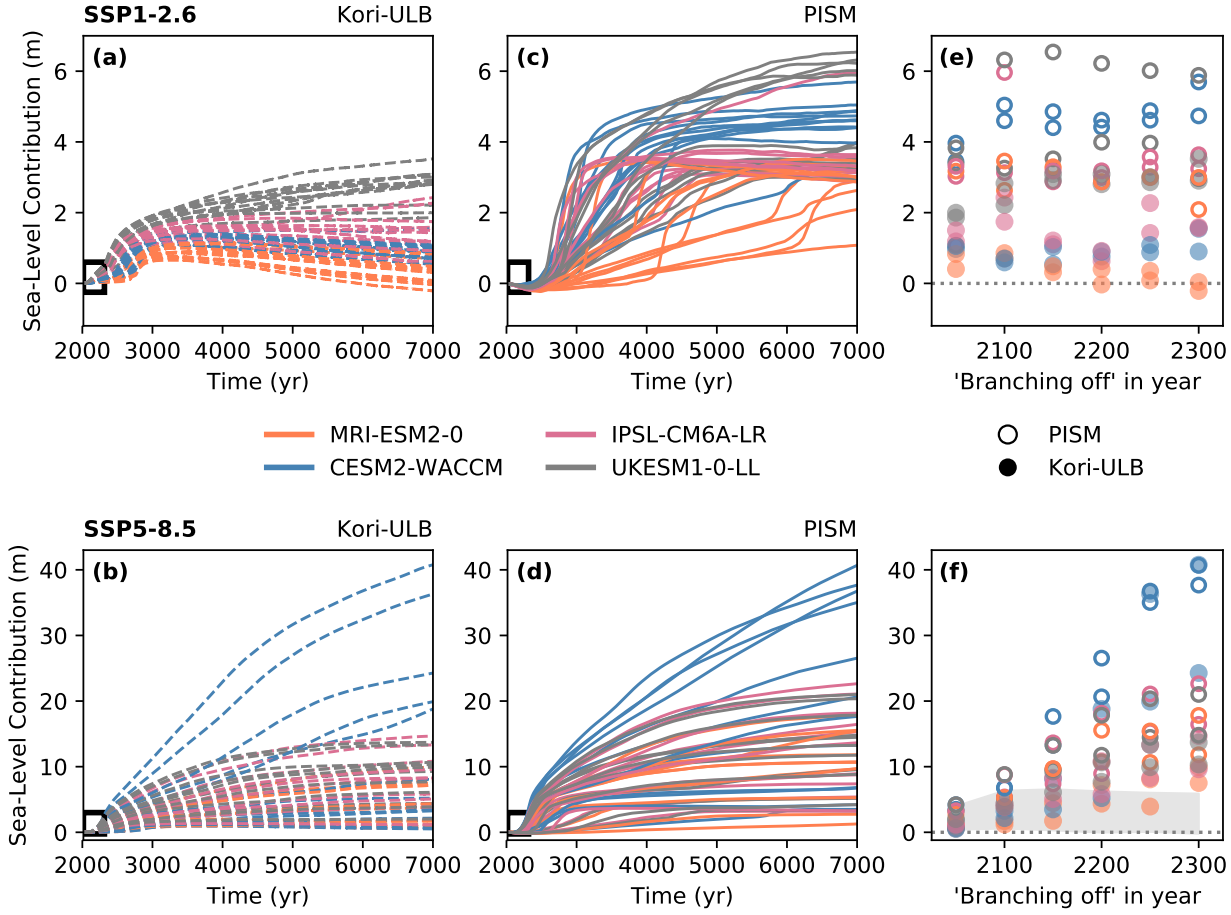

Figure 5. Projected Antarctic ice loss on multi-millennial timescales in response to changing climate conditions under emission pathways SSP1-2.6 (upper row) and SSP5-8.5 (lower row) as projected by four CMIP6 GCMs (given by colour). (a) - (d): Antarctic sea-level contribution (in meters sea-level equivalent) until the year 7000 to warming potentially reached at different points in time throughout the next centuries, as determined by the ice-sheet models Kori-ULB (dashed lines, left column) and PISM (solid lines, right column). (e) and (f): Committed Antarctic sea-level contribution in the year 7000 when stabilizing Antarctic climate at different points in time (that is, 'branching off' in the years 2050, 2100, 2150, 2200, 2250 and 2300; compare Sect. 2.2.1 and Fig. 1). Filled and open markers correspond to the long-term sea-level change determined by the ice-sheet models Kori-ULB and PISM, respectively. For comparison of the committed sea-level change under both emission pathways, the range of Antarctic ice loss by the year 7000 under SSP1-2.6 (e) is reported by the light grey shade in (f).

Irrespective of the timing of abrupt ice loss, the multi-millennial ice-sheet trajectories eventually are characterized by qualitatively different stages of ice-sheet decline with a very similar magnitude of the committed Antarctic sea-level contribution

determined by the applied GCM forcing for each ice-sheet model (Fig. 5a and c). That is, in our simulations under the SSP1-2.6 pathway, we do not find a strong dependency of the ~~long-term ice-sheet configuration reached in~~ long-term Antarctic sea-level commitment in the year 7000 on the point in time after which climatic boundary conditions are ~~kept constant~~ stabilized (Fig. ~~2e;~~ 5e, Fig. ~~3a, committed~~6a). When sustaining the warming level potentially reached until ~~year~~ 2050, ~~global mean sea-level~~ sea level may increase by +0.4 m to +~~3.8~~4.0 m on the ~~long-term~~ long term (Fig. ~~2e;~~ 5e, Tab. 1). For climatic boundary conditions representative of the end of this century and thereafter, Antarctic mass changes range between -0.2 m and +~~6.3 m of sea-level~~ 6.5 m sea-level equivalent, which unfolds over the next millennia (Fig. ~~2e;~~ 5e, Tab. 1). ~~The applied GCM forcing determines~~

This strong modulation of the magnitude of the committed Antarctic ~~sea-level contribution under SSP1-2.6 at a given (branchoff) point in time~~ sea-level contribution by the applied GCM forcing for each ice-sheet model (Fig. 5e, Fig. S2) is linked to substantial differences in the trajectories of atmospheric to oceanic warming between the applied GCMs under this lower-emission pathway (Fig. ~~2e). For both ice-sheet models , stronger ocean warming in the Wilkes basin projected by UKESM1-0-LL and~~ 4a and d). Their impact on the ice-sheet response plays out and becomes evident on longer timescales (on the order of millennia).

Across both ice-sheet models and all GCM forcings, we find a long-term recession of the grounding lines in the Amundsen Sea Embayment under this lower-emission pathway, with a connection from Pine Island Glacier to Ronne Ice Shelf (Fig. 6a).

Pronounced grounding-line retreat in the East Antarctic Wilkes subglacial basin in both Kori-ULB and PISM, potentially locked-in by 2050, adds up to +1.5 m to the long-term sea-level change (Fig. 5e, grey and pink, Fig. 6a). Long-term ice loss from this region is promoted by the abrupt and stronger ocean warming projected by IPSL-CM6A-LR and (especially) UKESM1-0-LL in the first half of this century compared to the other GCMs ~~may promote grounding-line retreat in this region (compare~~ (Fig. 4d, Fig. S2). The grounding line in Wilkes subglacial basin experiences only very limited or no retreat under the other GCM climate trajectories in Kori-ULB and PISM simulations (Fig. ~~S12–S15), giving rise to the upper limit of long-term ice loss found under the lower-emission pathway~~S2), respectively, despite stronger atmospheric warming levels when following CESM2-WACCM climate under the lower-emission pathway. This is linked to the less abrupt, more gradual change in ocean temperatures compared to UKESM1-0-LL and IPSL-CM6A-LR in the next two centuries (Fig. ~~2e).~~ 4a and d).

The magnitude of ~~mass loss~~ Antarctic sea-level commitment under SSP1-2.6 warming is further modulated by the long-term consequences of a potential collapse of ~~the~~ Ross and Ronne-Filchner ice shelves: In Kori-ULB, both large ice shelves are preserved to the year 7000, and we find a grounding-line advance and upstream thickening in the Siple Coast region (Fig. 6a). This long-term ice-sheet response in the Siple Coast may, in parts, result from a drift of the initialisation procedure, given lower sub-shelf melt rates obtained with PICO in this area compared to those that are obtained from the initialization approach to keep the ice sheet steady (Sect. 2.2.2). A thickening signal upstream of Ross Ice Shelf ~~as well as the extent of grounding-line recession in the~~ has also been observed over the past decades (with the stagnation of Kamb Ice Stream; Smith et al., 2020). The simulated thickening upstream of Ross Ice Shelf contributes to the decay in the long-term Antarctic sea-level contribution over time after the year 3000 in some Kori-ULB simulations, which is most pronounced for sustained MRI-ESM2-0 climate (Fig. 5a, orange). The preservation of these buttressing ice shelves limits the long-term sea-level change from Antarctica under

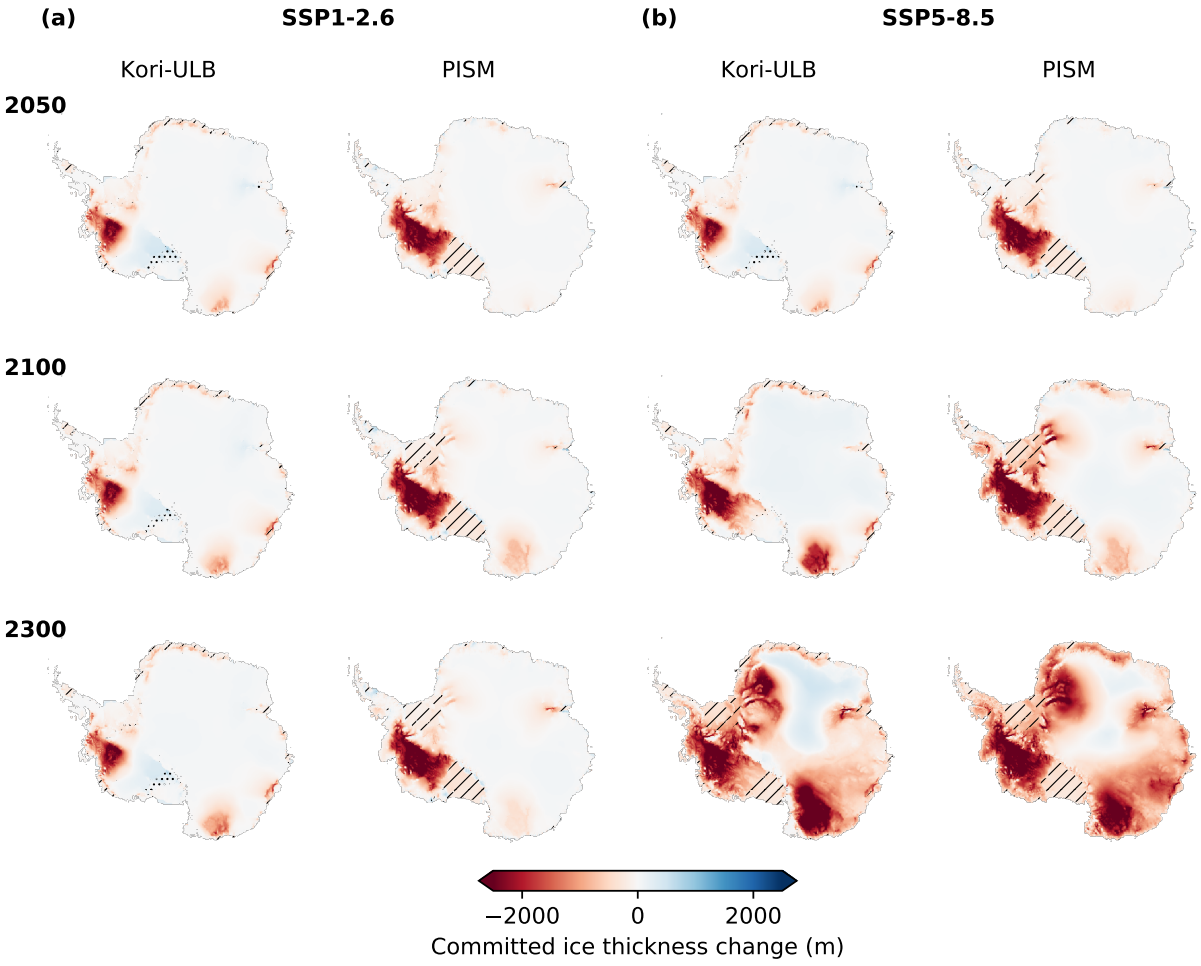

Figure 6. **Committed ice-sheet response** following emission pathways SSP1-2.6 (a) and SSP5-8.5 (b). Shown is the mean ice-thickness change in the year 7000 when stabilizing Antarctic climate in the years 2050, 2100 and 2300 (from top to bottom), as determined by the ice-sheet models Kori-ULB (left column) and PISM (right column). For each ice-sheet model, the ice-thickness change is averaged across the applied CMIP6 GCMs and the respective ice-sheet model configurations (Tab. S2). A potential loss of ice shelves is indicated by hatches. Dots mark areas of potential ice-sheet advance.

SSP1-2.6 to less than +3.5 m in the Kori-ULB simulations (with the upper bound reached under sustained UKESM1-0-LL and IPSL-CM6A-LR climate due to a combined grounding-line retreat in Wilkes subglacial basin and the Amundsen Sea Embayment~~.~~; Fig. 5a and e, grey and pink filled markers). In PISM, a substantial portion of the marine ~~ice–sheet~~ ice-sheet in West Antarctica is lost ~~by~~ with the collapse of Ross Ice Shelf and the subsequent retreat of the Siple Coast grounding line by the year 7000 under most considered climate trajectories (~~compare~~ Fig. ~~S14–S15), determining (in combination with apotential grounding–line retreat in the Wilkes basin) the upper range of Antarctic sea–level commitment under~~ 6a, Fig. S2). The loss of Ross Ice Shelf and the stronger sensitivity of the Siple Coast grounding line under SSP1-2~~.6 in our ensemble of~~ .6 climate in the PISM simulations may be related to the initialized upstream grounding-line location compared to observations at present-day (compare Sect. 2.2.2, Fig. S1; as previously seen in an ice-sheet model initialisation in a spin-up approach, e.g. Reese et al., 2023; Sutter e , and the simulated thinning in Ross Ice Shelf over the historical period (compare Sect. 3.1, Fig. 2c; also when determining the historical ice . In addition, the higher basal melt sensitivity (compare Sect. 2.2.3 and Sect. 3.1) also translates the projected ocean warming into pronounced ice-shelf thinning (Fig. 4f, Fig. 6a). Furthermore, once grounding-line retreat is triggered, a collapse of the West Antarctic Ice Sheet may be more likely in PISM than in Kori-ULB, where low slipperiness towards the interior of West Antarctica (given low basal sliding coefficients retrieved in the inverse simulations, Sect. 2.2.2) slows down ice-sheet retreat. The combined ice loss from West Antarctica and the East Antarctic Wilkes subglacial basin in PISM gives rise to the upper end of the Antarctic sea-level commitment of up to +6.5 m found under the lower-emission pathway in our simulations (Fig. ~~2e). While the Ross Ice Shelf collapses under SSP1-2.6 in PISM, Filchner–Ronne Ice Shelf~~ 5c and e, grey open markers).

Ronne-Filchner Ice Shelf remains intact in most of ~~these simulations (~~our simulations under SSP1-2.6, except for CESM2-WACCM ~~). In Kori-ULB~~with strong atmospheric and oceanic changes in the Weddell Sea region in combination with higher sub-shelf melt sensitivities in PISM (Fig. 6a, ~~grounding–line retreat is limited to Pine Island and Thwaites Glacier while both large ice shelves are preserved (with a slight grounding–line advance for Ross Ice Shelf, compare~~ Fig. ~~S12–S13). This limits the long–term sea–level change from Antarctica to approximately~~ S2). Its loss triggers ice-sheet retreat in the adjacent Recovery subglacial basin as a consequence of reduced buttressing, raising sea level by up to ~~+3.0 m in Kori-ULB (in combination with a retreating grounding line in Wilkes basin under UKESM1-0-LL and IPSL-CM6A-LR;~~ 5 m on the long term (Fig. ~~2e~~5c and e, blue open markers, Fig. 6a, Fig. S2).

Overall, both ice-sheet models agree on a substantial committed retreat in the Amundsen Sea Embayment, when following the lower-emission pathway over the coming centuries. With the loss of Ross Ice Shelf, a collapse of the West Antarctic Ice Sheet may even unfold on multi-millennial timescales, as shown in the simulations with PISM presented here. Committed mass loss in East Antarctica seems less likely, based on our set of simulations, and strongly depends on the projected Antarctic climate trajectory under the SSP1-2.6 scenario.

3.3.2 Antarctic sea-level commitment under higher-emission pathway SSP5-8.5

Under the **SSP5-8.5 emission scenario**, the potential magnitude as well as the range of the ~~long–term Antarctic sea–level response~~ long-term Antarctic sea-level commitment substantially increase with the point in time at which ~~ocean and atmospheric~~ atmospheric and oceanic warming is stabilized (Fig. ~~2~~5f). The growing spread of the Antarctic sea-level commitment for a given

(branchoff) point in time is, to a large part, caused by the divergence of the climate trajectories projected by the four GCMs under this higher-emission pathway (Figure 4a and d).

Under the sustained warming levels potentially reached during the next decades (that is, by 2050) under ~~this high-warming climate trajectory, long-term~~ these high-warming climate trajectories, committed ice-sheet changes are comparable to committed changes under the lower-emission pathway SSP1-2.6 (Sect. 3.3.1). This results from a very similar projected evolution of the Antarctic climate over the first half of this century, irrespective of the emission pathway (see above). That is, long-term mass losses are ~~projected to~~ likewise projected to mainly arise from marine regions in West Antarctica (Fig. ~~3b, committed~~6), leading to +0.5 m ~~–~~ - ~~+3.7~~4.2 m of ~~global mean sea-level rise (comparable to changes under SSP1-2.6; Tab. 1).~~ sea-level rise on multi-millennial timescales (Fig. ~~S16–S19 show the individual long-term ice-sheet response determined by both ice-sheet models to sustained warming levels reached by 2050 in the GCMs. Major portions of the catchment region of Thwaites and Pine Island Glaciers are drained in both ice-sheet models. In addition, the grounding line at the Siple Coast may retreat inland with a thinning of Ross Ice Shelf (or even a collapse, Fig. 3b, committed), as suggested in simulations by PISM. In response to changes in climatic boundary conditions~~ 5f, Tab. 1).

With significant changes in Antarctic climate projected for the end of this century ~~, we find the committed sea-level contribution to be substantially larger (Fig. 2f): Marine parts of the West Antarctic Ice Sheet show a significant retreat (in some cases the West Antarctic Ice Sheet even collapses entirely), accompanied by a strong inland retreat of the grounding line in the East Antarctic Wilkes basin on the long term (depending on the climate forcing,~~ and the atmosphere shifting towards an amplifying driver of mass loss in the transient ice-sheet response (Fig. ~~3b, committed; Fig. S16–S19). Compared to ice-sheet changes triggered within the next decades, this can lead to more than~~ 4a-d, Sect. 3.2), we also find the committed Antarctic sea-level contribution to be substantially larger, with a doubling of the ~~long-term~~ long-term mass loss ranging between +1.2 m and ~~+8.5 m sea-level equivalent (by year 7000,~~ 8.8 m sea-level equivalent compared to ice-sheet changes triggered within the next decades (Fig. ~~2f;~~ 5f, Tab. 1). The mass loss until the year 3000 amounts to +1.0 m ~~–~~ - ~~+4.9 m sea-level equivalent (compare~~ 5.2 m sea-level equivalent (Tab. 1), consistent with Chambers et al. (2022). Marine parts of the West Antarctic Ice Sheet (now also including the Ross Ice Shelf catchment in simulations with Kori-ULB) show a significant retreat in our entire ensemble of simulations across both ice-sheet models, potentially accompanied by an inland retreat of the grounding line in the East Antarctic Wilkes subglacial basin on the long term (Fig. 6b).

For warming levels that are reached under SSP5-8.5 for any of the branchoff points in time after 2100, ~~mass loss from Antarctica~~ the pattern of the committed ice-sheet response is overall consistent across Kori-ULB and PISM. For these branchoff points in time, the difference in future Antarctic climates projected by the four GCMs is significant (Fig. 4a and d, Tab. S1). Mass loss of the Antarctic Ice Sheet may continue well beyond the end of this millennium, with high rates of the Antarctic contribution to ~~sea-level~~ sea-level rise until the end of our simulations in the year 7000 (Fig. ~~2~~5b and d). ~~This is due to additional and persistent ice loss in the Aurora, Wilkes and Recovery~~ Depending on the GCM climate trajectory, the long-term ice loss is limited to West Antarctica and the East Antarctic marine Ronne-Filchner, Recovery, Wilkes and Aurora subglacial basins (Fig. ~~3b, committed).We also find a substantial ice thickness decrease in inner parts of East Antarctica~~ 6b, Fig. S3) or also includes parts of the ice sheet grounded above sea level ~~that is triggered under sustained high levels of warming~~

and possibly exacerbated by the melt–elevation feedback in East Antarctica, with very pronounced atmospheric warming in CESM2-WACCM (Fig. 3b, committed). In such cases, the long–term 4f, blue, Fig. 6b, Fig. S3). For sustained warming levels representative for 2300, the long-term contribution of the Antarctic Ice Sheet to global mean sea–level rise may sea-level rise may then be as high as +40.8 m for sustained warming levels representative for the year 2300 (in the year 7000(given sustained CESM2-WACCM climate; with ice loss of +7.5 m - +40.8 m, +5.9 m –- +31.7 m and +3.3 m –- +13.8 m sea–level 13.9 m sea-level equivalent by the year years 7000, 5000 and 3000, respectively, compare Tab. 1). Our upper range of long–term mass loss committed under constant

Overall, the multi-millennial Antarctic ice loss is strongly enhanced with a stabilization of climatic boundary conditions reached by the year 2300 is thus higher than previous estimates (under Representative Concentration Pathway RCP8.5, Golledge et al., 201 , likely caused by higher magnitudes of imposed warming in the selected GCMs employed here. later in time under the SSP5-8.5 emission pathway across both ice-sheet models, ranging from a long-term collapse of the West Antarctic Ice Sheet in response to warming projected by 2100 to the ice loss from major marine subglacial basins in East Antarctica with progressing atmospheric temperature changes after the end of this century. The Antarctic sea-level commitment could even increase up to +40 m with the decline of terrestrial parts of the East Antarctic Ice Sheet for warming reached after 2200, but this is associated with substantial GCM uncertainty.

In summary, comparing the long–term Comparing the long-term ice loss under both emission pathways, we find that the committed Antarctic sea–level sea-level contribution at a given point in time diverges beyond the end of this century (Fig. 25f, comparing projected multi–millennial multi-millennial ice loss under SSP5-8.5 to SSP1-2.6 indicated by light grey box). That is, the emission pathways also become increasingly relevant for the long–term long-term mass loss from Antarctica after 2100. 2100, as for the projected transient sea-level change (Sect. 3.2 and Coulon et al., 2024), and thus every decade of additional warming raises the Antarctic sea-level commitment substantially in our simulations. At the same time, even the lower–emission scenario poses lower-emission scenario may pose a considerable risk of Antarctic ice loss raising global mean sea–level sea level by multiple meters over the next millennia.–, depending on the GCM climate trajectory and ice-sheet modelling choices (Sect. 3.3.1).

It should be noted that our simulations end in the year 7000. As a consequence, in some cases the ice sheet has not yet reached a new equilibrium with the sustained climatic boundary conditions yet.(Fig. 5b and d). The complete loss of the East Antarctic Ice Sheet can thus not be ruled out on even longer timescales.

The growing spread of the Antarctic sea–level commitment for a given (branchoff) point in time is mainly caused by the divergence of the climate trajectories projected by the four GCMs (see discussion in Sect. **??**). Under equivalent warming, the long–term dynamical and topographical changes of the Antarctic Ice Sheet are largely consistent (for each ice–sheet model configuration) and uncertainty in Antarctic ice loss for a given warming level is due to inter– and intra–model uncertainty (e.g., arising in the ice–sheet model initialisation, compare Sect. 2.2.2, and by differences between applied atmospheric climatologies). The relationship between the committed Antarctic mass changes and sustained warming as well as potential thresholds in the long–term ice–sheet response are further studied in the following Sect. 3.4.

Projected ice loss from Antarctica on centennial to multi–millennial timescales (in meters sea–level equivalent) in response to changing climate conditions as projected by four different GCMs (given by the colour) under emission pathways SSP1-2.6 (upper row) and SSP5-8.5 (lower row), simulated by the ice–sheet models PISM (solid) and Kori-ULB (dashed). (a) and (b): Transient sea–level response from Antarctica until year 2300. (c) and (d): Multi–millennial Antarctic sea–level response until year 7000 to warming reached at different points in time throughout the next centuries. (e) and (f): Committed Antarctic sea–level contribution in the year 7000. Different atmospheric climatologies involved in the ice–sheet initialisation are indicated by the shape of the marker. Open and filled markers correspond to the long–term sea–level change determined by PISM and Kori-ULB, respectively. For comparison of the committed sea–level rise under both emission pathways, the range of long–term Antarctic ice loss by 7000 under SSP1-2.6 is indicated by the light grey box in (f).

Realized and committed ice–sheet evolution following emission pathways SSP1-2.6 (a) and SSP5-8.5 (b). Shown is the mean thickness change for the realized and committed ice–sheet response (from left to right) when stabilizing climatic boundary conditions at different points in time (from top to bottom). EAIS, East Antarctic Ice Sheet; WAIS, West Antarctic Ice Sheet; FRIS, Filchner–Ronne Ice Shelf.

3.4 Threshold behavior Potential threshold behaviour in response to changing climatic boundary conditions

The Antarctic Ice Sheet has been shown to exhibit a nonlinear response to warming and hysteresis behavior in quasi–equilibrium (that is, when temperatures change much slower than typical rates of change of an ice sheet; Garbe et al., 2020). In the following, we explore the relationship between climate boundary conditions potentially reached throughout the next centuries and sustained for several thousands of years and the configurations that the Antarctic Ice Sheet evolves to under these conditions on multi–millennial timescales. These ice–sheet states complement the quasi–equilibrium response of the Antarctic Ice Sheet (obtained by Garbe et al., 2020) as they record the long–term response to faster warming as projected under the different SSP scenarios. Figure 4 shows the committed sea–level contribution of Figure 7 summarizes the committed sea-level contribution from the Antarctic Ice Sheet (in the year 7000) for a given regional (Antarctic–averaged) Antarctic-averaged atmospheric warming level, thereby overcoming the dependency of ice loss on the diverging climate trajectories (Sect. 3.3). It also allows to explore potential thresholds in the relationship between climatic boundary conditions potentially reached throughout the next centuries and the long-term committed ice-sheet response.

In our simulations, we can identify distinct clusters of qualitatively different ice-sheet behaviour on the continental scale with increasing warming (Fig. 7) and locate critical thresholds in climatic boundary conditions inducing persistent ice loss on a basin scale (Fig. 8):

For **regional Antarctic atmospheric warming levels of up to 4°C**, as reached by 2300 under SSP1-2.6 and by 2050 under SSP5-8.5, we find a committed collapse of the Amundsen Sea basin, in some cases even a partial collapse of the West Antarctic Ice Sheet, resulting in a long–term an Antarctic mass loss of up to 6.0 m sea–level equivalent over multi–millennial +6.5 m sea-level equivalent over multi-millennial timescales (Fig. 47a and b as zoom-in, I and II). With both ice–sheet models, our experiments show a strong grounding–line

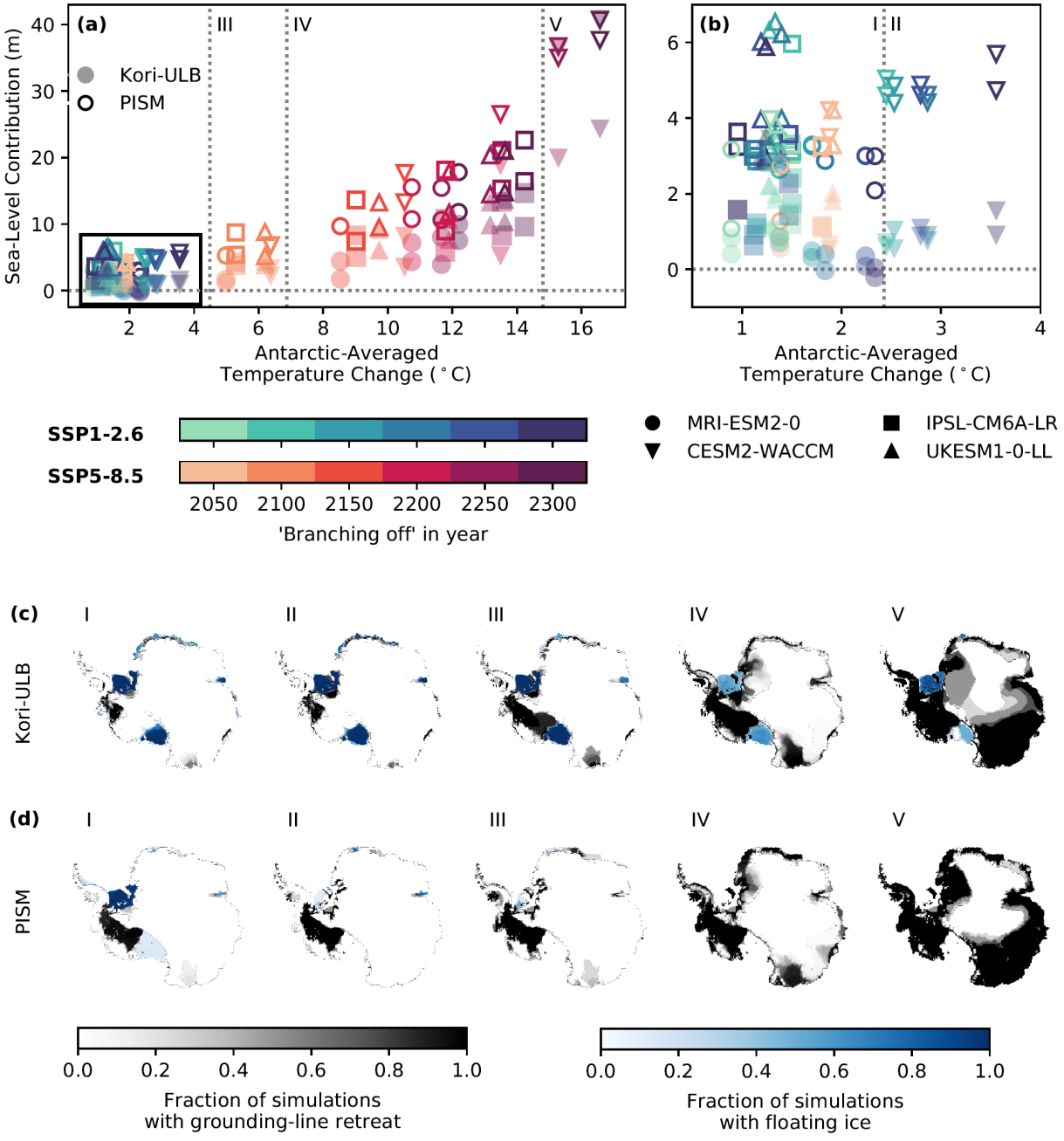

Figure 7. Committed sea-level contribution from the Antarctic Ice Sheet. (a) and (b): Long-term ice loss from the Antarctic Ice Sheet (in meters sea-level equivalent) for the year 7000 in response to Antarctic-averaged atmospheric temperature change (compared to 1995-2014) as projected by four CMIP6 GCMs (given by marker shape), as determined by the ice-sheet models Kori-ULB (filled markers) and PISM (open markers). The change in climatic boundary conditions is sustained for several millennia. (b) is a zoom into (a) for a low to intermediate Antarctic-averaged atmospheric temperature change. (c) and (d): Fractions of simulations that show grounding-line retreat in the year 7000 in Kori-ULB (c) and PISM (d). The fraction is determined for all simulations that are assigned to the distinct clusters I-V.

Table 1. Mean, minimum and maximum value of the combined realized and committed Antarctic ice loss (in meters ~~sea-level~~ sea-level equivalent) ~~as determined by the ice-sheet models PISM and Kori-ULB~~ under emission pathways SSP1-2.6 and SSP5-8.5, as determined by the ice-sheet models PISM and Kori-ULB. Ice loss is given for different points in time where climatic boundary conditions are stabilized. For a given point in time, upper rows represent SSP1-2.6 and lower rows correspond to SSP5-8.5.

		Realized	Committed in year 3000	Committed in year 5000	Committed in year 7000
2050	SSP1-2.6	-0.01	~~0.99~~ 0.96	~~1.97~~ 2.08	~~2.15~~ 2.19
		(-0.03,0.01)	(~~-0.14,2.27~~-0.11,2.63)	(~~0.65,3.82~~0.62,4.09)	(0.41,~~3.78~~3.97)
	SSP5-8.5	-0.01	~~0.93~~ 1.14	~~1.89~~ 2.05	~~2.06~~ 2.15
		(-0.03,0.01)	(~~-0.17,3.32~~-0.04,3.61)	(~~0.73,3.87~~0.69,3.94)	(0.51,~~3.73~~4.21)
2100	SSP1-2.6	0.00	~~1.32~~ 1.35	~~2.57~~ 2.64	~~2.77~~ 2.90
		(-0.05,0.08)	(~~0.18,3.76~~0.21,3.70)	(0.88,~~5.11~~5.17)	(0.59,~~6.08~~6.32)
	SSP5-8.5	-0.01	~~2.50~~ 2.56	~~4.31~~ 4.32	~~4.93~~ 4.81
		(-0.06,0.06)	(0.98,~~4.87~~5.17)	(1.07,~~7.88~~8.01)	(1.18,~~8.54~~8.81)
2150	SSP1-2.6	0.01	~~1.1~~ 1.31	~~2.5~~ 2.48	~~2.6~~ 2.66
		(-0.08,0.19)	(~~0.11,1.89~~0.10,3.36)	(0.67,~~5.55~~5.71)	(0.31,~~6.3~~6.54)
	SSP5-8.5	0.09	~~4.50~~ 4.51	~~7.33~~ 7.30	~~8.70~~ 8.79
		(~~-0.05~~-0.04,0.28)	(1.74,~~7.72~~7.61)	(1.84,~~13.45~~13.67)	(1.74,~~17.03~~17.66)
2200	SSP1-2.6	0.03	~~1.14~~ 1.10	~~2.20~~ 2.37	~~2.50~~ 2.54
		(-0.11,~~0.3~~0.30)	(~~-0.14,3.75~~-0.11,3.00)	(0.38,~~4.85~~5.52)	(-0.03,~~5.94~~6.22)
	SSP5-8.5	0.38	~~5.91~~ 5.81	~~10.48~~ 10.50	~~12.44~~ 12.55
		(~~0.18~~0.16,0.73)	(2.38,~~9.96~~9.88)	(3.54,~~19.36~~19.93)	(4.36,~~26.15~~26.54)
2250	SSP1-2.6	0.05	~~1.33~~ 1.24	~~2.49~~ 2.67	~~2.76~~2.77
		(~~-0.13,0.4~~-0.15,0.40)	(~~0.01,3.43~~0.03,2.94)	(0.45,~~5.14~~5.07)	(0.08,~~5.82~~6.01)
	SSP5-8.5	0.93	~~7.16~~ 7.15	~~14.20~~ 14.14	~~17.57~~ 17.63
		(~~0.4~~0.40,1.48)	(2.42,~~12.46~~12.44)	(3.21,~~27.20~~27.14)	(3.92,~~36.43~~36.76)
2300	SSP1-2.6	0.07	~~1.30~~ 1.22	~~2.56~~ 2.58	~~2.66~~ 2.69
		(~~-0.17~~-0.16,0.51)	(~~-0.14,4.10~~-0.13,2.94)	(0.26,~~5.67~~5.56)	(-0.21,~~5.98~~5.88)
	SSP5-8.5	~~1.82~~ 1.79	7.97	~~16.04~~ 16.10	~~19.51~~19.61
		(0.74,~~3.09~~3.07)	(3.27,~~13.79~~13.86)	(5.88,31.67)	(7.52,40.77)

The committed strong grounding-line retreat in the Amundsen Sea Embayment for this ~~temperature range (~~warming range (consistently shown by both ice-sheet models; Fig. ~~4~~7c and d, I and II, Fig. ~~5d and g) , consistent~~ 8a and b) is in line with previous work ~~(Garbe et al., 2020). This may be accompanied by a connection from Pine Island Glacier to Ronne Ice Shelf, giving rise to ice loss from this region (~~(Golledge et al., 2017; Garbe et al., 2020; Coulon et al., 2024).

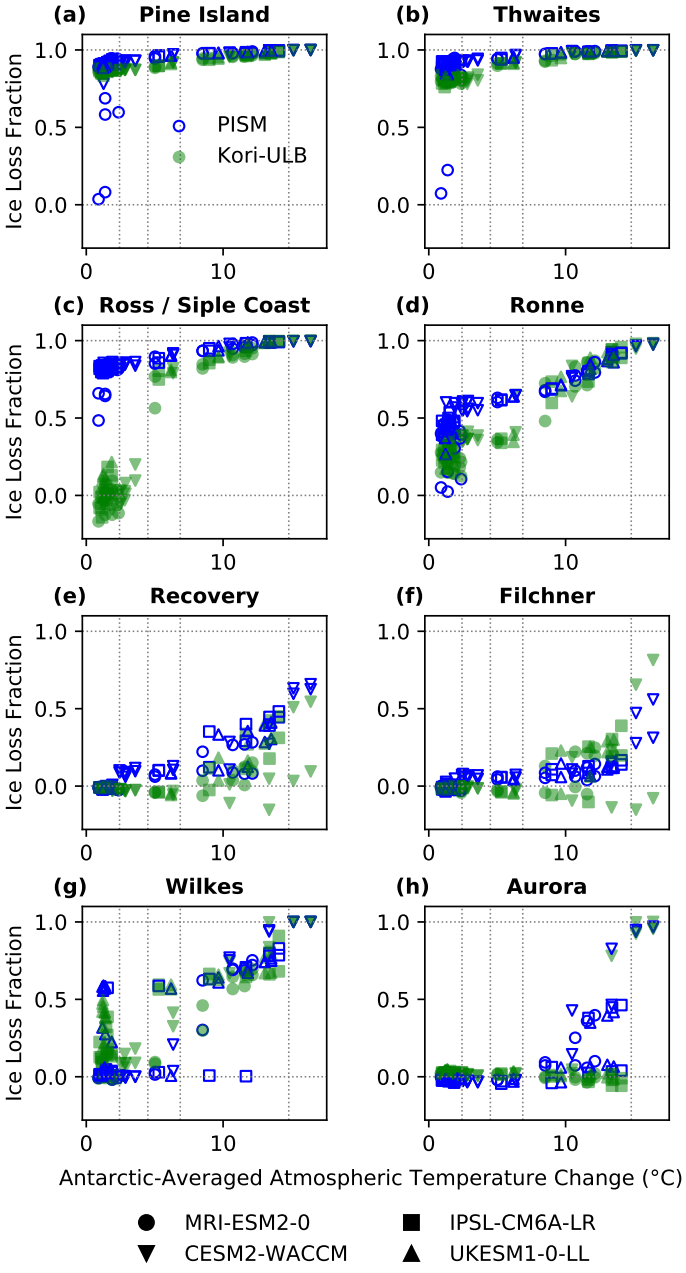

Figure 8. Ice loss from Antarctic drainage basins. Long-term ice loss from different Antarctic drainage basins (as fraction of respective sea-level rise potential) for the year 7000 in response to Antarctic-averaged atmospheric temperature change (compared to 1995-2014) as projected by four CMIP6 GCMs (given by marker shape). Filled, green and open, blue markers correspond to the long-term ice loss determined by the ice-sheet models Kori-ULB and PISM, respectively.

Uncertainties in the Antarctic sea-level commitment for an Antarctic-averaged atmospheric warming below 4°C (Fig. 7b) are related to (i) varying ice-sheet sensitivities in the Ross (Fig. 47c and d, I and II, Fig. 5a) . While Ross Ice Shelf is maintained in simulations with Kori-ULB, it is lost in most simulations with PISM (compare 8c) and Ronne-Filchner catchments (Fig. 47c and d, I). The collapse of Ross Ice Shelf is accompanied by the drainage of the corresponding catchment area (Fig. 4c, I and II, Fig. 5c and h), except for regional atmospheric warming below 1°C (projected by MRI-ESM2-0 under SSP1-2.6 until year 2050 only) which is comparable with the ice–sheet equilibrium response determined by means of PISM in Garbe et al. (2020) .While 2% of the initial ice mass in Antarctica contributing to global mean sea–level rise is lost in Kori-ULB (raising global mean sea–level by up to approximately +2.0 m), a slightly higher fraction of 6% (equivalent to a global mean sea–level change between +3.0 m and +4.0 m) is found in simulations with PISM (Fig. 4b) , due to the discharge of larger parts of the West Antarctic Ice Sheet as opposed to an advance of the grounding line in the Siple Coast area in Kori-ULB (compare 8e-f), depending on ice-sheet modelling choices (compare Sect. 3.3.1), and (ii) the onset of ice loss in the East Antarctic Wilkes subglacial basin, depending on the ocean warming in the applied GCMs (Fig. 47a, triangles, Fig.7c and d, I). The uncertainty in the initial ice–sheet configurations of each model results in differences on the order of decimeters in sea–level contribution in this warming range and is thus less significant than the inter–model spread. Overall, there is a good agreement also in the patterns of mass loss for the different initial configurations.

Some of our simulations (across both ice–sheet models) also show an onset of grounding–line ; compare Sect. 3.3.1). We find the committed grounding-line retreat in Wilkes basin in this range of atmospheric warming , shifting the upper bound of ice loss up to subglacial basin being triggered by ocean warming with exceeding a basin-averaged ocean temperature change of +6.0 m sea–level equivalent and widening the intra–model spread (Fig. 4b–d, I and Fig. 5i). This region contributes up to +1.5 m to the long–term sea–level change, which may occur for a mean ocean–temperature change exceeding +0.5°C – +1°C in this basin (depending on the ice–sheet model, with earlier onset of retreat in Kori-ULB; across both ice-sheet models (Fig. 7c and d, I, Fig. 5i8g, Fig. S4g). The loss of ice grounded below sea level in this particular (Wilkes) basin is triggered subglacial basin is initiated for slightly lower ocean warming than in Garbe et al. (2020) and Golledge et al. (2015) Golledge et al. (2015) and Garbe et al. (2020), but is located within the range of idealized experiments by Mengel and Levermann (2014).

The long–term response of the marine basins may further depend on the ratio of atmospheric to oceanic warming: Despite exposing the ice sheet to higher atmospheric warming levels as derived from CESM2–WACCM under the lower–emission pathway, the grounding line in Wilkes subglacial basin does not experience retreat under these forcing conditions (due to weaker ocean forcing compared to UKESM1-0-LL, A long-term collapse of the Ronne-Filchner Ice Shelf and ice loss from ice streams draining the Eastern Weddell Sea sector is found in PISM simulations when atmospheric warming in Antarctica exceeds 2.5°C (Fig. 4c, Hand 7b and d, II, Fig. 5i)in PISM experiments. While showing some limited grounding–line retreat in the Wilkes subglacial basin, the sea–level contribution of approximately 1.0 m determined by Kori-ULB is lower due to limited grounding–line retreat and subsequent ice loss in the basins draining Ross Ice Shelf as well as less pronounced thinning in Recovery basin (compared to PISM; Fig. 4d, II). Exceeding the regional atmospheric warming of 2.5°C projected by CESM2–WACCM under SSP1-2.6 also induces the long–term loss of Filchner–Ronne Ice Shelf in addition to Ross Ice Shelf in PISM experiments (comparable to the long–term 8e and f). This is in line with the long-term ice-sheet response found in

Golledge et al. (2015) after following emission pathway RCP4.5 with Antarctic atmospheric warming of about 2.2°C~~), which is accompanied by a retreat of the grounding line in Robin subglacial basin (Fig. 4b and c, II). Ice streams that drain the Recovery basin start showing a contribution to the long-term sea-level change (of about 5.0 m of sea-level equivalent in total for 2.5 °C to 4.0°C of Antarctic-averaged warming) (Fig. 4c, II), which further raises with enhanced warming (Fig. 5c). Such~~ . Given the lower sensitivity of the Ronne-Filchner Ice Shelf (Sect. 3.3.1), such a retreat of the basins connected to ~~Filchner-Ronne Ice Shelf occurs in Kori-ULB only at slightly~~ this major ice shelf occurs only at higher warming levels for Kori-ULB (see below, Fig. ~~4d~~8e and f).

Antarctic atmospheric warming levels of +5°C to +7°C are projected by the end of this century when following the ~~higher-emission pathway(Fig. 4 III). Under such climatic boundary conditions, the ice-sheet decline continues on the long-term in regions which are already affected by lower warming levels, resulting in an ice loss of~~ higher-emission pathway, resulting in a long-term ice loss ranging between +1.2 m and +~~8.5 m sea-level~~ 8.8 m sea-level equivalent (Fig. ~~4~~7a, III). This ~~wide spread~~ spread in Antarctic sea-level commitment contains the recent estimate by Van Breedam et al. (2020) of +6.6 m ~~sea-level~~ sea-level equivalent under warming of approximately +7°C over the next 10 000 years. In this warming range, ice loss from the Ross Ice Shelf catchment in West Antarctica substantially contributes to ~~sea-level~~ the long-term sea-level change also in Kori-ULB (Fig. ~~4d, IIIand~~ 7c, III, Fig. ~~5e and h~~8c). That is, we find a committed complete collapse of the West Antarctic Ice Sheet in both ~~ice-sheet~~ ice-sheet models for an ~~Antarctic-averaged~~ Antarctic-averaged atmospheric warming above +4°C ~~. The inter-model spread in~~ (Fig. 7c and d, III). The inter-model spread in Antarctic mass loss is explained by a stronger thinning of ice draining into the eastern Weddell Sea region in PISM (Fig. 7 c and d, III, Fig. 8e and f) in combination with a more pronounced thickening in the inner parts of East Antarctica in Kori-ULB within this warming range (~~compare~~ Fig. ~~S16–S17 for Kori-ULB with Fig. S18–S19 for PISM~~ S3, when sustaining warming projected for ~~year~~ 2100).

Exceeding an **atmospheric warming of +8°C in Antarctica** gives rise to a further increase in the fraction of ice that is lost on ~~multi-millennial timescales from 15 %~~ multi-millennial timescales to up to 40 % at +14°C (Fig. ~~4~~ 7, IV). Enhanced ~~long-term mass loss with stronger Antarctic~~ long-term mass loss aligned with progressing Antarctic atmospheric warming is found in particular for ~~Filchner-Ronne~~Ronne-Filchner, Recovery and Wilkes subglacial basins (Fig. ~~5a–c, i~~7c and d, IV, Fig. 8d - g). In addition, some of our ~~experiments~~ simulations suggest the onset of ice drainage from the East Antarctic Aurora ~~basin (Fig. 5f; in accordance with Golledge et al., 2015)~~subglacial basin for an Antarctic-averaged atmospheric temperature increase of +10°C (in accordance with Golledge et al., 2015), associated with a substantially increasing contribution to ~~sea-level~~ sea-level rise from this basin (for ~~RACMO initial state~~PISM, Fig. ~~S19~~7d, IV, Fig. 8h) in this warming range. The ice stored in the Aurora subglacial basin is lost completely in both ~~ice-sheet~~ ice-sheet models for even higher atmospheric warming levels (see below and Fig. ~~4V~~8h). While the general dependency of ice loss from the Aurora region on the atmospheric forcing in our simulations (Fig. 8h, compared to Fig. S4h) is in agreement with Golledge et al. (2017), stronger warming of the atmosphere is required here for triggering the retreat.

For sustained ~~**regional**~~ **Antarctic-averaged atmospheric warming above +15°C** (projected by ~~CESM2-WACCM after year~~ CESM2-WACCM after 2200), we find that large parts of the ~~marine basins in Antarctica~~ Antarctic marine basins are lost and ice grounded above sea level in East Antarctica starts to decline substantially on ~~multi-millennial timescales~~ multi-millennial

timescales in our entire ensemble of simulations (Fig. 47 V). Over the next millennia, this gives rise to an Antarctic ice loss equivalent to a ~~sea–level~~ sea-level change of up to +40.8 m. It cannot be ruled out that Antarctica could become ~~ice–free under the given climate conditions~~ice-free under these high-warming trajectories, consistent with ~~Garbe et al. (2020) and Winkelmann et al. (2015)~~ Winkelmann et al. (2015) and Garbe et al. (2020), given the continued increase of the Antarctic ~~sea–level~~ sea-level contribution at the end of our simulations (Fig. ~~2~~5c and d).

Overall, the ~~sea–level~~ sea-level commitment increases nonlinearly with increasing atmospheric ~~temperature change~~ warming in Antarctica (Fig. 47a), ~~with~~ consistent with the nonlinear response to warming in quasi-equilibrium (that is, when temperatures change mu . Our committed ice-sheet states complement this quasi-equilibrium response of the Antarctic Ice Sheet (obtained by Garbe et al., 2020) as they record the long-term response to faster warming as projected under the different SSP scenarios.

Under equivalent warming, the long-term dynamical and topographical changes of the Antarctic Ice Sheet are largely consistent for each ice-sheet model configuration (compare Table S2). We find a spread in long-term Antarctic mass loss at a given warming level due to ~~differences in parameter choices (here arising as part of the initialisation) and structural (model)uncertainty~~model uncertainties (e.g. arising in the ice-sheet model initialisation and physics), which is pronounced for low to intermediate warming levels in Antarctica covered by the lower-emission pathway SSP1-2.6 (Fig. 7b). In other words, the ~~ice–sheet~~ ice-sheet sensitivity to warming, in particular in some marine Antarctic basins, varies with the ~~initial Antarctic ice–sheet configuration and its characteristics.While we can identify distinct clusters of qualitatively different ice–sheet behavior on the continental–scale with changing atmospheric warming~~ ice-sheet model configuration (compare Tab. S2). In this warming range, varying trajectories of atmospheric to oceanic warming across GCMs may also play out and modulate Antarctica's sea-level contribution on longer timescales (Sect. 3.3.1). Beyond the low to intermediate warming levels covered by the lower emission pathway SSP1-2.6, the pattern of long-term mass loss and the resulting sea-level contribution from Antarctica are overall robust, with a step-wise long-term decline of the Antarctic Ice Sheet across two ice-sheet models (~~Fig. 4), critical thresholds in climatic boundary conditions inducing persistent ice loss are masked in the continent–wide committed sea–level contribution and can be located on a basin–scale~~ (Fig. ~~5). The importance of structural differences between the ice–sheet models, their initialisation and related parameter choices for Antarctic sea–level commitment and respective critical temperature thresholds is discussed in Sect. ??.~~ 7a, c and d): With increasing warming, our simulations suggest a committed partial collapse of the West Antarctic Ice Sheet (I and II), associated with a substantial retreat in the Amundsen Sea Embayment, up to its complete collapse (III), followed by enhanced mass loss from East Antarctic marine Wilkes, Recovery and Aurora subglacial basins (IV) and an eventual decline of terrestrial parts of the ice sheet (V).

~~**Committed sea–level contribution from the Antarctic Ice Sheet.** (a) and (b): Long–term ice loss from the Antarctic Ice Sheet (in meters sea–level equivalent) for year 7000 in response to Antarctic–averaged atmospheric temperature change (compared to 1995–2014). The change in climatic boundary conditions is sustained for several millennia. (b) is a zoom into (a) for a lower atmospheric temperature change. (c) and (d): Fractions of experiments that show grounding–line retreat in year 7000 in PISM and Kori-ULB, respectively. The fraction is determined for all experiments that are assigned to the distinct clusters I–V.~~

Ice loss from Antarctic drainage basins. Long–term ice loss from different Antarctic drainage basins (as fraction of respective sea–level rise potential) for the year 7000 in response to Antarctic–averaged atmospheric temperature change (compared to 1995–2014). The basin–averaged oceanic temperature change is represented by the colouring. Open and filled markers correspond to the long–term ice loss determined by PISM and Kori-ULB, respectively.

4 Discussion

In this paper, we determine the multi–millennial sea–level contribution from mass balance changes of multi-millennial sea-level contribution from the Antarctic Ice Sheet under a range of possible climate trajectories for both low– and high–emission low- and high-emission pathways. In particular, we quantify the long–term Antarctic sea–level long-term Antarctic sea-level commitment when stabilising climatic boundary conditions at different points in time. That is, the atmospheric and oceanic changes potentially established during the upcoming centuries decades and centuries in Antarctica are sustained for several thousands of years, and we explore their long–term long-term impacts on the Antarctic Ice Sheet. Experiments were Simulations are carried out systematically for stabilized climate Antarctic climates at different points in time over the course of the next centuries and in a consistent way with the stand–alone ice–sheet models PISM and stand-alone ice-sheet models Kori-ULB and PISM, thereby accounting for some inter– and intra–model model uncertainty.

Our experiments Our simulations illustrate a substantial gap between the difference between the transient *realized* and long-term *committed* sea–level sea-level change from the Antarctic Ice Sheet. While the projected Antarctic mass change by the end of this century may raise global mean sea–level by a few centimeters (or could potentially result in a sea–level drop, is limited (spanning a range from -0.1 m to +0.1 m sea–level sea-level equivalent), the Antarctic Ice Sheet may be committed to a strong grounding–line grounding-line retreat in the Amundsen Sea Embayment up to a potential collapse of the West Antarctic Ice Sheet for sustained climate climatic boundary conditions at levels projected to be reached during this century (that is, branching off in the years 2050 or 2100, depending on the GCM) even under the lower–emission pathwaylower-emission pathway, depending on ice-sheet modelling choices. Mass loss from the marine Wilkes subglacial basin in East Antarctica may unfold on multi–millennial timescales for warm ocean conditions multi-millennial timescales for strong ocean warming projected by some GCMs as early as the second half of this century under the lower–emission scenario. Stabilizing climate conditions later in time (for instance in the year 2300) and following the higher–emission lower-emission scenario. With a stabilization of climatic boundary conditions beyond the end of this century under the higher-emission pathway SSP5-8.5may additionally trigger , the long-term Antarctic sea-level contribution under these high-warming trajectories diverges from the sea-level commitment under SSP1-2.6. This is due to a successive ice-sheet retreat in major East Antarctic marine basins, additionally triggered by progressing warming. Next to ice loss from these marine parts, a substantial decline of the terrestrial non-marine East Antarctic Ice Sheet , resulting in long–term may eventually result in long-term mass losses of up to +40.8 m sea–level equivalentsea-level equivalent, subject to substantial uncertainties, especially due to the GCM climate forcing.

Determining the committed evolution of the Antarctic Ice Sheet triggered by the warming projected for the next decades and centuries extends previous studies of the long–term ice–sheet response (especially in the Amundsen Sea sector) under sustained

present–day long-term ice-sheet response under sustained *present-day* climate conditions. For example, Reese et al. (2023) and Golledge et al. (2019) Golledge et al. (2019), Reese et al. (2023) and Coulon et al. (2024) suggest a committed (potentially irreversible) grounding–line grounding-line retreat in West Antarctica under present–day conditions on centennial timescales present-day climate conditions in response to atmospheric and oceanic changes over the past decades. We also add to the assessment of the long–term Antarctic sea–level long-term Antarctic sea-level commitment to future warming by the end of this century (Chambers et al., 2022; Lowry et al., 2021) and by 2300 (Golledge et al., 2015; Bulthuis et al., 2019; Coulon et al., 2024) by exploring the multi–millennial multi-millennial consequences of stabilizing climatic boundary conditions at different points in time over the course of the next centuries, in a consistent way for two ice–sheet ice-sheet models. From a dynamical systems perspective, the long–term long-term stability of the Antarctic Ice Sheet under present and potential future rates of warming (being much faster than typical rates of change in an ice sheet) is studied. This complements the quasi–equilibrium ice–sheet quasi-equilibrium ice-sheet response to warming presented by Garbe et al. (2020) and, thereby, bridges the gap to the transient realized sea–level sea-level change from Antarctica (e.g., by the end of this century as in Seroussi et al., 2020) (e.g. by the end of this century as in Seroussi et al., 2020).

4.1 Uncertainties in Antarctic sea–level commitment

The committed Antarctic sea–level sea-level contribution is subject to growing uncertainties related to the substantial spread of warming projected by the selected GCMsfor a given point in time , in particular beyond the end of this century under SSP5-8.5 (*climate forcing uncertainty*, Sect. 3.3). Critical). Ice-sheet sensitivities and critical temperature thresholds giving rise to self–sustained self-sustained ice loss further vary in our experiments simulations as a result of *inter–and intra–model uncertainties (Sect. 3.4). model uncertainties*. These uncertainties may be induced by differences in the model structure and the parameterisation of certain processes (e.g., Seroussi et al., 2020), initialisation procedures (e.g., Seroussi et al., 2019; Aðalgeirsdóttir et al., as well as parameter choices (e.g., Bulthuis et al., 2019; Nias et al., 2016; Coulon et al., 2024). The ice-sheet processes (e.g. Seroussi et al., , parameter choices (e.g. Bulthuis et al., 2019; Nias et al., 2016; Coulon et al., 2024) and well as initialisation approaches (e.g. Aschwander . In the following, the role of these different sources of uncertainties for the multi–millennial Antarctic sea–level uncertainty for the multi-millennial Antarctic sea-level response presented in this work is discussedin the following.

Uncertainty due to climate forcing

4.1 Uncertainties in Antarctic sea-level commitment due to climate forcing

The climate Following recent efforts in projecting the Antarctic sea-level contribution on different timescales ranging from the next decades until 2100 to several millennia (Seroussi et al., 2020; Payne et al., 2021; Golledge et al., 2015), we base the imposed changes in Antarctic climate on state-of-the-art GCMs from the Coupled Model Intercomparison Project CMIP6. Biases in the chosen GCMs and a poor representation of conditions at the ice-sheet margins due to their coarse resolution (Beadling et al., 2020; Bracegirdle et al., 2020; Purich and England, 2021) may influence the simulated mass changes of the Antarctic Ice Sheet. In our simulations, the climate forcing from the four GCMs employed here employed GCMs results in

a wide spread of the realized and especially committed ~~sea–level~~ sea-level contribution from Antarctica, making it one of the most important sources of uncertainty.

For low to intermediate warming levels covered by the ~~lower–emission~~ lower-emission pathway SSP1-2.6, the uncertainty introduced by the climate forcing at a given point in time is comparable to the uncertainty caused by ~~inter–model differences~~ ice-sheet modelling choices (compare Fig. ~~2e), except for the response to CESM2–WACCM under SSP1-2.6.Here, PISM shows an onset of ice discharge from the Recovery basin after Filchner–Ronne Ice Shelf is lost (Fig. S14–15), while corresponding ice loss is triggered for stronger changes in climatic boundary conditions in Kori-ULB (compare~~ 5e and the following Sect. 4.2). Here, the Antarctic sea-level commitment is modulated by varying trajectories of atmospheric to oceanic warming across the GCMs for each ice-sheet model (Fig. ~~S12–S13 for SSP1-2.6 to Fig. S16–S17 for SSP5-8.5). This gives rise to a larger difference in the Antarctic sea–level contribution determined by both ice–sheet models.~~

4a and d). We find that the growing spread of the committed Antarctic ~~sea–level~~ sea-level contribution under the ~~higher–emission~~ higher-emission scenario SSP5-8.5 for stabilizing the ~~ice–sheet~~ ice-sheet boundary conditions later in time ~~can (~~(Fig. 5e) can, to a large part~~)~~ , be attributed to the divergence of the climate trajectories projected by the four GCMs ~~. They~~ beyond the end of this century (Fig. 4a and d).

The GCMs providing available future changes in Antarctic climate until 2300, on which our analysis is based, are characterized by different warming rates and a large range of climate sensitivities, ~~resulting in~~ with a high upper bound (Meehl et al., 2020) , which may not be in accordance with paleoclimatic evidence (Zhu et al., 2021). This introduces a substantial climate forcing uncertainty at a specific point in time: While for MRI-ESM2-0 a comparably low equilibrium climate sensitivity was determined (3.2°C, below the multimodel mean of 3.7°C; Meehl et al., 2020), the equilibrium climate sensitivities of UKESM1-0-LL (5.3°C), CESM2-WACCM (4.8°C) and IPSL-CM6A-LR (4.6°C) are at the upper end of the range of climate sensitivities reported for CMIP6. CESM2-WACCM also shows a significantly stronger ~~regional~~ Antarctic-averaged atmospheric warming under SSP5-8.5 beyond ~~2150~~ 2200 than the other GCMs (Tab. S1).

This translates into a growing uncertainty in ~~projected long–term~~ the projected long-term Antarctic ice loss under SSP5-8.5 with a substantially higher committed ~~sea–level~~ sea-level contribution from Antarctica for the same year under sustained CESM2-WACCM climate compared to the other applied CMIP6 GCMs. For example, the committed Antarctic ~~sea–level~~ sea-level contribution determined by Kori-ULB and PISM under CESM2-WACCM ~~ranges between~~ climate ranges between +24.3 m and +40.8 m (when assuming a stabilization of climatic boundary conditions representative for ~~the year~~ 2300). In contrast, we find an Antarctic mass loss of up to ~~22.0 m~~ +22.6 m sea-level equivalent for the other CMIP6 GCMs. These higher magnitudes of imposed warming in some of the selected GCMs employed here may also explain the substantially higher upper range of the long-term Antarctic mass loss committed under stabilized climatic boundary conditions reached by 2300 in our simulations (with committed ice loss of +3.3 m - +13.9 m, +5.9 m - +31.7 m and +7.5 m - 40.8 m sea-level equivalent by the years 3000, 5000 and 7000; Tab. 1) compared to some previous estimates (under Representative Concentration Pathway RCP8.5, Golledge , Consequently, the derived future climate trajectories and respective projected multi-millennial Antarctic ice loss should only be related to emissions with care and can rather be seen as a potential range of long-term futures for Antarctica.

~~Uncertainty arising from intra– and inter–model differences~~

As noted above, the majority of projections of future Antarctic climate to date covers this century only (O'Neill et al., 2016; Tebaldi et al., 2
. The pronounced projected changes in Antarctic climate and the substantial GCM uncertainty especially beyond the end of the century reflected in our assessment of the Antarctic sea-level commitment highlight the need for a through assessment of potential multi-centennial Antarctic climate trajectories in future research, as a basis for improving our understanding of the associated long-term Antarctic Ice Sheet response (on timescales on the order of centuries to multiple millennia).

~~On multi–millennial timescales, both ice–sheet models show a good agreement in the pattern of mass loss and the resulting sea–level contribution from Antarctica for~~ For determining the long-term Antarctic sea-level commitment, we here assume constant climatic boundary conditions on multi-millennial timescales. This allows us to assess the committed sea-level contribution from the Antarctic Ice Sheet and its stability under an idealized combination of atmospheric and oceanic changes with respect to present-day. This approach has been invoked previously (e.g. Golledge et al., 2015), but comes with certain assumptions: For instance, a continued ocean response to changing CO_2 conditions and atmospheric warming (Li et al., 2013) may result in an altered ratio of atmospheric and oceanic changes beyond the point in time where a stabilization of climatic boundary conditions is assumed here. Observed interannual and decadal variability (Paolo et al., 2018; Jenkins et al., 2018) is neglected in the imposed constant climatic boundary conditions for simplicity, which has been shown to potentially result in a lower long-term ice-sheet volume (compared to a stable climate; Mikkelsen et al., 2018) up to ice-sheet retreat (Christian et al., 2020; Robel et al., 2019)
.

In addition, climate trajectories distinct from such climate stabilization scenarios, e.g. temperature overshoot pathways (Tokarska et al., 2019), may impact the ice-sheet response in the near and far future. The response of the Antarctic Ice Sheet to a reversal of climatic boundary conditions after exceeding a warming of, e.g., 1.5°C, including the potential for 'safe' overshoots (Ritchie et al., 2021), is not well constrained. Based on the long-term Antarctic sea-level contribution presented here, the (ir-)reversibility of this committed Antarctic mass loss for a reversal of climatic boundary conditions and relevant timescales can be assessed in a next step.

4.2 Uncertainties in Antarctic sea-level commitment arising from model uncertainties

Under strong atmospheric warming (~~above 15°C of regional~~ with an Antarctic atmospheric temperature change above 8°C in our simulations), where the ~~ice–sheet~~ice-sheet's decline ~~(predominantly of its terrestrial parts grounded above sea level) is driven~~ is amplified by atmospheric changes rather than ~~ocean warming. The onset of grounding–line retreat in~~ being mostly driven by ocean warming (compare Coulon et al., 2024), the pattern of long-term mass loss and the resulting sea-level contribution from Antarctica on multi-millennial timescales are overall robust across both ice-sheet models, irrespective of their initialization approaches and structural differences. This includes enhanced ice loss from major East Antarctic marine basins ~~is located at different~~ with progressing warming, following a committed collapse of the West Antarctic Ice Sheet (for warming projected for the end of this century under SSP5-8.5; Sect. 3.3.2, Sect. 3.4).

Model uncertainty is most pronounced for ice loss from Antarctic marine basins located within low to intermediate warming levels ~~due to *inter–model differences*.Both ice–sheet~~ as covered by the lower-emission pathway SSP1-2.6. Depending on ice-sheet modelling choices, we find varying timings, basin-scale temperature thresholds and rates of grounding-line retreat in West Antarctica (Sect. 3.3.1, Sec. 3.4, Fig. 8).

On shorter, multi-centennial timescales, Kori-ULB projections are characterized by a higher sensitivity and an earlier onset of ice loss from the Amundsen Sea Embayment compared to the simulations with PISM under the lower-emission pathway (Fig. 3a and b). This stronger dynamical response of Thwaites and Pine Island glaciers in Kori-ULB results in a higher Antarctic sea-level contribution by 2300, continuing the simulated trends in this region over the historical period (Fig. 2). Both ice-sheet models agree on ~~an early~~ a long-term retreat of grounding lines of Pine Island and Thwaites ~~Glacier in the Amundsen Sea Embayment~~glaciers already under SSP1-2.6, consistent with previous findings that the ~~grounding–lines may at present~~ grounding lines at present might already be undergoing a ~~self–sustained~~ self-sustained retreat or that this retreat ~~has been locked in~~ might be imminent due to changes in ~~the climatic boundary conditions~~ Antarctic climate over the past decades ~~(Favier et al., 2014; Golledge et al., 2019; Reese et al., 2023). Ice loss from the catchment draining Ross Ice Shelf and a (partial) collapse of the West Antarctic Ice Sheet is triggered, however, for lower warming in PISM than in Kori-ULB, resulting in a multi–meter~~ (Favier et al., 2014; Golledge et al., 2019; Reese et al., 2023; Coulon et al., 2024).

The multi-meter spread of the ~~long–term committed sea–level contribution for Antarctic–averaged~~ sea-level contribution on longer, multi-millennial timescales for an Antarctic-averaged atmospheric warming up to 4°C (~~Fig. 4) . This grounded ice–sheet response isaccompanied by a different response of the major ice shelves in both ice–sheet models.Sequential collapse of the Ross and Filchner–Ronne Ice Shelf is projected by PISM for the change in oceanic and atmospheric conditions projected under SSP1-2.6, while both shelves are preserved in Kori-ULB under this~~ covered by the lower–emission ~~pathway and in some cases even under the higher–emission~~ pathway ~~SSP5-8.5. Ice–sheet sensitivities of the marine Wilkes and Recovery subglacial basins in East Antarctica to changes in atmospheric and oceanic boundary conditions also vary depending on the ice–sheet model configuration, such that persistent ice loss is triggered for different magnitudes of warming.~~SSP1-2.6) is, to a large part, associated with varying ice-sheet sensitivities in the catchments draining Ross and Ronne-Filchner ice shelves, accompanied by different responses of these major buttressing Antarctic ice shelves (Fig. 7; Sect. 3.3.1 and Sect. 3.4).

~~This inter–model discrepancy may be the result of several factors related to the characteristics of both ice–sheet models: The grounding line in the Siple Coast area is relatively sensitive~~ Here, the uncertainty in the onset of ice-sheet retreat can be linked to certain geometrical features of the initial ice-sheet state as an outcome of the applied initialization approaches (Sect. 2.2.2) as well as different, but all plausible ice-sheet modelling choices e.g. for determining sub-shelf melt (Sect. 2.2.3): For example, Ross and Ronne-Filchner ice shelves, restraining the ice flowing from the grounded ice sheet, are overall sustained longer in Kori-ULB, potentially related to a combination of the calving schemes employed in the ice-sheet models (Levermann et al., 2012; Pollard et al., 2015; DeConto and Pollard, 2016) and different PICO sub-shelf melt sensitivities to changes in ~~climatic boundary conditions in PISM, being located upstream~~ ocean temperatures (Sect. 2.2.3; Reese et al., 2018, 2023) . A simulated upstream location of the Siple Coast grounding line (Fig. S1; Reese et al., 2023; Sutter et al., 2023) and thinning of ~~the observed grounding line at present–day (compare Fig. S1; as often observed in a model initialisation in a spin–up approach, e.g., Ree~~

and showing thinning in Ross Ice Shelf over the historical period (compare Fig. S2; also when determining the historical ice–sheet evolution. The grounding–line advance in (Fig. 2; Reese et al., 2020, 2023) following a spin-up approach in PISM (Sect. 2.2.2) as well as a potential drift of the Siple Coast found grounding line in Kori-ULB under SSP1-2.6 may result from a drift of the initialisation procedure, which could be due to an underestimation of the sub–shelf (Sect. 3.3.1), given lower sub-shelf melt rates obtained from PICO compared to the balance melt rates derived during the nudging procedure with PICO in this area compared to those that are obtained from the initialization approach to keep the ice sheet steady (Sect. 2.2.2). Finally, some ice shelves are sustained longer in Kori-ULB, which could be due to the different calving schemes employed in the ice–sheet models (Levermann et al., 2012; Pollard et al., 2015; DeConto and Pollard, 2016), may also contribute to these varying ice-sheet sensitivities in the Siple Coast region.

Our simulations are performed on a comparably coarse horizontal resolution of 16 km, allowing for a large number of experiments as presented here, which is needed to cover the wide range of uncertainties. The migration of the grounding line in PISM is captured reasonably well, even on such a coarse resolution, with a sub–grid interpolation scheme (Feldmann et al., 2014), which allows to reproduce glacial cycles of the Antarctic Ice Sheet (Albrecht et al., 2020).Garbe et al. (2020) showed (using PISM)that the overall hysteresis behavior of the The rates of grounding-line retreat are then dictated by basal friction (e.g. Cornford et al., 20, that deviates spatially between both ice-sheet models: Once triggered, faster and large-scale West Antarctic grounding-line retreat unfolds in PISM for low to intermediate warming, promoted by overall slippery bed conditions in the interior of marine subglacial basins given the parameterized, bed-elevation dependent material properties of the subglacial till (in particular, the till friction angle; Sect. 2.1). Grounding lines face less slippery bed conditions when retreating towards the interior of the West Antarctic Ice Sheet is robust across model resolution. In in Kori-ULB, resolving grounding–line dynamics at a coarse resolution is addressed by imposing a flux condition (Pollard and DeConto, 2012a, 2020), which results in a good agreement with high–resolution models.

Characteristics of the initial states give rise to an *intra–model* spread in the projected multi–millennial sea–level contribution for a given warming level. In our experiments, we rely on two different present–day atmospheric climatologies (Kittel et al., 2021; van Wess that are involved in building the respective initial ice–sheet configurations based on the optimized lower sliding coefficients from the inverse simulation (Sect. 2.2.2). While a recent intercomparison concluded that Antarctic climate isrepresented reasonably well compared to observations in state–of–the–art RCMs, disagreement with respect to precipitation and atmospheric temperatures between the RCMs still exists for some areas (Mottram et al., 2021). For enhanced atmospheric warming , the difference between the initial states of Kori-ULB constructed with the atmospheric climatologies derived from MAR and RACMO increases in terms of sea–level contribution. For warming covered by the lower–emission Therefore, stronger forcing (that is, warming levels reached by the end of this century under SSP5-8.5) is required to overcome this low slipperiness towards the interior of West Antarctica and to induce a complete collapse of the West Antarctic Ice Sheet.

Overall, the uncertainty in Antarctic sea-level commitment to warming projected by 2300 under this lower-emission pathway SSP1-2.6 , the difference on the order of decimeters of sea–level equivalent (Fig. S20) isdue to varying ice–sheet sensitivities of both initial states in associated with ice-sheet modelling choices (ranging from -0.13 m to 2.94 m; Tab. 1) is, in the year 3000, comparable to the spread in Antarctic ice-sheet trajectories in terms of the Wilkes suglacial basin and the Siple

Coast (Fig. S12–S13). The gap in mass loss amounts to multiple meters of sea–level equivalent for an Antarctic–averaged atmospheric warming above 15°C (compare Fig. S20). Most of the marine–based portions of Antarctica are lost already before reaching this warming range, such that this difference arises from a stronger decline of ice grounded above sea level for the atmospheric climatology derived from MAR than from RACMO, potentially caused by enhanced surface melting with the former. The initial states built in a spin–up approach with PISM differ in their dynamical response due to the distinct parameter combinations favoured by the scoring in the initial–state ensembles for the distinct atmospheric climatologies (Reese et al., 2023; Albrecht et al., 2020, see Sect. 2.2.2). Overall, we find that mass loss is higher for the RACMO initial state with a lower pseudo–plastic sliding exponent $q = 0.5$ (compared to $q = 0.75$ as an outcome of the initialisation given the MAR atmospheri . This is the case both during the historical period and for a large range of the covered projected atmospheric temperature changes (Fig. S20). For a regional atmospheric warming of up to about 4°C the difference in sea–level contribution between the PISM initial states is generally on the order of decimeters. Given an initialisation with the atmospheric climatology derived from RACMO, the ice sheet is more sensitive to changes in its climatic boundary conditions in the Recovery and Aurora basin (occurring for Antarctic–averaged atmospheric temperature changes above approximately +8°C), with a global mean sea–level change being up to +9.0 m higher compared to the MAR initial state. The response of both present–day representations of Antarctica to strong regional warming above +15°C (where the decline of remaining terrestrial parts in East Antarctica dominates) agrees well. Here, a slightly more pronounced mass loss is found for the ice–sheet initialisation involving the MAR atmospheric climatology (with higher atmospheric temperatures enhancing surface melt and runoff of the remaining ice grounded above sea level). sea-level change related to parametric uncertainties in ice-climate interactions by the end of the millennium (with -0.73 m - 2.90 m; Coulon et al., 2024).

The range of possible long-term ice-sheet trajectories under SSP1-2.6 suggests the Ross Ice Shelf catchment as an important focus region for future assessments of the multi-millennial Antarctic sea-level contribution, also given a possible intrusion of modified Circumpolar Deep Water into the eastern Ross Sea continental shelf followed by strong sub-shelf melting (Siahaan et al., 2022) as previously simulated for the Filchner Trough (e.g. Hellmer et al., 2012) and its potential to lead to a complete collapse of the West Antarctic Ice Sheet (e.g. Martin et al., 2019).

In a next step, the long-term ice-sheet response when including larger parts of the parameter space covered in the initial-state ensemble and beyond should also be explored, to quantify how parametric uncertainties translate into Antarctic sea-level commitment and extending Coulon et al. (2024) to multi-millennial timescales. While taking into account distinct Antarctic ice–sheet ice-sheet representations as a result of an initial–state initial-state ensemble covering relevant model parameters , some sources of intra–model and including two ice-sheet models, parametric uncertainties cannot be further fully explored here due to computational constraints in favor of sampling a wide range of possible future climates. One of these is the uncertainty related to the sub–shelf melt parameterisation: To determine sub–shelf

For example, to determine sub-shelf melt, PICO (Reese et al., 2018) with a fixed combination of the overturning parameter and the effective turbulent heat exchange coefficient parameter (Reese et al., 2018, 2023) is chosen out of a diverse set of available sub–shelf melt parameterisations (recently compared in Burgard et al., 2022)sub-shelf melt parameterisations (recently compared in e. . PICO has been shown to reproduce observed basal sub-shelf melt rates averaged over Antarctic ice shelves related to the ver-

tical overturning circulation in ~~ice–shelf~~ ice-shelf cavities and to resemble the typical pattern of strongest melt near the grounding line (Reese et al., 2018, 2023). However, smoother spatial fields of ~~basal~~ sub-shelf melt in PICO compared to observations (Reese et al., 2018) and ~~determining~~ here quantifying melt as linearly related to temperature (Reese et al., 2018; Burgard et al., 2022) may ~~eventually impact long–term ice dynamics. In a next step, the long–term ice–sheet responsewhen including larger parts of the parameter space covered in the initial–state ensemble and beyond could be explored, allowing to quantify how parametric uncertainty translates into multi–millennial Antarctic sea–level commitment~~underestimate the long-term ice-sheet response. While the chosen combinations of the overturning parameter and the effective turbulent heat exchange coefficient parameter resemble sub-shelf melt sensitivities and / or observed melt rates (Sect. 2.2.3, Sect. 3.1), substantial parametric uncertainty related to sub-shelf melt exists (e.g. Coulon et al., 2024; Seroussi et al., 2023) and cannot be further explored here.

4.3 ~~Limitations in assessing Antarctic sea–level commitment~~

~~**Boundary conditions**~~

~~Following recent efforts in projecting the Antarctic sea–level contribution on different timescales ranging from the next decades until 2100 to several millennia (Seroussi et al., 2020; Payne et al., 2021; Golledge et al., 2019, 2015), we base the imposed changes in climatic conditions in Antarctica on state–of–the–art GCMs from the Coupled Model Intercomparison Project CMIP6. Biases in the chosen GCMs and a poor representation of conditions at the ice–sheet margins due to their coarse resolution (Beadling et al., 2020; Bracegirdle et al., 2020; Purich and England, 2021) may influence the simulated mass changes of the Antarctic Ice Sheet presented here. First of all, this is relevant for interpreting the simulated historic evolution of the ice sheet because it captures the response to the changes in atmospheric and oceanic conditions over the past decades simulated by one selected GCM (NorESM1-M; Barthel et al., 2020; Bentsen et al., 2013) only. Including the historic ice–sheet trajectory was shown to be essential for Antarctic sea–level projections by 2100 (Reese et al., 2020). Potential biases in the historic ice–sheet evolution (due to biases in the forcing, but likewise in the ice–sheet models itself) may also play a role for the multi–millennial ice–sheet response presented here. The GCMs available to provide future changes in boundary conditions until 2300 are characterized by a large range of climate sensitivities with a high upper bound (Meehl et al., 2020), which has been suggested to not be in accordance with paleoclimate evidence (Zhu et al., 2021). It introduces large uncertainties in the Antarctic sea–level commitment for fixing climatic boundary conditions at the same point in time (as discussed above). Consequently, the derived future climate trajectories and respective projected multi–millennial Antarctic ice loss should only be related to emissions with care and can rather be seen as a potential range of climate futures for Antarctica.~~

~~For determining the long–term~~ Finally, our simulations are performed on a comparably coarse horizontal resolution of 16 km, allowing for a large number of long-term simulations as presented here, which is needed to cover a wide range of uncertainties. The migration of the grounding line in PISM is captured reasonably well, even on such a coarse resolution, with a sub-grid interpolation scheme (Feldmann et al., 2014), that allows to reproduce glacial cycles of the Antarctic ~~sea–level commitment, we assume constant climate conditions on multi–millennial timescales. Keeping climatic boundary conditions constant on multi–millennial timescales allows us to assess the long–term ice–sheet stability and committed sea–level contribution under~~

an idealized combination of atmospheric and oceanic changes with respect to present-day. This approach has been invoked previously (e.g., Golledge et al., 2015), but comes with certain assumptions: For instance, a continued ocean response to changing CO_2 conditions and atmospheric warming (Li et al., 2013) may result in an altered ratio of atmospheric and oceanic changes beyond the point in time where a stabilization of climatic boundary conditions is assumed here. In addition, observed interannual and decadal variability (Paolo et al., 2018; Jenkins et al., 2018) is neglected in the imposed constant climate conditions for simplicity, which has been shown to potentially result in a lower long-term ice-sheet volume (compared to a stable climate; Mikkelsen e up to ice-sheet retreat (Christian et al., 2020; Robel et al., 2019).

Finally, climate trajectories distinct from climate stabilization scenarios may impact the Antarctic Ice Sheet response in the near and far future. This includes increasingly discussed (temperature) overshoot pathways showing a reversal of climate conditions after exceeding a warming of, e.g., 1.5°C (Tokarska et al., 2019). The corresponding response of (Albrecht et al., 2020) . Garbe et al. (2020) showed (using PISM) that the overall hysteresis behaviour of the Antarctic Ice Sheet is , however, not well constrained. In particular, the timescale difference between the ice sheet's response and the potentially high rates of future warming may allow for trajectories deviating from the equilibrium response of the ice sheet. That is , large-scale ice-sheet changes described here may potentially be reversible despite having crossed a critical threshold upon reverting temperatures to present-day or pre-industrial climate conditions in a 'safe' overshoot (Ritchie et al., 2021). Our experiments form the basis for assessing the response of the Antarctic Ice Sheet to a reversal of climatic boundary conditions and relevant timescales. It will allow us to characterize the (ir-)reversibility of the Antarctic mass loss presented here. robust across model resolution. In Kori-ULB, resolving grounding-line dynamics at a coarse resolution is addressed by imposing a flux condition (Pollard and DeConto, 2012a, 2020), which results in a good agreement with high-resolution models.

Missing feedback mechanisms relevant for long-term Antarctic mass loss

Several positive and negative feedbacks (Fyke et al., 2018)

4.3 Limitations related to processes and feedback mechanisms

Several amplifying and dampening feedbacks between the Antarctic Ice Sheet and the Earth system (Fyke et al., 2018) are missing in stand-alone ice-sheet stand-alone ice-sheet model projections such as the ones presented here, but may be relevant for the long-term long-term mass changes and stability of the Antarctic Ice Sheet. Including the missing feedbacks in future fully-coupled fully-coupled assessments of the Antarctic sea-level sea-level commitment could change the timing and rates of (abrupt) mass loss determined in our experimentssimulations, either by dampening or by accelerating accelerating or by dampening Antarctic ice loss. However, such fully-coupled fully-coupled Earth system models including the ice sheets, which are capable of simulating the multi-millennial multi-millennial ice-sheet response as needed for this study, are not yet available.

We here include some of the relevant feedbacks using parametrisations: Atmospheric temperature imposed to the Antarctic Ice Sheet is modified in our experiments simulations using the atmospheric lapse rate to account for the impact of a changing ice-surface ice-surface elevation. This also feeds into the surface melt determined by the positive-degree-day

positive-degree-day approach, depicting the surface ~~melt–elevation~~ melt-elevation feedback (Levermann and Winkelmann, 2016).

The potentially strong decline of ice volume under warming projected for ~~higher–emission~~ higher-emission pathways may, however, additionally result in changes of the atmospheric circulation and respective precipitation patterns ~~(compare e.g., Merz et al., 2014,~~ (compare e.g. Merz et al., 2014, for Greenland), which are not covered in our ~~experiments~~simulations. By applying the ~~positive–degree–day~~ positive-degree-day approach to determine the future ~~ice–sheet~~ ice-sheet surface melt, we do not account for the ~~self–amplifying melt–albedo~~ amplifying melt-albedo feedback (Jakobs et al., 2019, 2021). While ~~polar–oriented~~ polar-oriented regional climate models cannot provide boundary conditions (or dynamically interact with ice sheets) on ~~multi–millennial~~ multi-millennial timescales considered here as of yet, approaches of intermediate complexity such as the recently introduced (simple) diurnal Energy Balance Model ~~(Garbe et al., 2023; Zeitz et al., 2021)~~ (Zeitz et al., 2021; Garbe et al., 2023) may allow to include the potentially accelerating effect of changes in albedo on projected ice loss through enhanced surface melting (Garbe et al., 2023) in the future.

Surface melt on Antarctic ice shelves facilitates hydrofracturing and may, thereby, trigger ice-shelf collapse (Pollard et al., 2015; Trusel e and potentially the Marine Ice Cliff Instability (MICI; Bassis and Walker, 2012; Pollard et al., 2015). While temperature thresholds for melt pond formation as a precursor for such ice-shelf loss may be exceeded by the end of the century (van Wessem et al., 2023) , the availability of parameterisations to include these processes in ice-sheet models is still limited (Pollard et al., 2015; DeConto and Pollard , Considering hydrofracturing (following Pollard et al., 2015; DeConto and Pollard, 2016; Seroussi et al., 2020) may speed-up grounding-line retreat in marine Antarctic basins due to an earlier ice-shelf breakup (Seroussi et al., 2020; Coulon et al., 2024) .

In addition, freshwater fluxes from mass balance changes of the Antarctic Ice Sheet into the surrounding ocean have been suggested to result in atmospheric cooling in the Southern Hemisphere competing with a potential enhancement of ice loss by the end of the century in ~~a positive~~ an amplifying feedback due to subsurface ocean warming ~~(Golledge et al., 2019). This self–amplifying~~ (Golledge et al., 2019; DeConto et al., 2021). This amplifying feedback could have played a role in abrupt ice discharge events during the last deglaciation (Weber et al., 2014). It remains to be explored how such ~~ice–ocean~~ ice-ocean feedbacks could play out on ~~multi–millennial~~ multi-millennial timescales in Antarctica's future.

Finally, while bedrock adjustment to changes in ice load is included in our ~~experiments~~simulations, opposing Earth structures between West and East Antarctica are not considered: By assuming uniform ~~solid–Earth properties, ocean–driven~~ solid-Earth properties, ocean-driven ice loss from marine basins in East Antarctica may be underestimated on millennial timescales (Coulon et al., 2021), such that our estimates of the committed East Antarctic mass loss may be seen as conservative. On the other hand, taking into account characteristic rheological properties of the solid Earth in West Antarctica could promote rapid bedrock uplift, thereby delaying ~~ice–sheet changes .~~ ice-sheet changes (Coulon et al., 2021).

5 Conclusion

While various sources of ~~uncertainties~~ uncertainty remain to be explored for quantifying the ~~long–term Antarctic sea–level~~ long-term Antarctic sea-level commitment, our analysis shows ~~(across distinct ice–sheet models) that the long–term multi–millennial~~ across two ice-sheet models and a multitude of varying climate, model and parametric uncertainties that the multi-millennial impacts on the Antarctic Ice Sheet of warming projected ~~for a given point in time~~ over the next decades and centuries are profound when compared to ~~the sea–level change realized at this point in time.~~ typical sea-level projections as for instance in the IPCC assessments. The Antarctic sea-level commitment to warming projected over the next centuries increases nonlinearly. The multi-millennial ice-sheet response grows steps-wise from a pronounced grounding-line retreat of Thwaites and Pine Island glaciers under lower–emission pathway SSP1-2.6 to a complete long-term collapse of the West Antarctic Ice Sheet triggered at latest for higher–emission warming trajectories in 2100 followed by mass loss from major marine basins in East Antarctica. It is possible that pronounced ice loss also from terrestrial ice-sheet parts of up to +40 m sea-level equivalent is locked in in response to projected warming after 2200 under SSP5-8.5. Our findings thus stress the importance of complementing typical ~~decadal–to–centennial~~ decadal-to-centennial projections of the future evolution of the Antarctic Ice Sheet by the respective committed Antarctic ~~sea–level contribution for long–term~~ sea-level contribution for long-term decision making.

Code and data availability. The source code of PISM is publicly available on GitHub via https://www.pism.io. The exact PISM version used in this paper will be archived within the open access repository Zenodo upon publication of the manuscript. The code of the Kori-ULB ice-sheet model is publicly available on GitHub via https://github.com/FrankPat/Kori-dev. All datasets used in this study are freely accessible through their original references. The CMIP6 forcing data used in this study are accessible through the CMIP6 search interface (https://esgf-node.llnl.gov/search/cmip6/). The simulations outputs, the data needed to produce the figures and tables, and the scripts will be hosted on Zenodo upon publication of the final paper.

Author contributions. R.W. conceived the study. A.K.K. and V.C. processed the forcing data, initialized the ice-sheet models and ran the model simulations. A.K.K. performed the data analysis, produced the figures and wrote the original manuscript with regular inputs from V.C. All authors contributed to the final version of the manuscript.

Competing interests. The authors declare that they have no conflict of interest.

Acknowledgements. This project has received funding from the European Union's Horizon 2020 research and innovation programme under grant agreement No. 869304 (PROTECT). The authors gratefully acknowledge the European Regional Development Fund (ERDF), the German Federal Ministry of Education and Research (BMBF) and the Land Brandenburg for supporting this project by providing resources

on the high-performance computer system at the Potsdam Institute for Climate Impact Research. Development of PISM is supported by NASA grants 20-CRYO2020-0052 and 80NSSC22K0274 and NSF grant OAC-2118285. Computational resources for Kori-ULB simulations have been provided by the Consortium des Équipements de Calcul Intensif (CÉCI), funded by the Fonds de la Recherche Scientifique de Belgique (F.R.S.-FNRS) under Grant No. 2.5020.11 and by the Walloon Region. A.K.K. and R.W. further acknowledge support by the European Union's Horizon 2020 research and innovation programme under Grant Agreement No. 820575 (TiPACCs). We acknowledge the World Climate Research Programme's Working Group on Coupled Modelling, which is responsible for CMIP, and we thank the climate modelling groups (whose models are listed in Table S1 of this paper) for producing and making their model output available. This work has been performed in the context of the FutureLab on Earth Resilience in the Anthropocene at the Potsdam Institute for Climate Impact Research.

References

Aðalgeirsdóttir, G., Aschwanden, A., Khroulev, C., Boberg, F., Mottram, R., Lucas-Picher, P., and Christensen, J.: Role of model initialization for projections of 21st-century Greenland ice sheet mass loss, Journal of Glaciology, 60, 782–794, https://doi.org/10.3189/2014JoG13J202, 2014.

Adusumilli, S., Fricker, H. A., Medley, B., Padman, L., and Siegfried, M. R.: Interannual variations in meltwater input to the Southern Ocean from Antarctic ice shelves, Nature Geoscience, 13, 616–620, https://doi.org/10.1038/s41561-020-0616-z, 2020.

Aitken, A., Roberts, J., Van Ommen, T., Young, D., Golledge, N., Greenbaum, J., Blankenship, D., and Siegert, M.: Repeated large-scale retreat and advance of Totten Glacier indicated by inland bed erosion, Nature, 533, 385–389, https://doi.org/10.1038/nature17447, 2016.

Albrecht, T., Winkelmann, R., and Levermann, A.: Glacial-cycle simulations of the Antarctic Ice Sheet with the Parallel Ice Sheet Model (PISM) – Part 1: Boundary conditions and climatic forcing, The Cryosphere, 14, 599–632, https://doi.org/10.5194/tc-14-599-2020, 2020.

Armstrong McKay, D. I., Staal, A., Abrams, J. F., Winkelmann, R., Sakschewski, B., Loriani, S., Fetzer, I., Cornell, S. E., Rockström, J., and Lenton, T. M.: Exceeding 1.5° C global warming could trigger multiple climate tipping points, Science, 377, eabn7950, https://doi.org/10.1126/science.abn7950, 2022.

Arthern, R. J. and Williams, C. R.: The sensitivity of West Antarctica to the submarine melting feedback, Geophysical Research Letters, 44, 2352–2359, https://doi.org/10.1002/2017GL072514, 2017.

Aschwanden, A., Aðalgeirsdóttir, G., and Khroulev, C.: Hindcasting to measure ice sheet model sensitivity to initial states, The Cryosphere, 7, 1083–1093, https://doi.org/10.5194/tc-7-1083-2013, 2013.

Barletta, V. R., Bevis, M., Smith, B. E., Wilson, T., Brown, A., Bordoni, A., Willis, M., Khan, S. A., Rovira-Navarro, M., Dalziel, I., et al.: Observed rapid bedrock uplift in Amundsen Sea Embayment promotes ice-sheet stability, Science, 360, 1335–1339, https://doi.org/10.1126/science.aao1447, 2018.

Barthel, A., Agosta, C., Little, C. M., Hattermann, T., Jourdain, N. C., Goelzer, H., Nowicki, S., Seroussi, H., Straneo, F., and Bracegirdle, T. J.: CMIP5 model selection for ISMIP6 ice sheet model forcing: Greenland and Antarctica, The Cryosphere, 14, 855–879, https://doi.org/10.5194/tc-14-855-2020, 2020.

Bassis, J. N. and Walker, C. C.: Upper and lower limits on the stability of calving glaciers from the yield strength envelope of ice, Proceedings of the Royal Society A: Mathematical, Physical and Engineering Sciences, 468, 913–931, https://doi.org/10.1098/rspa.2011.0422, 2012.

Beadling, R. L., Russell, J., Stouffer, R., Mazloff, M., Talley, L., Goodman, P., Sallée, J.-B., Hewitt, H., Hyder, P., and Pandde, A.: Representation of Southern Ocean properties across coupled model intercomparison project generations: CMIP3 to CMIP6, Journal of Climate, 33, 6555–6581, https://doi.org/10.1175/JCLI-D-19-0970.1, 2020.

Bentsen, M., Bethke, I., Debernard, J. B., Iversen, T., Kirkevåg, A., Seland, Ø., Drange, H., Roelandt, C., Seierstad, I. A., Hoose, C., et al.: The Norwegian Earth System Model, NorESM1-M–Part 1: description and basic evaluation of the physical climate, Geoscientific Model Development, 6, 687–720, https://doi.org/10.5194/gmd-6-687-2013, 2013.

Berends, C. J., Stap, L. B., and van de Wal, R. S.: Strong impact of sub-shelf melt parameterisation on ice-sheet retreat in idealised and realistic Antarctic topography, Journal of Glaciology, 69, 1434–1448, https://doi.org/10.1017/jog.2023.33, 2023a.

Berends, C. J., Van De Wal, R. S., Van Den Akker, T., and Lipscomb, W. H.: Compensating errors in inversions for subglacial bed roughness: same steady state, different dynamic response, The Cryosphere, 17, 1585–1600, https://doi.org/10.5194/tc-17-1585-2023, 2023b.

Bernales, J., Rogozhina, I., and Thomas, M.: Melting and freezing under Antarctic ice shelves from a combination of ice-sheet modelling and observations, Journal of Glaciology, 63, 731–744, https://doi.org/10.1017/jog.2017.42, 2017.

Blackburn, T., Edwards, G., Tulaczyk, S., Scudder, M., Piccione, G., Hallet, B., McLean, N., Zachos, J., Cheney, B., and Babbe, J.: Ice retreat in Wilkes Basin of East Antarctica during a warm interglacial, Nature, 583, 554–559, https://doi.org/10.1038/s41586-020-2484-5, 2020.

Bracegirdle, T., Holmes, C., Hosking, J., Marshall, G., Osman, M., Patterson, M., and Rackow, T.: Improvements in circumpolar Southern Hemisphere extratropical atmospheric circulation in CMIP6 compared to CMIP5, Earth and Space Science, 7, e2019EA001 065, https://doi.org/10.1029/2019EA001065, 2020.

Bueler, E. and Brown, J.: Shallow shelf approximation as a "sliding law" in a thermomechanically coupled ice sheet model, Journal of Geophysical Research: Earth Surface, 114, https://doi.org/10.1029/2008JF001179, 2009.

Bueler, E. and van Pelt, W.: Mass-conserving subglacial hydrology in the Parallel Ice Sheet Model version 0.6, Geoscientific Model Development, 8, 1613–1635, https://doi.org/gmd-8-1613-2015, 2015.

Bueler, E., Lingle, C. S., and Brown, J.: Fast computation of a viscoelastic deformable Earth model for ice-sheet simulations, Annals of Glaciology, 46, 97–105, https://doi.org/10.3189/172756407782871567, 2007.

Bulthuis, K., Arnst, M., Sun, S., and Pattyn, F.: Uncertainty quantification of the multi-centennial response of the Antarctic ice sheet to climate change, The Cryosphere, 13, 1349–1380, https://doi.org/10.5194/tc-13-1349-2019, 2019.

Burgard, C., Jourdain, N. C., Reese, R., Jenkins, A., and Mathiot, P.: An assessment of basal melt parameterisations for Antarctic ice shelves, The Cryosphere, 16, 4931–4975, https://doi.org/tc-16-4931-2022, 2022.

Calov, R. and Greve, R.: A semi-analytical solution for the positive degree-day model with stochastic temperature variations, Journal of Glaciology, 51, 173–175, https://doi.org/10.3189/172756505781829601, 2005.

Chambers, C., Greve, R., Obase, T., Saito, F., and Abe-Ouchi, A.: Mass loss of the Antarctic ice sheet until the year 3000 under a sustained late-21st-century climate, Journal of Glaciology, 68, 605–617, https://doi.org/10.1017/jog.2021.124, 2022.

Christian, J. E., Robel, A. A., Proistosescu, C., Roe, G., Koutnik, M., and Christianson, K.: The contrasting response of outlet glaciers to interior and ocean forcing, The Cryosphere, 14, 2515–2535, https://doi.org/10.5194/tc-14-2515-2020, 2020.

Clark, P. U., Shakun, J. D., Marcott, S. A., Mix, A. C., Eby, M., Kulp, S., Levermann, A., Milne, G. A., Pfister, P. L., Santer, B. D., et al.: Consequences of twenty-first-century policy for multi-millennial climate and sea-level change, Nature Climate Change, 6, 360–369, https://doi.org/10.1038/nclimate2923, 2016.

Clarke, G. K., Nitsan, U., and Paterson, W.: Strain heating and creep instability in glaciers and ice sheets, Reviews of Geophysics, 15, 235–247, https://doi.org/10.1029/RG015i002p00235, 1977.

Cook, C. P., Van De Flierdt, T., Williams, T., Hemming, S. R., Iwai, M., Kobayashi, M., Jimenez-Espejo, F. J., Escutia, C., González, J. J., Khim, B.-K., et al.: Dynamic behaviour of the East Antarctic ice sheet during Pliocene warmth, Nature Geoscience, 6, 765–769, https://doi.org/10.1038/ngeo1889, 2013.

Cornford, S. L., Seroussi, H., Asay-Davis, X. S., Gudmundsson, G. H., Arthern, R., Borstad, C., Christmann, J., Dias dos Santos, T., Feldmann, J., Goldberg, D., Hoffman, M. J., Humbert, A., Kleiner, T., Leguy, G., Lipscomb, W. H., Merino, N., Durand, G., Morlighem, M., Pollard, D., Rückamp, M., Williams, C. R., and Yu, H.: Results of the third marine ice sheet model intercomparison project (MISMIP+), The Cryosphere, 14, 2283–2301, https://doi.org/10.5194/tc-14-2283-2020, 2020.

Coulon, V., Bulthuis, K., Whitehouse, P. L., Sun, S., Haubner, K., Zipf, L., and Pattyn, F.: Contrasting response of West and East Antarctic ice sheets to glacial isostatic adjustment, Journal of Geophysical Research: Earth Surface, 126, e2020JF006 003, https://doi.org/10.1029/2020JF006003, 2021.

Coulon, V., Klose, A. K., Kittel, C., Edwards, T., Turner, F., Winkelmann, R., and Pattyn, F.: Disentangling the drivers of future Antarctic ice loss with a historically-calibrated ice-sheet model, The Cryosphere, 18, 653–681, https://doi.org/10.5194/tc-18-653-2024, 2024.

Cuffey, K. M. and Paterson, W. S. B.: The Physics of Glaciers, Academic Press, 2010.

DeConto, R. M. and Pollard, D.: Rapid Cenozoic glaciation of Antarctica induced by declining atmospheric CO2, Nature, 421, 245–249, https://doi.org/10.1038/nature01290, 2003.

DeConto, R. M. and Pollard, D.: Contribution of Antarctica to past and future sea-level rise, Nature, 531, 591–597, https://doi.org/10.1038/nature17145, 2016.

DeConto, R. M., Pollard, D., Alley, R. B., Velicogna, I., Gasson, E., Gomez, N., Sadai, S., Condron, A., Gilford, D. M., Ashe, E. L., et al.: The Paris Climate Agreement and future sea-level rise from Antarctica, Nature, 593, 83–89, https://doi.org/10.1038/s41586-021-03427-0, 2021.

Dutton, A., Carlson, A. E., Long, A. J., Milne, G. A., Clark, P. U., DeConto, R., Horton, B. P., Rahmstorf, S., and Raymo, M. E.: Sea-level rise due to polar ice-sheet mass loss during past warm periods, Science, 349, aaa4019, https://doi.org/10.1126/science.aaa4019, 2015.

Edwards, T. L., Nowicki, S., Marzeion, B., Hock, R., Goelzer, H., Seroussi, H., Jourdain, N. C., Slater, D. A., Turner, F. E., Smith, C. J., et al.: Projected land ice contributions to twenty-first-century sea level rise, Nature, 593, 74–82, https://doi.org/10.1038/s41586-021-03302-y, 2021.

Favier, L., Durand, G., Cornford, S. L., Gudmundsson, G. H., Gagliardini, O., Gillet-Chaulet, F., Zwinger, T., Payne, A., and Le Brocq, A. M.: Retreat of Pine Island Glacier controlled by marine ice-sheet instability, Nature Climate Change, 4, 117–121, https://doi.org/10.1038/nclimate2094, 2014.

Feldmann, J., Albrecht, T., Khroulev, C., Pattyn, F., and Levermann, A.: Resolution-dependent performance of grounding line motion in a shallow model compared with a full-Stokes model according to the MISMIP3d intercomparison, Journal of Glaciology, 60, 353–360, https://doi.org/10.3189/2014JoG13J093, 2014.

Fox-Kemper, B., Hewitt, H., Xiao, C., Aðalgeirsdóttir, G., Drijfhout, S., Edwards, T., Golledge, N., Hemer, M., Kopp, R., Krinner, G., Mix, A., Notz, D., Nowicki, S., Nurhati, I., Ruiz, L., Sallée, J.-B., Slangen, A., and Yu, Y.: Ocean, Cryosphere and Sea Level Change. In Climate Change 2021: The Physical Science Basis. Contribution of Working Group I to the Sixth Assessment Report of the Intergovernmental Panel on Climate Change [Masson-Delmotte, V., P. Zhai, A. Pirani, S.L. Connors, C. Péan, S. Berger, N. Caud, Y. Chen, L. Goldfarb, M.I. Gomis, M. Huang, K. Leitzell, E. Lonnoy, J.B.R. Matthews, T.K. Maycock, T. Waterfield, O. Yelekçi, R. Yu, and B. Zhou (eds.)], Cambridge University Press, pp. 1211–1362, 2021.

Fretwell, P., Pritchard, H. D., Vaughan, D. G., Bamber, J. L., Barrand, N. E., Bell, R., Bianchi, C., Bingham, R., Blankenship, D. D., Casassa, G., et al.: Bedmap2: improved ice bed, surface and thickness datasets for Antarctica, The Cryosphere, 7, 375–393, https://doi.org/10.5194/tc-7-375-2013, 2013.

Fyke, J., Sergienko, O., Löfverström, M., Price, S., and Lenaerts, J. T.: An overview of interactions and feedbacks between ice sheets and the Earth system, Reviews of Geophysics, 56, 361–408, https://doi.org/10.1029/2018RG000600, 2018.

Garbe, J., Albrecht, T., Levermann, A., Donges, J. F., and Winkelmann, R.: The hysteresis of the Antarctic Ice Sheet, Nature, 585, 538–544, https://doi.org/10.1038/s41586-020-2727-5, 2020.

Garbe, J., Zeitz, M., Krebs-Kanzow, U., and Winkelmann, R.: The evolution of future Antarctic surface melt using PISM-dEBM-simple, The Cryosphere, 17, 4571–4599, https://doi.org/10.5194/tc-17-4571-2023, 2023.

Golledge, N., Levy, R., McKay, R., and Naish, T.: East Antarctic ice sheet most vulnerable to Weddell Sea warming, Geophysical Research Letters, 44, 2343–2351, https://doi.org/10.1002/2016GL072422, 2017.

Golledge, N. R., Kowalewski, D. E., Naish, T. R., Levy, R. H., Fogwill, C. J., and Gasson, E. G.: The multi-millennial Antarctic commitment to future sea-level rise, Nature, 526, 421–425, https://doi.org/10.1038/nature15706, 2015.

Golledge, N. R., Keller, E. D., Gomez, N., Naughten, K. A., Bernales, J., Trusel, L. D., and Edwards, T. L.: Global environmental consequences of twenty-first-century ice-sheet melt, Nature, 566, 65–72, https://doi.org/10.1038/s41586-019-0889-9, 2019.

Golledge, N. R., Clark, P. U., He, F., Dutton, A., Turney, C., Fogwill, C., Naish, T., Levy, R. H., McKay, R. M., Lowry, D. P., et al.: Retreat of the Antarctic Ice Sheet during the Last Interglaciation and implications for future change, Geophysical Research Letters, 48, e2021GL094 513, https://doi.org/10.1029/2021GL094513, 2021.

Goosse, H., Brovkin, V., Fichefet, T., Haarsma, R., Huybrechts, P., Jongma, J., Mouchet, A., Selten, F., Barriat, P.-Y., Campin, J.-M., Deleersnijder, E., Driesschaert, E., Goelzer, H., Janssens, I., Loutre, M.-F., Morales Maqueda, M. A., Opsteegh, T., Mathieu, P.-P., Munhoven, G., Pettersson, E. J., Renssen, H., Roche, D. M., Schaeffer, M., Tartinville, B., Timmermann, A., and Weber, S. L.: Description of the Earth system model of intermediate complexity LOVECLIM version 1.2, Geoscientific Model Development, 3, 603–633, https://doi.org/10.5194/gmd-3-603-2010, 2010.

Gudmundsson, G. H., Krug, J., Durand, G., Favier, L., and Gagliardini, O.: The stability of grounding lines on retrograde slopes, The Cryosphere, 6, 1497–1505, https://doi.org/10.5194/tc-6-1497-2012, 2012.

Gulev, S., Thorne, P., Ahn, J., Dentener, F., Domingues, C., Gerland, S., Gong, D., Kaufman, D., Nnamchi, H., Quaas, J., Rivera, J., Sathyendranath, S., Smith, S., Trewin, B., von Schuckmann, K., and Vose, R.: Changing State of the Climate System. In Climate Change 2021: The Physical Science Basis. Contribution of Working Group I to the Sixth Assessment Report of the Intergovernmental Panel on Climate Change [Masson-Delmotte, V., P. Zhai, A. Pirani, S.L. Connors, C. Péan, S. Berger, N. Caud, Y. Chen, L. Goldfarb, M.I. Gomis, M. Huang, K. Leitzell, E. Lonnoy, J.B.R. Matthews, T.K. Maycock, T. Waterfield, O. Yelekçi, R. Yu, and B. Zhou (eds.)], Cambridge University Press, p. 287–422, 2021.

Haseloff, M. and Sergienko, O. V.: The effect of buttressing on grounding line dynamics, Journal of Glaciology, 64, 417–431, https://doi.org/10.1017/jog.2018.30, 2018.

Haseloff, M. and Sergienko, O. V.: Effects of calving and submarine melting on steady states and stability of buttressed marine ice sheets, Journal of Glaciology, 68, 1149–1166, https://doi.org/10.1017/jog.2022.29, 2022.

Hellmer, H. H., Kauker, F., Timmermann, R., Determann, J., and Rae, J.: Twenty-first-century warming of a large Antarctic ice-shelf cavity by a redirected coastal current, Nature, 485, 225–228, https://doi.org/10.1038/nature11064, 2012.

Huybrechts, P. and De Wolde, J.: The dynamic response of the Greenland and Antarctic ice sheets to multiple-century climatic warming, Journal of Climate, 12, 2169–2188, https://doi.org/10.1175/1520-0442(1999)012<2169:TDROTG>2.0.CO;2, 1999.

Jakobs, C. L., Reijmer, C. H., Kuipers Munneke, P., König-Langlo, G., and Van Den Broeke, M. R.: Quantifying the snowmelt–albedo feedback at Neumayer Station, East Antarctica, The Cryosphere, 13, 1473–1485, https://doi.org/10.5194/tc-13-1473-2019, 2019.

Jakobs, C. L., Reijmer, C. H., van den Broeke, M. R., Van de Berg, W., and van Wessem, J.: Spatial Variability of the Snowmelt-Albedo Feedback in Antarctica, Journal of Geophysical Research: Earth Surface, 126, e2020JF005 696, https://doi.org/10.1029/2020JF005696, 2021.

Jenkins, A., Shoosmith, D., Dutrieux, P., Jacobs, S., Kim, T. W., Lee, S. H., Ha, H. K., and Stammerjohn, S.: West Antarctic Ice Sheet retreat in the Amundsen Sea driven by decadal oceanic variability, Nature Geoscience, 11, 733–738, https://doi.org/10.1038/s41561-018-0207-4, 2018.

Joughin, I., Smith, B. E., and Medley, B.: Marine ice sheet collapse potentially under way for the Thwaites Glacier Basin, West Antarctica, Science, 344, 735–738, https://doi.org/10.1126/science.1249055, 2014.

Kittel, C., Amory, C., Agosta, C., Jourdain, N. C., Hofer, S., Delhasse, A., Doutreloup, S., Huot, P.-V., Lang, C., Fichefet, T., and Fettweis, X.: Diverging future surface mass balance between the Antarctic ice shelves and grounded ice sheet, The Cryosphere, 15, 1215–1236, https://doi.org/10.5194/tc-15-1215-2021, 2021.

Kreuzer, M., Reese, R., Huiskamp, W. N., Petri, S., Albrecht, T., Feulner, G., and Winkelmann, R.: Coupling framework (1.0) for the PISM (1.1.4) ice sheet model and the MOM5 (5.1.0) ocean model via the PICO ice shelf cavity model in an Antarctic domain, Geoscientific Model Development, 14, 3697–3714, https://doi.org/10.5194/gmd-14-3697-2021, 2021.

Lai, C.-Y., Kingslake, J., Wearing, M. G., Chen, P.-H. C., Gentine, P., Li, H., Spergel, J. J., and van Wessem, J. M.: Vulnerability of Antarctica's ice shelves to meltwater-driven fracture, Nature, 584, 574–578, https://doi.org/10.1038/s41586-020-2627-8, 2020.

Le Meur, E. and Huybrechts, P.: A comparison of different ways of dealing with isostasy: examples from modelling the Antarctic ice sheet during the last glacial cycle, Annals of Glaciology, 23, 309–317, https://doi.org/10.3189/S0260305500013586, 1996.

Lee, J.-Y., Marotzke, J., Bala, G., Cao, L., Corti, S., Dunne, J., Engelbrecht, F., Fischer, E., Fyfe, J., Jones, C., Maycock, A., Mutemi, J., Ndiaye, O., Panickal, S., and Zhou, T.: Future Global Climate: Scenario-Based Projections and Near- Term Information. In Climate Change 2021: The Physical Science Basis. Contribution of Working Group I to the Sixth Assessment Report of the Intergovernmental Panel on Climate Change [Masson-Delmotte, V., P. Zhai, A. Pirani, S.L. Connors, C. Péan, S. Berger, N. Caud, Y. Chen, L. Goldfarb, M.I. Gomis, M. Huang, K. Leitzell, E. Lonnoy, J.B.R. Matthews, T.K. Maycock, T. Waterfield, O. Yelekçi, R. Yu, and B. Zhou (eds.)], Cambridge University Press, pp. 553–672, 2021.

Lenton, T. M., Held, H., Kriegler, E., Hall, J. W., Lucht, W., Rahmstorf, S., and Schellnhuber, H. J.: Tipping elements in the Earth's climate system, Proceedings of the National Academy of Sciences, 105, 1786–1793, https://doi.org/10.1073/pnas.0705414105, 2008.

Lenton, T. M., Armstrong McKay, D., Loriani, S., Abrams, J., Lade, S., Donges, J., Milkoreit, M., Powell, M., Smith, S., Zimm, C., Buxton, C., Bailey, E., Laybourn, L., Ghadiali, A., and Dyke, J. e.: The Global Tipping Points Report 2023, University of Exeter, Exeter, UK., 2023.

Levermann, A. and Winkelmann, R.: A simple equation for the melt elevation feedback of ice sheets, The Cryosphere, 10, 1799–1807, https://doi.org/10.5194/tc-10-1799-2016, 2016.

Levermann, A., Albrecht, T., Winkelmann, R., Martin, M. A., Haseloff, M., and Joughin, I.: Kinematic first-order calving law implies potential for abrupt ice-shelf retreat, The Cryosphere, 6, 273–286, https://doi.org/10.5194/tc-6-273-2012, 2012.

Levy, R., Harwood, D., Florindo, F., Sangiorgi, F., Tripati, R., Von Eynatten, H., Gasson, E., Kuhn, G., Tripati, A., DeConto, R., et al.: Antarctic ice sheet sensitivity to atmospheric CO2 variations in the early to mid-Miocene, Proceedings of the National Academy of Sciences, 113, 3453–3458, https://doi.org/10.1073/pnas.1516030113, 2016.

Li, C., von Storch, J.-S., and Marotzke, J.: Deep-ocean heat uptake and equilibrium climate response, Climate Dynamics, 40, 1071–1086, https://doi.org/10.1007/s00382-012-1350-z, 2013.

Li, X., Rignot, E., Mouginot, J., and Scheuchl, B.: Ice flow dynamics and mass loss of Totten Glacier, East Antarctica, from 1989 to 2015, Geophysical Research Letters, 43, 6366–6373, https://doi.org/10.1002/2016GL069173, 2016.

Lingle, C. S. and Clark, J. A.: A numerical model of interactions between a marine ice sheet and the solid earth: Application to a West Antarctic ice stream, Journal of Geophysical Research: Oceans, 90, 1100–1114, https://doi.org/10.1029/JC090iC01p01100, 1985.

Lowry, D. P., Krapp, M., Golledge, N. R., and Alevropoulos-Borrill, A.: The influence of emissions scenarios on future Antarctic ice loss is unlikely to emerge this century, Communications Earth & Environment, 2, 1–14, https://doi.org/10.1038/s43247-021-00289-2, 2021.

Martin, D. F., Cornford, S. L., and Payne, A. J.: Millennial-scale vulnerability of the Antarctic ice sheet to regional ice shelf collapse, Geophysical Research Letters, 46, 1467–1475, https://doi.org/10.1029/2018GL081229, 2019.

Martin, M. A., Winkelmann, R., Haseloff, M., Albrecht, T., Bueler, E., Khroulev, C., and Levermann, A.: The Potsdam Parallel Ice Sheet Model (PISM-PIK)–Part 2: dynamic equilibrium simulation of the Antarctic ice sheet, The Cryosphere, 5, 727–740, https://doi.org/10.5194/tc-5-727-2011, 2011.

Meehl, G. A., Senior, C. A., Eyring, V., Flato, G., Lamarque, J.-F., Stouffer, R. J., Taylor, K. E., and Schlund, M.: Context for interpreting equilibrium climate sensitivity and transient climate response from the CMIP6 Earth system models, Science Advances, 6, eaba1981, https://doi.org/10.1126/sciadv.aba1981, 2020.

Mengel, M. and Levermann, A.: Ice plug prevents irreversible discharge from East Antarctica, Nature Climate Change, 4, 451–455, https://doi.org/10.1038/nclimate2226, 2014.

Merz, N., Gfeller, G., Born, A., Raible, C., Stocker, T., and Fischer, H.: Influence of ice sheet topography on Greenland precipitation during the Eemian interglacial, Journal of Geophysical Research: Atmospheres, 119, 10,749–10,768, https://doi.org/10.1002/2014JD021940, 2014.

Mikkelsen, T. B., Grinsted, A., and Ditlevsen, P.: Influence of temperature fluctuations on equilibrium ice sheet volume, The Cryosphere, 12, 39–47, https://doi.org/10.5194/tc-12-39-2018, 2018.

Miles, B. W., Jordan, J. R., Stokes, C. R., Jamieson, S. S., Gudmundsson, G. H., and Jenkins, A.: Recent acceleration of Denman Glacier (1972–2017), East Antarctica, driven by grounding line retreat and changes in ice tongue configuration, The Cryosphere, 15, 663–676, https://doi.org/10.5194/tc-15-663-2021, 2021.

Morlighem, M., Rignot, E., Binder, T., Blankenship, D., Drews, R., Eagles, G., Eisen, O., Ferraccioli, F., Forsberg, R., Fretwell, P., et al.: Deep glacial troughs and stabilizing ridges unveiled beneath the margins of the Antarctic ice sheet, Nature Geoscience, 13, 132–137, https://doi.org/10.1038/s41561-019-0510-8, 2020.

Mottram, R., Hansen, N., Kittel, C., van Wessem, J. M., Agosta, C., Amory, C., Boberg, F., van de Berg, W. J., Fettweis, X., Gossart, A., et al.: What is the surface mass balance of Antarctica? An intercomparison of regional climate model estimates, The Cryosphere, 15, 3751–3784, https://doi.org/10.5194/tc-15-3751-2021, 2021.

Naish, T., Powell, R., Levy, R., Wilson, G., Scherer, R., Talarico, F., Krissek, L., Niessen, F., Pompilio, M., Wilson, T., et al.: Obliquity-paced Pliocene West Antarctic ice sheet oscillations, Nature, 458, 322–328, https://doi.org/10.1038/nature07867, 2009.

Naish, T. R., Woolfe, K. J., Barrett, P. J., Wilson, G. S., Atkins, C., Bohaty, S. M., Bücker, C. J., Claps, M., Davey, F. J., Dunbar, G. B., et al.: Orbitally induced oscillations in the East Antarctic ice sheet at the Oligocene/Miocene boundary, Nature, 413, 719–723, https://doi.org/10.1038/35099534, 2001.

Nias, I. J., Cornford, S. L., and Payne, A. J.: Contrasting the modelled sensitivity of the Amundsen Sea Embayment ice streams, Journal of Glaciology, 62, 552–562, https://doi.org/10.1017/jog.2016.40, 2016.

Nowicki, S., Goelzer, H., Seroussi, H., Payne, A. J., Lipscomb, W. H., Abe-Ouchi, A., Agosta, C., Alexander, P., Asay-Davis, X. S., Barthel, A., Bracegirdle, T. J., Cullather, R., Felikson, D., Fettweis, X., Gregory, J. M., Hattermann, T., Jourdain, N. C., Kuipers Munneke, P., Larour, E., Little, C. M., Morlighem, M., Nias, I., Shepherd, A., Simon, E., Slater, D., Smith, R. S., Straneo, F., Trusel, L. D., van den Broeke, M. R., and van de Wal, R.: Experimental protocol for sea level projections from ISMIP6 stand-alone ice sheet models, The Cryosphere, 14, 2331–2368, https://doi.org/10.5194/tc-14-2331-2020, 2020.

Oerlemans, J.: Some basic experiments with a vertically-integrated ice sheet model, Tellus, 33, 1–11, https://doi.org/10.3402/tellusa.v33i1.10690, 1981.

O'Neill, B. C., Tebaldi, C., Van Vuuren, D. P., Eyring, V., Friedlingstein, P., Hurtt, G., Knutti, R., Kriegler, E., Lamarque, J.-F., Lowe, J., et al.: The scenario model intercomparison project (ScenarioMIP) for CMIP6, Geoscientific Model Development, 9, 3461–3482, https://doi.org/10.5194/gmd-9-3461-2016, 2016.

Otosaka, I. N., Shepherd, A., Ivins, E. R., Schlegel, N.-J., Amory, C., van den Broeke, M. R., Horwath, M., Joughin, I., King, M. D., Krinner, G., Nowicki, S., Payne, A. J., Rignot, E., Scambos, T., Simon, K. M., Smith, B. E., Sørensen, L. S., Velicogna, I., Whitehouse, P. L., A, G., Agosta, C., Ahlstrøm, A. P., Blazquez, A., Colgan, W., Engdahl, M. E., Fettweis, X., Forsberg, R., Gallée, H., Gardner, A., Gilbert, L., Gourmelen, N., Groh, A., Gunter, B. C., Harig, C., Helm, V., Khan, S. A., Kittel, C., Konrad, H., Langen, P. L., Lecavalier, B. S., Liang, C.-C., Loomis, B. D., McMillan, M., Melini, D., Mernild, S. H., Mottram, R., Mouginot, J., Nilsson, J., Noël, B., Pattle, M. E., Peltier, W. R., Pie, N., Roca, M., Sasgen, I., Save, H. V., Seo, K.-W., Scheuchl, B., Schrama, E. J. O., Schröder, L., Simonsen, S. B., Slater, T., Spada, G., Sutterley, T. C., Vishwakarma, B. D., van Wessem, J. M., Wiese, D., van der Wal, W., and Wouters, B.: Mass balance of the Greenland and Antarctic ice sheets from 1992 to 2020, Earth System Science Data, 15, 1597–1616, https://doi.org/10.5194/essd-15-1597-2023, 2023.

Paolo, F., Padman, L., Fricker, H., Adusumilli, S., Howard, S., and Siegfried, M.: Response of Pacific-sector Antarctic ice shelves to the El Niño/Southern oscillation, Nature Geoscience, 11, 121–126, https://doi.org/10.1038/s41561-017-0033-0, 2018.

Paolo, F. S., Fricker, H. A., and Padman, L.: Volume loss from Antarctic ice shelves is accelerating, Science, 348, 327–331, https://doi.org/10.1126/science.aaa0940, 2015.

Patterson, M. O., McKay, R., Naish, T., Escutia, C., Jimenez-Espejo, F., Raymo, M., Meyers, S., Tauxe, L., and Brinkhuis, H.: Orbital forcing of the East Antarctic ice sheet during the Pliocene and Early Pleistocene, Nature Geoscience, 7, 841–847, https://doi.org/10.1038/ngeo2273, 2014.

Pattyn, F.: Sea-level response to melting of Antarctic ice shelves on multi-centennial timescales with the fast Elementary Thermomechanical Ice Sheet model (f.ETISh v1.0), The Cryosphere, 11, 1851–1878, https://doi.org/10.5194/tc-11-1851-2017, 2017.

Pattyn, F., Perichon, L., Durand, G., Favier, L., Gagliardini, O., Hindmarsh, R. C., Zwinger, T., Albrecht, T., Cornford, S., Docquier, D., and et al.: Grounding-line migration in plan-view marine ice-sheet models: results of the ice2sea MISMIP3d intercomparison, Journal of Glaciology, 59, 410–422, https://doi.org/10.3189/2013JoG12J129, 2013.

Payne, A. J., Nowicki, S., Abe-Ouchi, A., Agosta, C., Alexander, P., Albrecht, T., Asay-Davis, X., Aschwanden, A., Barthel, A., Bracegirdle, T. J., et al.: Future sea level change under Coupled Model Intercomparison Project Phase 5 and Phase 6 scenarios from the Greenland and Antarctic ice sheets, Geophysical Research Letters, 48, e2020GL091 741, https://doi.org/10.1029/2020GL091741, 2021.

Pegler, S. S.: Marine ice sheet dynamics: the impacts of ice-shelf buttressing, Journal of Fluid Mechanics, 857, 605–647, https://doi.org/10.1038/s41561-017-0033-0, 2018.

Pollard, D. and DeConto, R. M.: Modelling West Antarctic ice sheet growth and collapse through the past five million years, Nature, 458, 329–332, https://doi.org/10.1038/nature07809, 2009.

Pollard, D. and DeConto, R. M.: Description of a hybrid ice sheet-shelf model, and application to Antarctica, Geoscientific Model Development, 5, 1273–1295, https://doi.org/10.5194/gmd-5-1273-2012, 2012a.

Pollard, D. and DeConto, R. M.: A simple inverse method for the distribution of basal sliding coefficients under ice sheets, applied to Antarctica, The Cryosphere, 6, 953–971, https://doi.org/10.5194/tc-6-953-2012, 2012b.

Pollard, D. and DeConto, R. M.: Improvements in one-dimensional grounding-line parameterizations in an ice-sheet model with lateral variations (PSUICE3D v2.1), Geoscientific Model Development, 13, 6481–6500, https://doi.org/10.5194/gmd-13-6481-2020, 2020.

Pollard, D., DeConto, R. M., and Alley, R. B.: Potential Antarctic Ice Sheet retreat driven by hydrofracturing and ice cliff failure, Earth and Planetary Science Letters, 412, 112–121, https://doi.org/10.1016/j.epsl.2014.12.035, 2015.

Purich, A. and England, M. H.: Historical and future projected warming of Antarctic Shelf Bottom Water in CMIP6 models, Geophysical Research Letters, 48, e2021GL092 752, https://doi.org/10.1029/2021GL092752, 2021.

Reeh, N.: Parameterization of melt rate and surface temperature on the Greenland ice sheet, Polarforschung, 59, 113–128, 1991.

Reese, R., Albrecht, T., Mengel, M., Asay-Davis, X., and Winkelmann, R.: Antarctic sub-shelf melt rates via PICO, The Cryosphere, 12, 1969–1985, https://doi.org/10.5194/tc-12-1969-2018, 2018.

Reese, R., Levermann, A., Albrecht, T., Seroussi, H., and Winkelmann, R.: The role of history and strength of the oceanic forcing in sea level projections from Antarctica with the Parallel Ice Sheet Model, The Cryosphere, 14, 3097–3110, https://doi.org/10.5194/tc-14-3097-2020, 2020.

Reese, R., Garbe, J., Hill, E. A., Urruty, B., Naughten, K. A., Gagliardini, O., Durand, G., Gillet-Chaulet, F., Gudmundsson, G. H., Chandler, D., et al.: The stability of present-day Antarctic grounding lines–Part 2: Onset of irreversible retreat of Amundsen Sea glaciers under current climate on centennial timescales cannot be excluded, The Cryosphere, 17, 3761–3783, https://doi.org/10.5194/tc-17-3761-2023, 2023.

Rignot, E., Mouginot, J., and Scheuchl, B.: Ice flow of the Antarctic Ice Sheet, Science, 333, 1427–1430, https://doi.org/10.1126/science.1208336, 2011.

Rignot, E., Mouginot, J., Scheuchl, B., Van Den Broeke, M., van Wessem, M. J., and Morlighem, M.: Four decades of Antarctic Ice Sheet mass balance from 1979–2017, Proceedings of the National Academy of Sciences, 116, 1095–1103, https://doi.org/10.1073/pnas.1812883116, 2019.

Ritchie, P. D., Clarke, J. J., Cox, P. M., and Huntingford, C.: Overshooting tipping point thresholds in a changing climate, Nature, 592, 517–523, https://doi.org/10.1038/s41586-021-03263-2, 2021.

Robel, A. A., Seroussi, H., and Roe, G. H.: Marine ice sheet instability amplifies and skews uncertainty in projections of future sea-level rise, Proceedings of the National Academy of Sciences, 116, 14 887–14 892, https://doi.org/10.1073/pnas.1904822116, 2019.

Robinson, A., Calov, R., and Ganopolski, A.: Multistability and critical thresholds of the Greenland ice sheet, Nature Climate Change, 2, 429–432, https://doi.org/10.1038/nclimate1449, 2012.

Rosier, S. H., Reese, R., Donges, J. F., De Rydt, J., Gudmundsson, G. H., and Winkelmann, R.: The tipping points and early warning indicators for Pine Island Glacier, West Antarctica, The Cryosphere, 15, 1501–1516, https://doi.org/10.5194/tc-15-1501-2021, 2021.

Schmidtko, S., Heywood, K. J., Thompson, A. F., and Aoki, S.: Multidecadal warming of Antarctic waters, Science, 346, 1227–1231, https://doi.org/10.1126/science.1256117, 2014.

Schoof, C.: Ice sheet grounding line dynamics: Steady states, stability, and hysteresis, Journal of Geophysical Research: Earth Surface, 112, https://doi.org/10.1029/2006JF000664, 2007.

Sergienko, O. V.: No general stability conditions for marine ice-sheet grounding lines in the presence of feedbacks, Nature Communications, 13, 2265, https://doi.org/10.1038/s41467-022-29892-3, 2022.

Seroussi, H., Nakayama, Y., Larour, E., Menemenlis, D., Morlighem, M., Rignot, E., and Khazendar, A.: Continued retreat of Thwaites Glacier, West Antarctica, controlled by bed topography and ocean circulation, Geophysical Research Letters, 44, 6191–6199, https://doi.org/10.1002/2017GL072910, 2017.

Seroussi, H., Nowicki, S., Simon, E., Abe-Ouchi, A., Albrecht, T., Brondex, J., Cornford, S., Dumas, C., Gillet-Chaulet, F., Goelzer, H., et al.: initMIP-Antarctica: an ice sheet model initialization experiment of ISMIP6, The Cryosphere, 13, 1441–1471, https://doi.org/10.5194/tc-13-1441-2019, 2019.

Seroussi, H., Nowicki, S., Payne, A. J., Goelzer, H., Lipscomb, W. H., Abe-Ouchi, A., Agosta, C., Albrecht, T., Asay-Davis, X., Barthel, A., et al.: ISMIP6 Antarctica: a multi-model ensemble of the Antarctic ice sheet evolution over the 21st century, The Cryosphere, 14, 3033–3070, https://doi.org/10.5194/tc-14-3033-2020, 2020.

Seroussi, H., Verjans, V., Nowicki, S., Payne, A. J., Goelzer, H., Lipscomb, W. H., Abe-Ouchi, A., Agosta, C., Albrecht, T., Asay-Davis, X., Barthel, A., Calov, R., Cullather, R., Dumas, C., Galton-Fenzi, B. K., Gladstone, R., Golledge, N. R., Gregory, J. M., Greve, R., Hattermann, T., Hoffman, M. J., Humbert, A., Huybrechts, P., Jourdain, N. C., Kleiner, T., Larour, E., Leguy, G. R., Lowry, D. P., Little, C. M., Morlighem, M., Pattyn, F., Pelle, T., Price, S. F., Quiquet, A., Reese, R., Schlegel, N.-J., Shepherd, A., Simon, E., Smith, R. S., Straneo, F., Sun, S., Trusel, L. D., Van Breedam, J., Van Katwyk, P., van de Wal, R. S. W., Winkelmann, R., Zhao, C., Zhang, T., and Zwinger, T.: Insights into the vulnerability of Antarctic glaciers from the ISMIP6 ice sheet model ensemble and associated uncertainty, The Cryosphere, 17, 5197–5217, https://doi.org/10.5194/tc-17-5197-2023, 2023.

Shakun, J. D., Corbett, L. B., Bierman, P. R., Underwood, K., Rizzo, D. M., Zimmerman, S. R., Caffee, M. W., Naish, T., Golledge, N. R., and Hay, C. C.: Minimal East Antarctic Ice Sheet retreat onto land during the past eight million years, Nature, 558, 284–287, https://doi.org/10.1038/s41586-018-0155-6, 2018.

Siahaan, A., Smith, R. S., Holland, P. R., Jenkins, A., Gregory, J. M., Lee, V., Mathiot, P., Payne, A. J., Ridley, J. K., and Jones, C. G.: The Antarctic contribution to 21st-century sea-level rise predicted by the UK Earth System Model with an interactive ice sheet, The Cryosphere, 16, 4053–4086, https://doi.org/10.5194/tc-16-4053-2022, 2022.

Smith, B., Fricker, H. A., Gardner, A. S., Medley, B., Nilsson, J., Paolo, F. S., Holschuh, N., Adusumilli, S., Brunt, K., Csatho, B., et al.: Pervasive ice sheet mass loss reflects competing ocean and atmosphere processes, Science, 368, 1239–1242, https://doi.org/10.1126/science.aaz5845, 2020.

Sugden, D. E., Marchant, D. R., Potter, N., Souchez, R. A., Denton, G. H., Swisher III, C. C., and Tison, J.-L.: Preservation of Miocene glacier ice in East Antarctica, Nature, 376, 412–414, https://doi.org/10.1038/376412a0, 1995.

Sun, S., Pattyn, F., Simon, E. G., Albrecht, T., Cornford, S., Calov, R., Dumas, C., Gillet-Chaulet, F., Goelzer, H., Golledge, N. R., and et al.: Antarctic ice sheet response to sudden and sustained ice-shelf collapse (ABUMIP), Journal of Glaciology, 66, 891–904, https://doi.org/0.1017/jog.2020.67, 2020.

Sutter, J., Jones, A., Frölicher, T., Wirths, C., and Stocker, T.: Climate intervention on a high-emissions pathway could delay but not prevent West Antarctic Ice Sheet demise, Nature Climate Change, 13, 951–960, https://doi.org/10.1038/s41558-023-01738-w, 2023.

Tebaldi, C., Debeire, K., Eyring, V., Fischer, E., Fyfe, J., Friedlingstein, P., Knutti, R., Lowe, J., O'Neill, B., Sanderson, B., van Vuuren, D., Riahi, K., Meinshausen, M., Nicholls, Z., Tokarska, K. B., Hurtt, G., Kriegler, E., Lamarque, J.-F., Meehl, G., Moss, R., Bauer, S. E., Boucher, O., Brovkin, V., Byun, Y.-H., Dix, M., Gualdi, S., Guo, H., John, J. G., Kharin, S., Kim, Y., Koshiro, T., Ma, L., Olivié, D., Panickal, S., Qiao, F., Rong, X., Rosenbloom, N., Schupfner, M., Séférian, R., Sellar, A., Semmler, T., Shi, X., Song, Z., Steger, C., Stouffer, R., Swart, N., Tachiiri, K., Tang, Q., Tatebe, H., Voldoire, A., Volodin, E., Wyser, K., Xin, X., Yang, S., Yu, Y., and Ziehn, T.: Climate model projections from the Scenario Model Intercomparison Project (ScenarioMIP) of CMIP6, Earth System Dynamics, 12, 253–293, https://doi.org/10.5194/esd-12-253-2021, 2021.

Tokarska, K. B., Zickfeld, K., and Rogelj, J.: Path independence of carbon budgets when meeting a stringent global mean temperature target after an overshoot, Earth's Future, 7, 1283–1295, https://doi.org/10.1029/2019EF001312, 2019.

Trusel, L. D., Frey, K. E., Das, S. B., Karnauskas, K. B., Kuipers Munneke, P., Van Meijgaard, E., and Van Den Broeke, M. R.: Divergent trajectories of Antarctic surface melt under two twenty-first-century climate scenarios, Nature Geoscience, 8, 927–932, https://doi.org/10.1038/ngeo2563, 2015.

Turney, C. S., Fogwill, C. J., Golledge, N. R., McKay, N. P., van Sebille, E., Jones, R. T., Etheridge, D., Rubino, M., Thornton, D. P., Davies, S. M., et al.: Early Last Interglacial ocean warming drove substantial ice mass loss from Antarctica, Proceedings of the National Academy of Sciences, 117, 3996–4006, https://doi.org/10.1073/pnas.1902469117, 2020.

Van Breedam, J., Goelzer, H., and Huybrechts, P.: Semi-equilibrated global sea-level change projections for the next 10 000 years, Earth System Dynamics, 11, 953–976, https://doi.org/10.5194/esd-11-953-2020, 2020.

van Wessem, J. M., Van De Berg, W. J., Noël, B. P., Van Meijgaard, E., Amory, C., Birnbaum, G., Jakobs, C. L., Krüger, K., Lenaerts, J., Lhermitte, S., et al.: Modelling the climate and surface mass balance of polar ice sheets using RACMO2–Part 2: Antarctica (1979–2016), The Cryosphere, 12, 1479–1498, https://doi.org/10.5194/tc-12-1479-2018, 2018.

van Wessem, J. M., van den Broeke, M. R., Wouters, B., and Lhermitte, S.: Variable temperature thresholds of melt pond formation on Antarctic ice shelves, Nature Climate Change, 13, 161–166, https://doi.org/10.1038/s41558-022-01577-1, 2023.

Weber, M., Clark, P., Kuhn, G., Timmermann, A., Sprenk, D., Gladstone, R., Zhang, X., Lohmann, G., Menviel, L., Chikamoto, M., et al.: Millennial-scale variability in Antarctic ice-sheet discharge during the last deglaciation, Nature, 510, 134–138, https://doi.org/10.1038/nature13397, 2014.

Weertman, J.: Stability of the junction of an ice sheet and an ice shelf, Journal of Glaciology, 13, 3–11, https://doi.org/10.3189/S0022143000023327, 1974.

Wilson, D. J., Bertram, R. A., Needham, E. F., van de Flierdt, T., Welsh, K. J., McKay, R. M., Mazumder, A., Riesselman, C. R., Jimenez-Espejo, F. J., and Escutia, C.: Ice loss from the East Antarctic Ice Sheet during late Pleistocene interglacials, Nature, 561, 383–386, https://doi.org/10.1038/s41586-018-0501-8, 2018.

Winkelmann, R., Martin, M. A., Haseloff, M., Albrecht, T., Bueler, E., Khroulev, C., and Levermann, A.: The Potsdam Parallel Ice Sheet Model (PISM-PIK)–Part 1: Model description, The Cryosphere, 5, 715–726, https://doi.org/10.5194/tc-5-715-2011, 2011.

Winkelmann, R., Levermann, A., Ridgwell, A., and Caldeira, K.: Combustion of available fossil fuel resources sufficient to eliminate the Antarctic Ice Sheet, Science Advances, 1, e1500 589, https://doi.org/10.1126/sciadv.1500589, 2015.

Zachos, J., Pagani, M., Sloan, L., Thomas, E., and Billups, K.: Trends, rhythms, and aberrations in global climate 65 Ma to present, Science, 292, 686–693, https://doi.org/10.1126/science.1059412, 2001.

Zeitz, M., Reese, R., Beckmann, J., Krebs-Kanzow, U., and Winkelmann, R.: Impact of the melt–albedo feedback on the future evolution of the Greenland Ice Sheet with PISM-dEBM-simple, The Cryosphere, 15, 5739–5764, https://doi.org/10.5194/tc-15-5739-2021, 2021.

Zhu, J., Otto-Bliesner, B. L., Brady, E. C., Poulsen, C. J., Tierney, J. E., Lofverstrom, M., and DiNezio, P.: Assessment of equilibrium climate sensitivity of the Community Earth System Model version 2 through simulation of the Last Glacial Maximum, Geophysical Research Letters, 48, e2020GL091 220, https://doi.org/10.1029/2020GL091220, 2021.